9-21-2010

System Identification and State Estimation for Intake Manifold Charge Flow Temperature of a Compression Ignition Diesel Engine

Ryle D. Maxson
Embry-Riddle Aeronautical University - Daytona Beach

SYSTEM IDENTIFICATION AND STATE ESTIMATION FOR INTAKE MANIFOLD CHARGE FLOW TEMPERATURE OF A COMPRESSION IGNITION DIESEL ENGINE

Ryle Maxson

A Thesis Submitted to the
Graduate Studies Office
In Partial Fulfillment of the Requirements for the Degree of
Master of Science in Mechanical Engineering

September 21, 2010

Embry-Riddle Aeronautical University
Daytona Beach, Florida

SYSTEM IDENTIFICATION AND STATE ESTIMATION
FOR INTAKE MANIFOLD CHARGE FLOW TEMPERATURE
OF A COMPRESSION IGNITION DIESEL ENGINE

by

Ryle Maxson

This thesis was prepared under the direction of the candidate's thesis committee chairman, Dr. Darris White, Department of Mechanical Engineering, and has been approved by the members of his thesis committee. It was submitted to the Mechanical Engineering Department and was accepted in partial fulfillment of the requirements for the degree of Masters of Science in Mechanical Engineering.

THESIS COMMITTEE:

Dr. Darris White
Chairman

Dr. Charles Reinholtz
Member
Department Chair, Mechanical Engineering

Dr. William Engblom
Member

Dr. James Cunningham
Associate Vice President for Academics

9/27/10
Date

ACKNOWLEDGEMENTS

The author would like to gratefully acknowledge the contributions of the entire Diesel Combustion and Emissions Control group at GM, including Ognyan Yanakiev, Charles Solbrig, Ping Ge, and Sharon Li. Without their guidance and support, this project would not have been possible. The author would also like to thank the Faculty and Staff at Embry-Riddle Aeronautical University, most notably those of the Department of Mechanical Engineering. Lastly, I would like to thank my family for their continual support in all my endeavors.

ABSTRACT

Author: Ryle D. Maxson

Title: System Identification and State Estimation for Intake Manifold Charge Flow Temperature of a Compression Ignition Diesel Engine

Institution: Embry-Riddle Aeronautical University

Degree: Master of Science in Mechanical Engineering

Year: 2010

Intake manifold charge temperature is a factor used in mean value engine models (MVEMs) for the calculation of intake mass air charge and oxygen flow. More stringent emission requirements have led to increased deployment of more advanced engine combustion models onto production engine controllers. Measurement of the temperature via physical thermocouple sensors mounted to the engine intake manifold is both slow, in comparison to the changing conditions of an engine, and undesirable due to the cost and increased complexity of extra sensors. A state estimation model has been evaluated that imitates the function of the intake manifold temperature sensor reading, but uses the fusion of data acquired from other sensor locations on the engine. Steady-state and Federal Test Procedure (FTP) cycle analysis was used to evaluate the development model on a rapid prototyping system. The model showed substantial agreement with the measured values over a range of operating conditions.

TABLE OF CONTENTS

TABLE OF FIGURES

LIST OF ACRONYMS

CAC:	Charge Air Cooler
ECT:	Engine Coolant Temperature
EGR:	Exhaust Gas Recirculation
FTP:	Federal Test Procedure
f_{AIR}:	Fresh Air Fraction in Intake Manifold
f_{EGR}:	EGR Air Fraction in Intake Manifold
ICE:	Internal Combustion Engine
MAF:	Mass Air Flowrate
MAF_{Delay}:	Transport Delay Time (seconds)
MAP:	Manifold Absolute Pressure
MY:	Model Year
MVEM	Mean Value Engine Model
$\dot{m}_{tot}$:	Total Charge Mass Flow
$N_{Eng.Speed}$:	Engine Speed in RPM
P_{im}:	Intake Manifold Pressure
R:	Ideal Gas Constant
RMS:	Root Mean Square
T_{act} :	Actual Temperature to which the Sensor is exposed
T_{chg}:	Estimated Intake Charge Flow Temperature
VGT:	Variable Geometry Turbine

V_{disp}:	Engine Displacement (Liters)
η_{eff}:	Volumetric Efficiency
τ :	Sensor Time Constant

CHAPTER 1: INTRODUCTION

Modern diesel engines utilize highly developed charge airflow paths controlled by a number of advanced techniques. They include the use of intake throttle bodies, exhaust gas recirculation (EGR) valves with cooled and un-cooled by-pass flow paths, variable geometry turbines (VGT), and charge air coolers (CAC) which can condition intake charge airflow; all in an effort to increase power and efficiency, while still meeting ever more stringent emissions regulations (1) (2). Several methods of controlling and modeling of the intake charge flow reference the intake manifold temperature parameter (3) (4). Mean value engine modeling (MVEM), where complete combustion models of internal combustion engines (ICEs) are developed, is becoming more important as vehicle manufacturers investigate precise and efficient forms of combustion and emission control (5) (6) including calculating the mass air charge flow, or oxygen estimates in real-time (7). New combustion methods made possible by more powerful engine controllers are narrowing the gaps in achievable and desirable emissions (8) (9). Moving from directly from a universal theoretical model of an engine, to a deployable controller has become the preferred method of development. For engine air charge estimation the temperature parameter can be measured with a thermocouple placed directly in the manifold.

In ICEs, thermocouples are common measurement devices for determining temperatures, or for providing important diagnostic feedback. This method of measurement for intake charge flow is employed on European style inline 4-cylinder diesel engines with single plenum intake manifold designs. Unfortunately, thermocouples have inherent limitations, besides the added cost of adding a new sensor or sensors in a production setting (10). While the measured temperature of a thermocouple exposed to steady state flows can be useful in calculating the intake charge flow air mass, in transient flow conditions the temperature measurement often lags behind the actual temperature of the flow itself. In addition, larger V8 engines can have complex physical manifold layouts that make the actual temperature distribution of the flow in the manifold difficult to measure in production settings. The desire to eliminate unnecessary or difficult to implement sensor components and reduce the number of calibration hours on modern vehicles has lead to the development of new estimation and control techniques (11) (12) (13).

The temperature parameter can also be used in the control and estimation of the EGR fraction of gas in the intake manifold. The EGR fraction effects both smoke (particulate) and NOx formations in the engine (14) (15) (16). Accurate control of the EGR fraction and its corresponding temperature effect on the engine can lead to better emissions and fuel economy in the engine (17) and directly effects the amount of usable oxygen in the intake manifold (18) (19). The manifold pressure state equation is another commonly used algorithm in modeling and requires the intake manifold temperature to accurately estimate the manifold filling dynamics (20).

This report assesses an estimate algorithm used for the state estimation of the intake manifold charge flow temperature variable to facilitate in the calculation and control of a diesel engine in conjunction with the models mentioned. The layout of the next generation LML style Duramax V8 engine makes it desirable to estimate the temperature without the use of an intake manifold mounted thermocouple in production, given the deviations in manifold style from the original Duramax 6600 Diesel (21). A production ready fresh air thermocouple is already mounted downstream of the charge air cooler to measure the temperature of the fresh air mixture coming into the manifold for diagnostic purposes (see Figure 1). An additional thermocouple measures the temperature of air leaving the EGR cooler/by-pass valve, also originally for diagnostic purposes. Fusing the inputs of these two sensors with that of other production sensors provides an estimate of the intake manifold charge flow temperature after mixing of the EGR cooler air and the fresh air.

Evaluation for the algorithm is performed using Matlab and Simulink in conjunction with test data gathered on test cell D217 for an LML style Duramax Diesel engine. Final testing is performed on a rapid prototyping system. The application is intended for use on the 2015 Model Year (MY) engine.

TOTAL CHARGE MASS FLOW

The total charge mass flow calculation (Equation 5 below) was evaluated using two different methods. The primary estimate was done assuming constant Cp and Cv (Const R). This assumption proved reasonable based on the analysis of the secondary model that used a variable R. It should be noted that the temperatures observed in the intake were of relatively low temperature (<180°C) facilitating the assumption of constant Cp and Cv. Figure 9 shows the two calculations being done in parallel for model comparison.

$$\dot{m}_{tot} = \left(\frac{P_{im} \times N_{Eng.spd} \times \eta_{eff}}{T_{chg}}\right) \times \frac{V_{disp} \times 100}{60 \times 2 \times R}$$

Equation 5 Total Charge Mass Flow

One major limitation to both of these estimates was the reliance on a calibrated volumetric efficiency table for the final estimate.

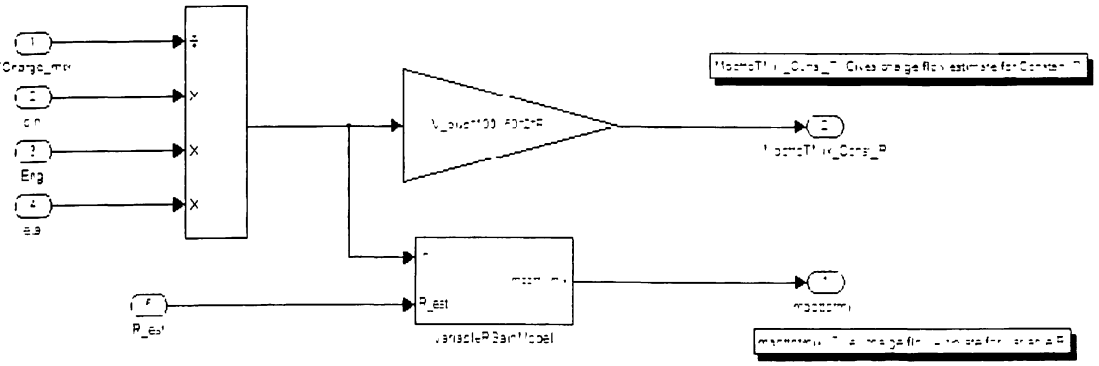

Figure 9: Cylinder Mass Flow Estimation

The variable R cylinder mass flow estimation utilizes a previous value of R determined in the last time step, since R is based on EGR fraction on the intake, assuming there is a negligible change over a small step size. If the time step size is to large, this assumption becomes less accurate.

EGR FRACTION ESTIMATION

The EGR Fraction estimate is performed based on the difference between the Mass Air Flow sensor reading and the estimated total cylinder charge flow. The estimation of the EGR Fraction is not trivial and has a very large effect on many other engine parameters as seen in many MVEMs (28) (29). This method of estimation requires that the previous estimate of the cylinder charge mass flow is accurate. Checks are done (see saturation blocks and EGR valve position input in Figure 10) to prevent unsteady behavior during low circulation values. When the EGR valve is closed the EGR fraction is set to zero.

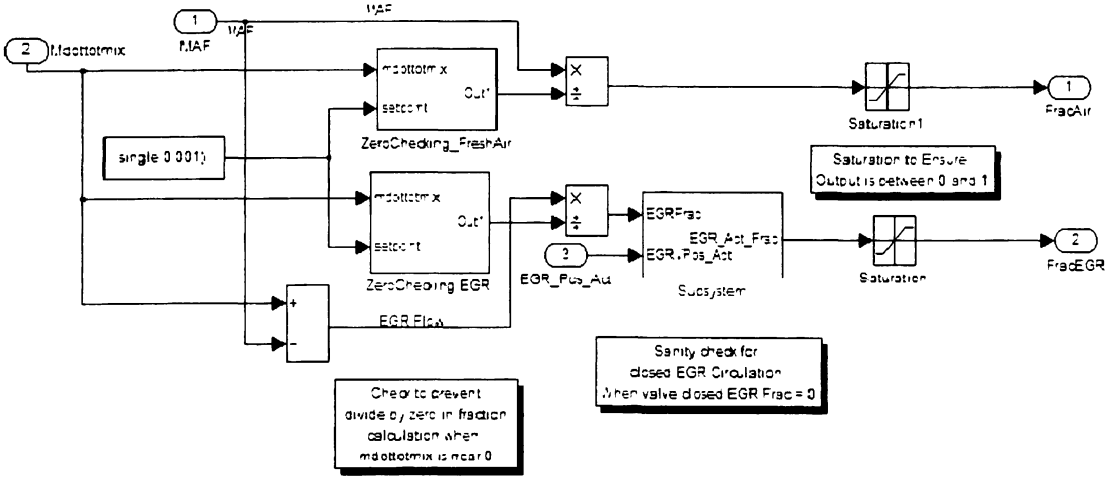

Figure 10: EGR Fraction and Air Fraction Calculation

The EGR fraction could alternatively be estimated by a look-up table based on the known mass flow of the EGR under certain operating conditions (fuel and speed) and valve positions (30). The valve flow can be approximated using common flow equations through an orifice. This method has drawbacks however, as EGR flow typically degrades with age, necessitating offset corrections overtime (31). A model of the exhaust gas pressure combined with the known pressure drop across the EGR cooler and by-pass valve would be beneficial in estimating the actual flow into the intake. As mentioned above, in the development model, EGR position is used only as a diagnostic check to ensure that when the valve is closed, the EGR fraction becomes zero.

MAF DELAY CALCULATION

Depending on engine speed and the full volume of the engine air intake system, there can be a measurable delay between the time the air mass from the mass airflow sensor reaches the mixture point in the manifold. To account for this delay a subsystem was created to estimate this time and implement a variable delay. The block uses Equation 6 to estimate the delay time based on the known volume of the intake and the engine speed.

$$MAF_{Delay} = \frac{N_{Eng.Speed} \times \frac{2}{60} \times \eta_{eff} \times \frac{V_{disp}}{8}}{V_{INTAKE}}$$

Equation 6 MAF Intake Manifold Delay

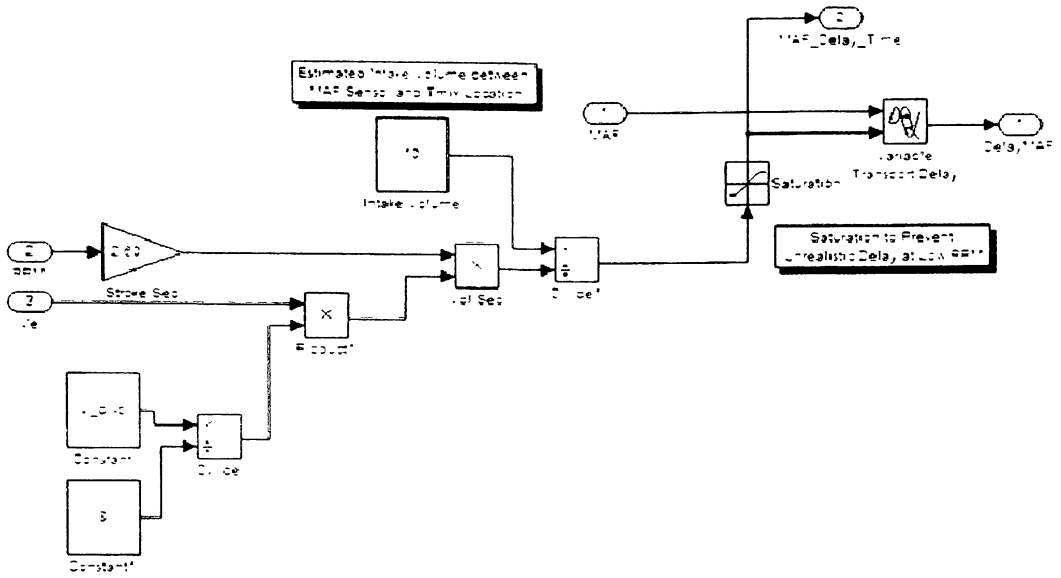

Figure 11: MAF Delay Calculation

Figure 11 above shows the method for calculating the delay. This could also be implemented as a 1-D lookup table based on engine speed. For the purposes of this study, it was important to minimize the amount of calibration needed; therefore, a theoretical relationship is used. The system can be tuned by adjusting the volume parameter for the intake in Equation 6. For the Duramax, the intake volume was estimated based on the physical dimensions of the dynamometer test cell intake system. The production vehicle system may contain a different final airbox and intake track length.

TEMPERATURE CORRECTION CALIBRATION

The final step in the calculation of the intake charge temperature is to account for the heat transfer across the intake manifold, and to calibrate the estimate to actual test cell data.

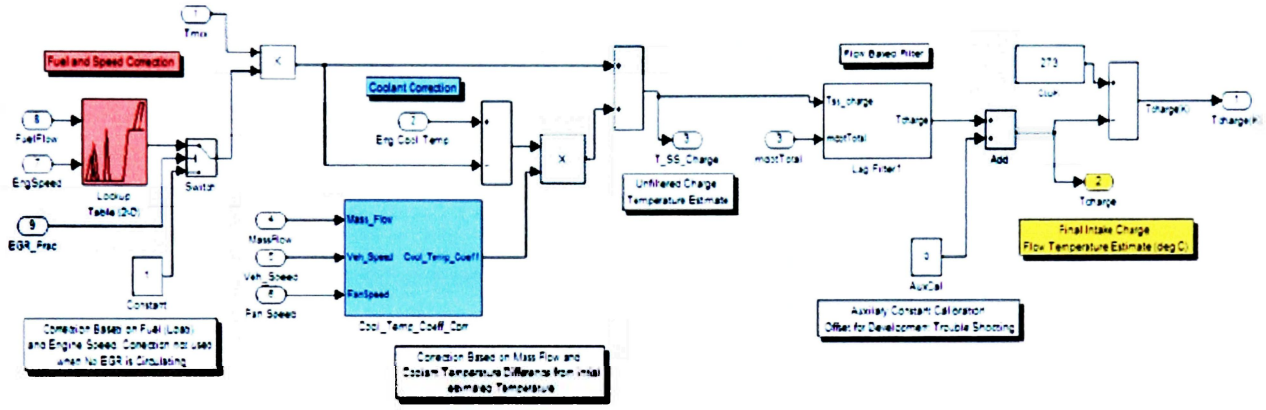

Figure 12: Temperature Correction and Calibration Factors

Figure 12 shows the several stages involved in calculating the final charge temperature estimate. The first section consists of a 2-D lookup table based on engine speed and fuel flow. The second stage is to account for the heat transfer across the manifold based on the difference between the engine coolant temperature and the initial mixture temperature estimate (the engine is assumed to initially be heat soaked to this temperature). Vehicle speed, cooling fan influence and other ambient effects are taken into account in this stage. The coolant correction block utilized a 1-D lookup table for cell testing, however an integrated 2-D table is also provided. The 2-D table references the vehicle speed and fan-operating condition to provide a gain to the coolant correction factor. For this application, it is assumed that airflow through the engine

compartment with the vehicle moving, or the fan operating will be greatly influenced by the coolant temperature due to heat rejection to the air across the radiator as well as the coolant channels near the engine intake manifold. There is an additional lag filter for smoothing the output signal as necessary based on the flow rate, and an auxiliary constant offset calibration parameter for development model testing.

UNIVERSAL GAS CONSTANT ESTIMATION

As EGR rate increases, the intake charge flow percentage of O_2 decreases. Figure 14 below shows a simplified model of the intake charge speciation based on the amount of EGR Fraction in the charge. This model was established based on work performed by Ladommatos in (18). It is assumed that the initial charge is simply fresh air, with mostly nitrogen and oxygen. As EGR use increases, the charge tends towards that of the burned mixture of carbon dioxide, and water, in addition to the nitrogen and oxygen already present. It can be seen in Figure 15, which is the calculated R-value based on the percentage of gas distribution in Figure 14, that the value is dominated by the relatively unchanging nitrogen composition in the mixture. These models were implemented in the Simulink system as a simple 1-D Lookup table as seen in Figure 13.

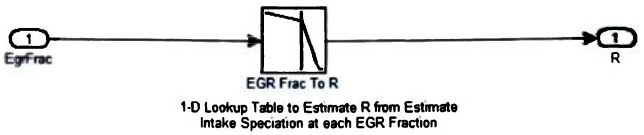

Figure 13: 1-D Lookup Table for R

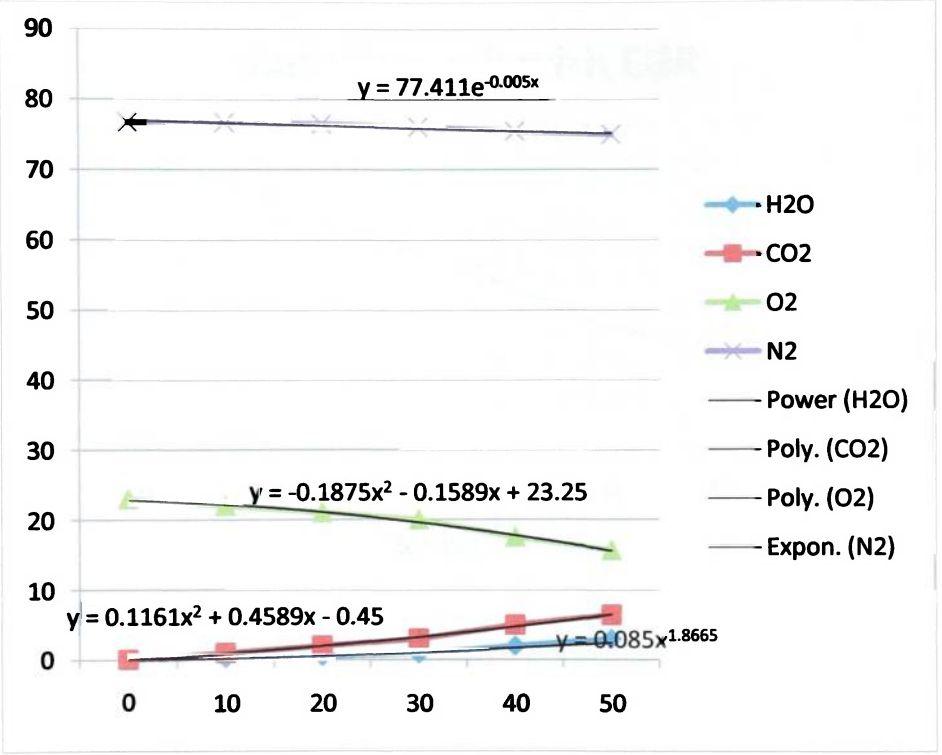

Figure 14: Variation of Speciation with Changes in EGR

Figure 14 above is a plot of the intake charge airflow species for a diesel engine based on simplified combustion parameters for the re-circulated exhaust gas mixture. The intake charge is primarily dominated by Nitrogen, with decreasing amounts of Oxygen, and subsequently increasing amounts of Carbon Dioxide as the EGR fraction increases.

The effect of these speciation amounts is seen in Figure 15 below. As the EGR fraction increases, the value of R changes by only a small percentage, indicating this may not be an important factor in the overall temperature estimation strategy. This was confirmed by testing on the dynamometer in the test cell as seen in Chapter 3.

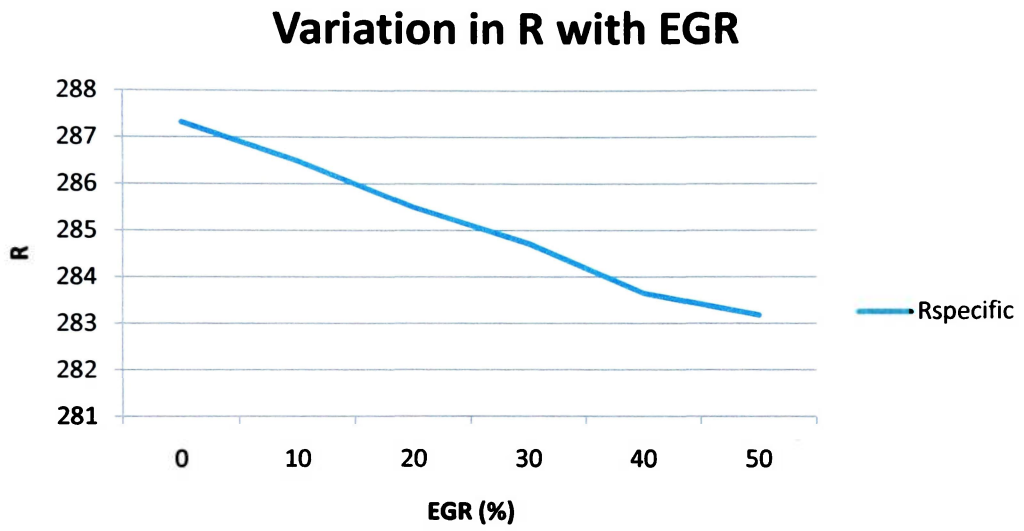

Figure 15: Variation of R with EGR

CHAPTER 3: RESULTS AND ANALYSIS

The baseline model was evaluated over a steady state cycle with step changes as seen in Figure 16. The model showed it could accurately predict trends in temperature changes; however, with no heat transfer outside of the gases, there was a large offset in the estimate.

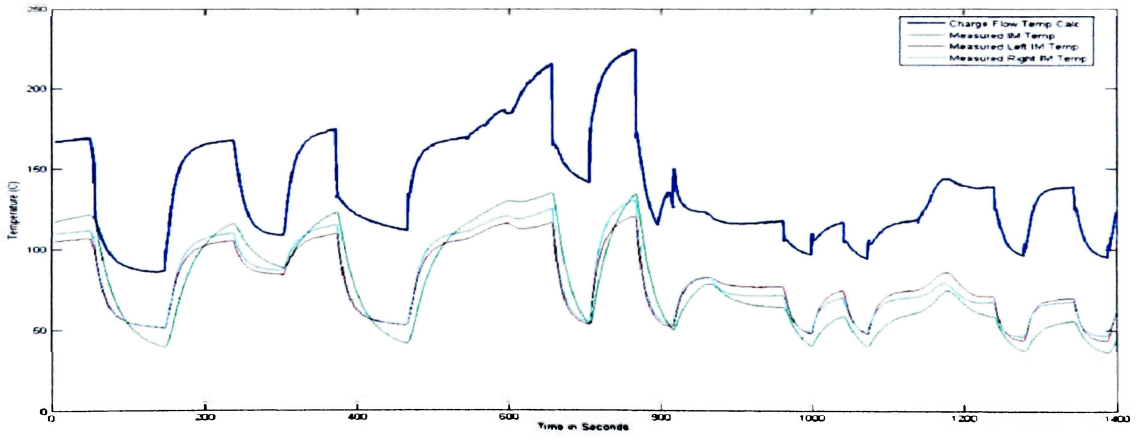

Figure 16: Initial Steady State Charge Flow Temperature Estimation

Similarly, as seen in Figure 17 the FTP cycle analysis showed varying offsets that illustrated the need for heat transfer corrections.

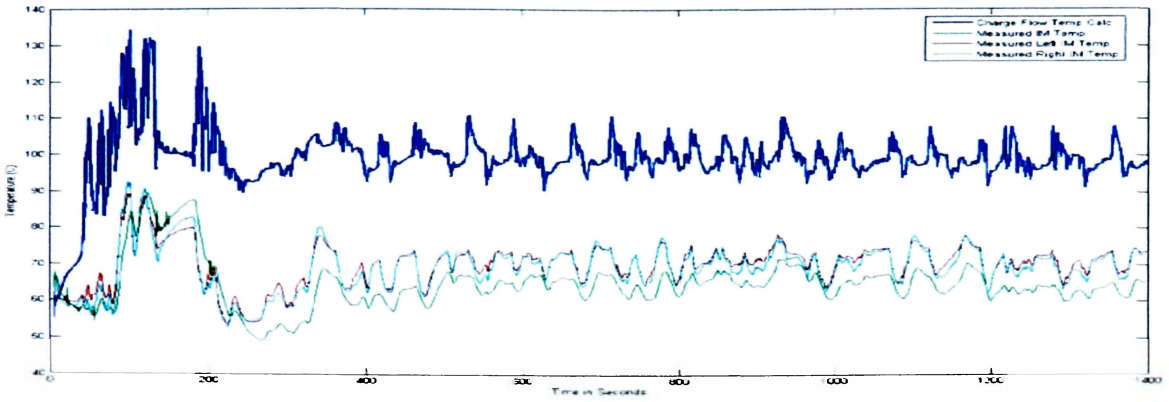

Figure 17: FTP75 Charge Flow Temperature Estimation

TEMPERATURE SIGNAL RESOLUTION

Regardless of the offset present, increasing the resolution of the available thermocouple temperature sensor signals was required. The results of the three signal enhancement methods are seen in Figure 18 below. All three methods are capable of providing a predicative trend through which the magnitude of the gain of the sensor input can be adjusted by varying constants in the algorithm. If the signal is reconstructed beyond a certain point, it becomes difficult to distinguish the actual signal from noise present. This has been studied in detail in other reports (32) (33) (34). As seen in Equation 3, the time constant of the sensor has a direct relationship on the estimate, and it is important that this time constant be adjusted to the appropriate value for each sensor. Evaluating the exact time constant of the sensor can also been done in real-time, but often methods call for two sensors in similar locations as in (32) to accurately estimate their behavior.

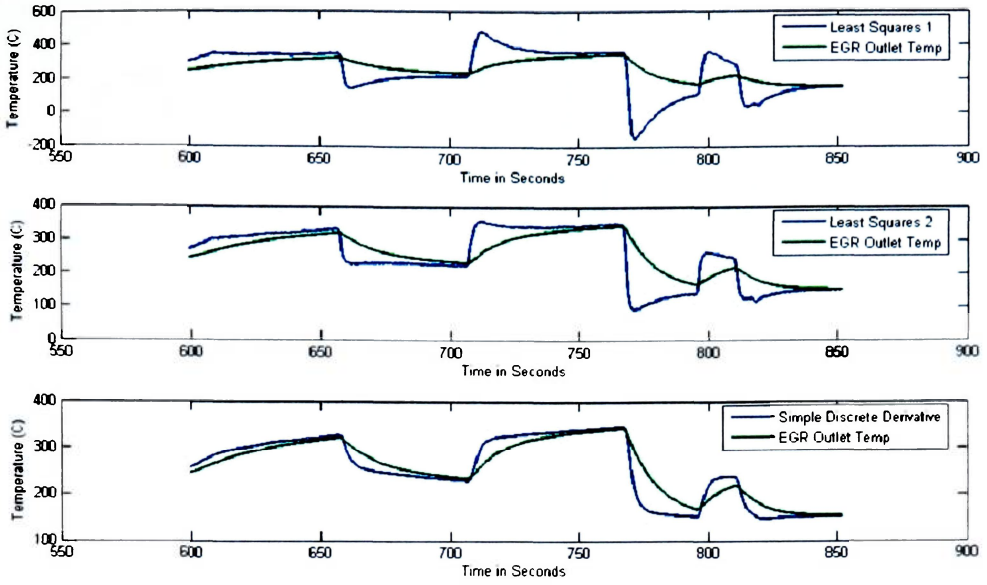

Figure 18: Temperature Sensor Enhancement

CHARGE FLOW SPECIFIC HEAT CORRECTION

The results of the variable gas constant correction versus EGR fraction were negligible in terms of overall temperature estimation strategy. Figure 19 below illustrates the minimal change seen. The effect is greater under very high EGR ratios. The maximum deviation observed between the two estimates over an FTP cycle was 0.7°C.

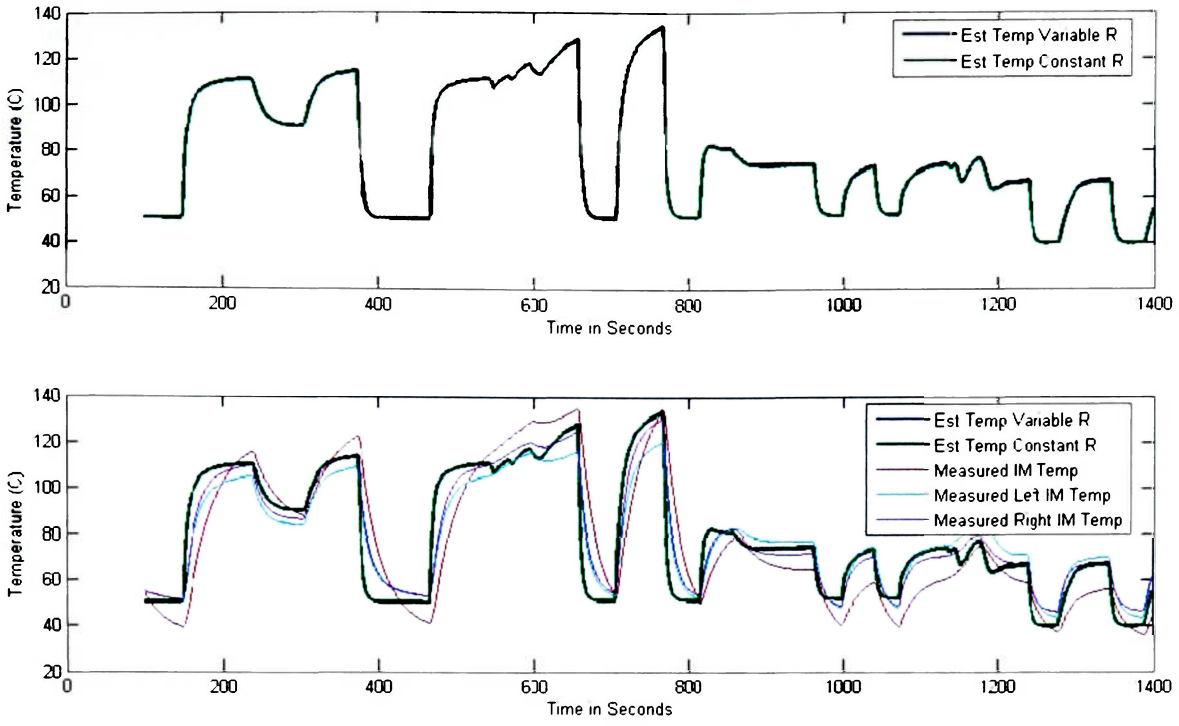

Figure 19: Effects of R Variation on Charge Flow Temperature Estimation

TRANSPORT DELAY CORRECTION

The MAF delay calculation, performed as expected, but like variable R, the effects on overall temperature estimation is minimal. Figure 20 demonstrates the capabilities of the MAF delay block. Calibrated to provide small changes in the estimate of the total calculation, it is not seen as necessary adjustment, given the noise and inherent variation in the manifold. However, if hardware memory and processing power are not limitations, it is a valid correction to the estimate.

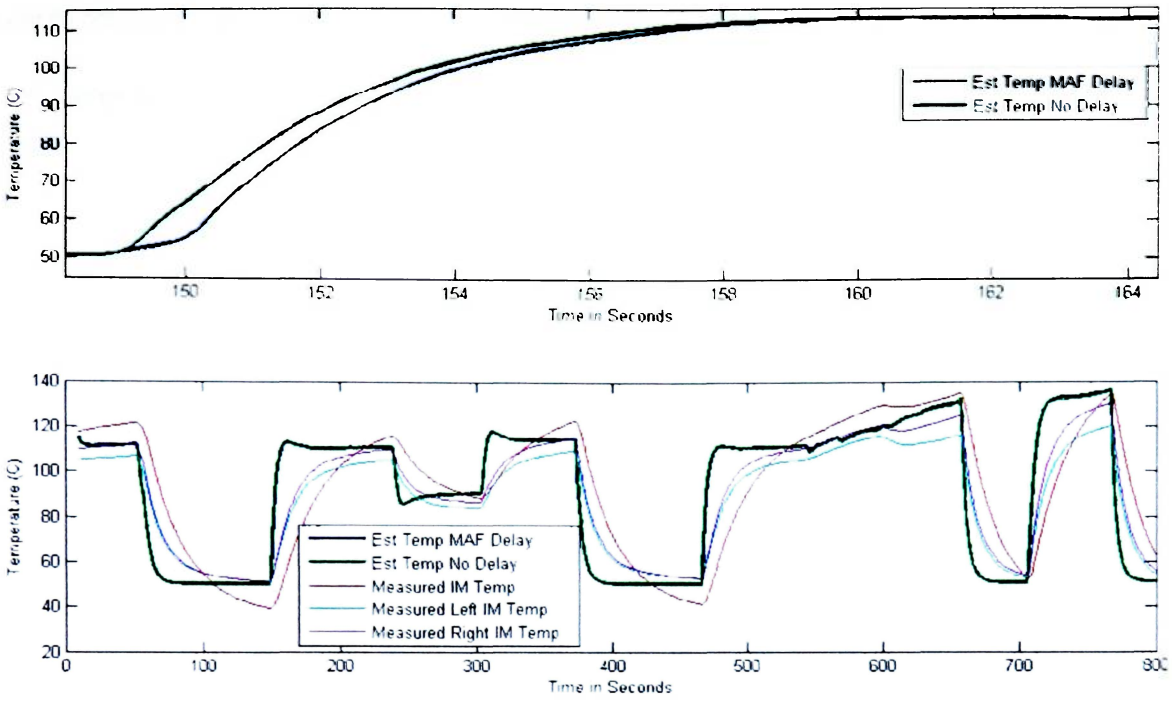

Figure 20: Mass Air Flow Sensor Delay

HEAT TRANSFER THROUGH INTAKE MANIFOLD

Heat transfer in an engine model is commonly broken into 4 sections: intake line, in-cylinder, exhaust port flow, and exhaust line flow (35). For the intake charge flow air temperature estimation the intake line heat transfer is simplified into a series of correction factors to the original mixture temperature. The heat transfer correction is the effect of the engine manifold temperature on the overall flow temperature. Mixing occurs well into the manifold; in addition, it was assumed initially that the manifold in a stationary vehicle is relatively near the coolant temperature. The correction can be seen below in Figure 21. After t = 800s the correction does not bring the temperature

fully in line with the measurements however. To correct for this offset the fueling correction was implemented.

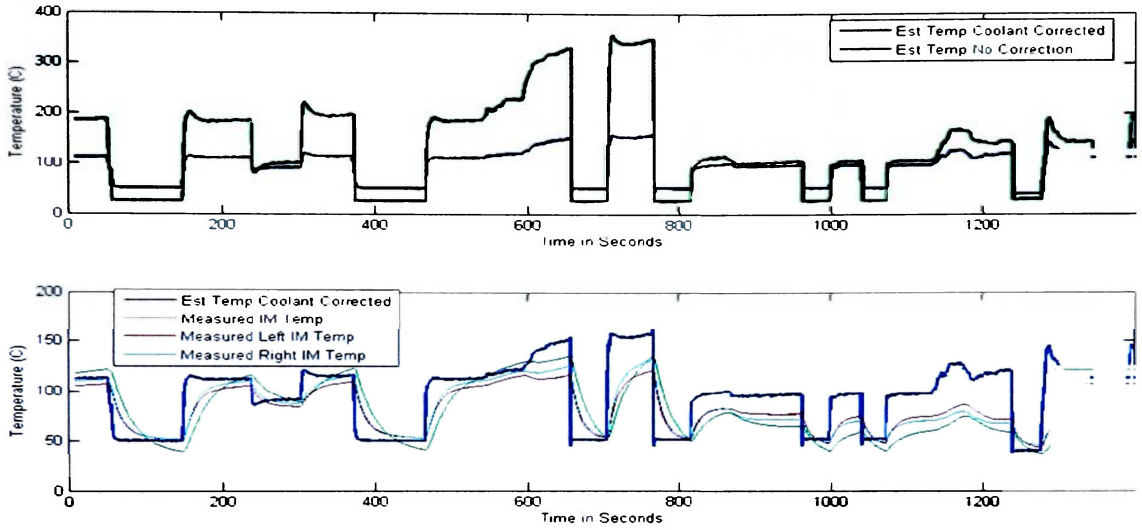

Figure 21: Coolant Correction

ENGINE LOAD CALIBRATION CORRECTION

Figure 22 shows a final estimate for the Charge Flow Temperature based on the correction factors applied above, and an additional correction for fuel/load and speed. Engine load, and exhaust pressure can have significant impacts on the upstream cylinder air charge, as seen in (36). The estimate leads the actual sensor readings, and falls in line with the variation between the measurements.

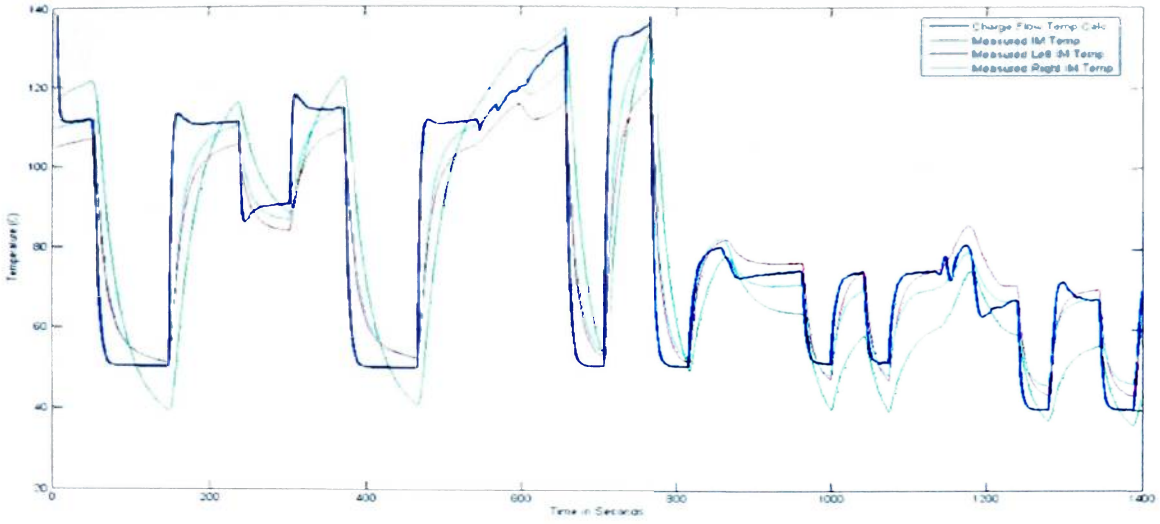

Figure 22: Steady State Charge Flow Temperature Estimation

Perhaps more importantly, the FTP cycle analysis, like that seen below in Figure 23, Figure 24, and Figure 25 shows a high degree of repeatability over cycles. This repeatability is critical if the estimate is to be considered for further calibration and production use.

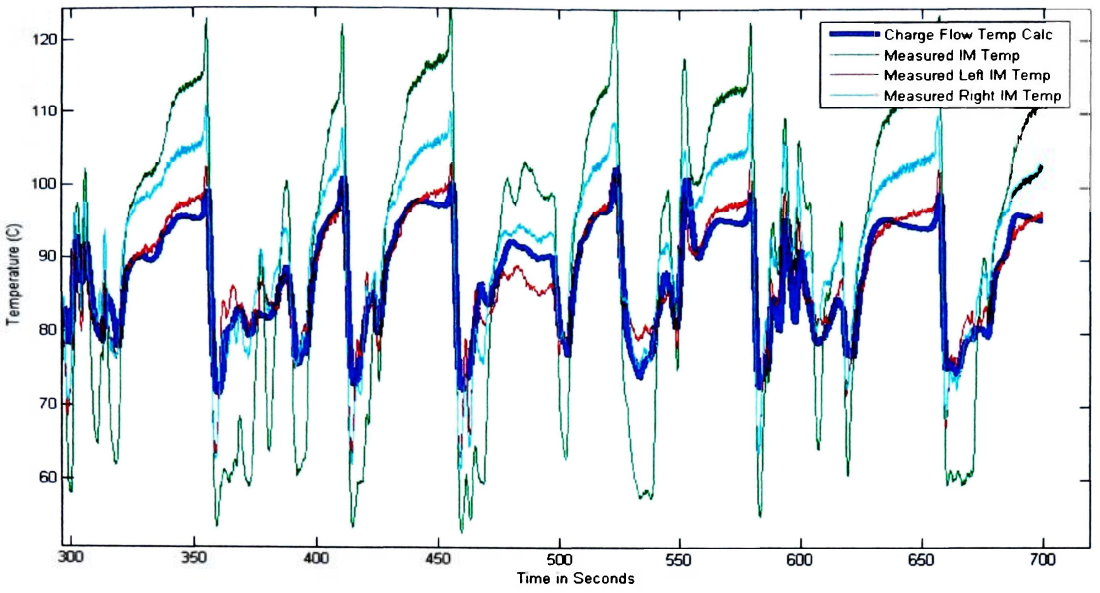

Figure 23: FTP Charge Flow Temperature Estimation

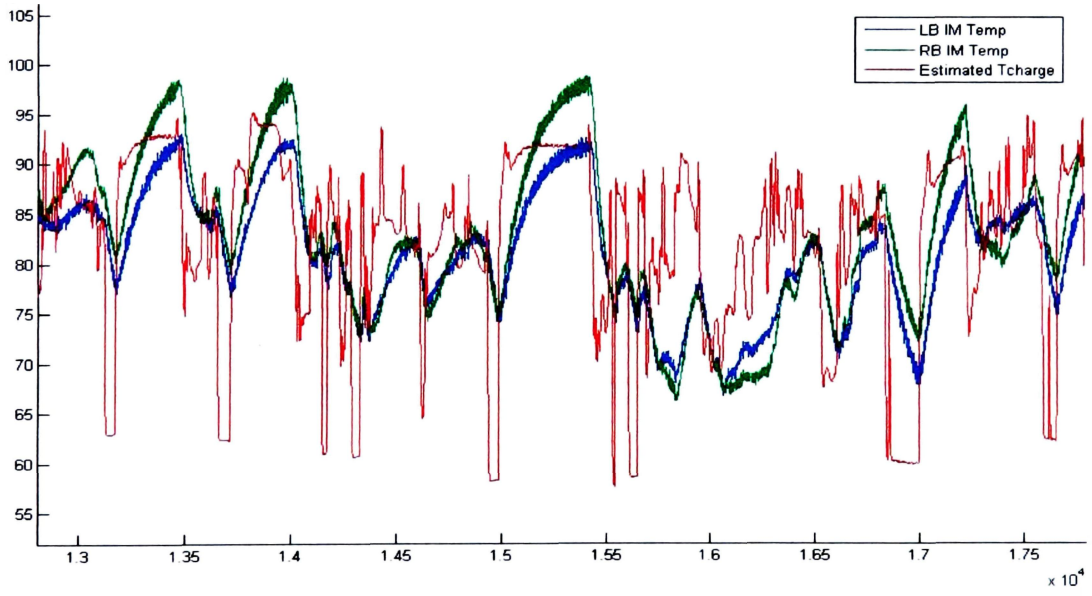

Figure 24: Estimated Tcharge over FTP72 on E41 O2 Model

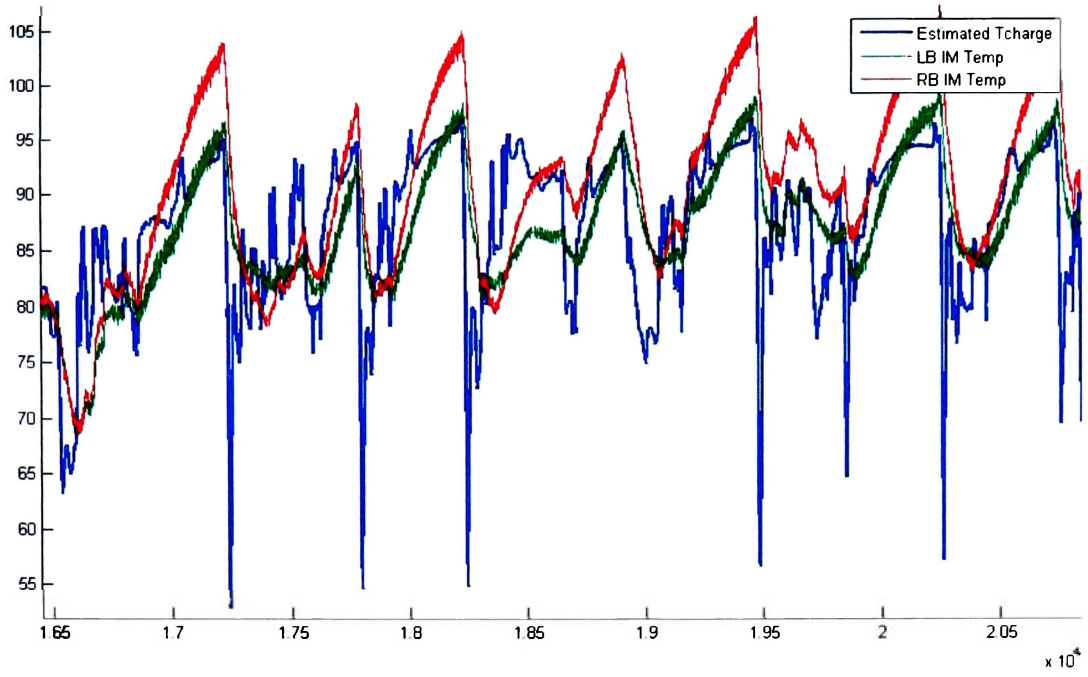

Figure 25: Estimated Tcharge over FTP72 on E41 MAF Model

Figure 24, an FTP cycle utilizing the O_2 control method, and Figure 25, utilizing the more traditional MAF control method, represent the estimated temperature as given by the rapid prototyping system run in D217 over several test cycles. There is a useable estimate of the temperature at this point. The spikes in the estimated temperature indicate areas where the resolution of the estimate is much greater than the resolution of the sensor. The thermocouples filter short duration temperature step changes (green and red lines in Figure 25), while the model estimate is able to fuse data from other areas, such as the EGR position and MAF sensor, to better estimate the higher rate of change temperature profile (blue line).

Table 1 Qualitative Analysis of Charge Flow Temperature Model

Model System	Processing	Memory	Repeatability
Baseline	Lo	Lo	Lo
Variable R	Lo	Medium	Lo
MAF Delay	Lo	Lo	Lo
Thermocouple Correction	Hi	Medium	Medium
Coolant Correction/Vehicle Speed	Medium	Hi	Medium/Hi
Fuel/Eng. Speed Correction	Lo	Hi	Hi
Full Model	Hi	Hi	Hi

Table 1 shows the processing and memory requirements versus the overall repeatability of the development model with respect to the baseline model of the intake charge mixture without heat transfer. The model baseline (without heat transfer) has the least reliable estimate of temperature, but also the lowest processing and memory requirements. Both the MAF delay calculation and the variable R correction have minimal impacts on the baseline models reliability. The Full model, which incorporates all of the corrections to date, is considered the most repeatable, but inherently the highest hardware requirements.

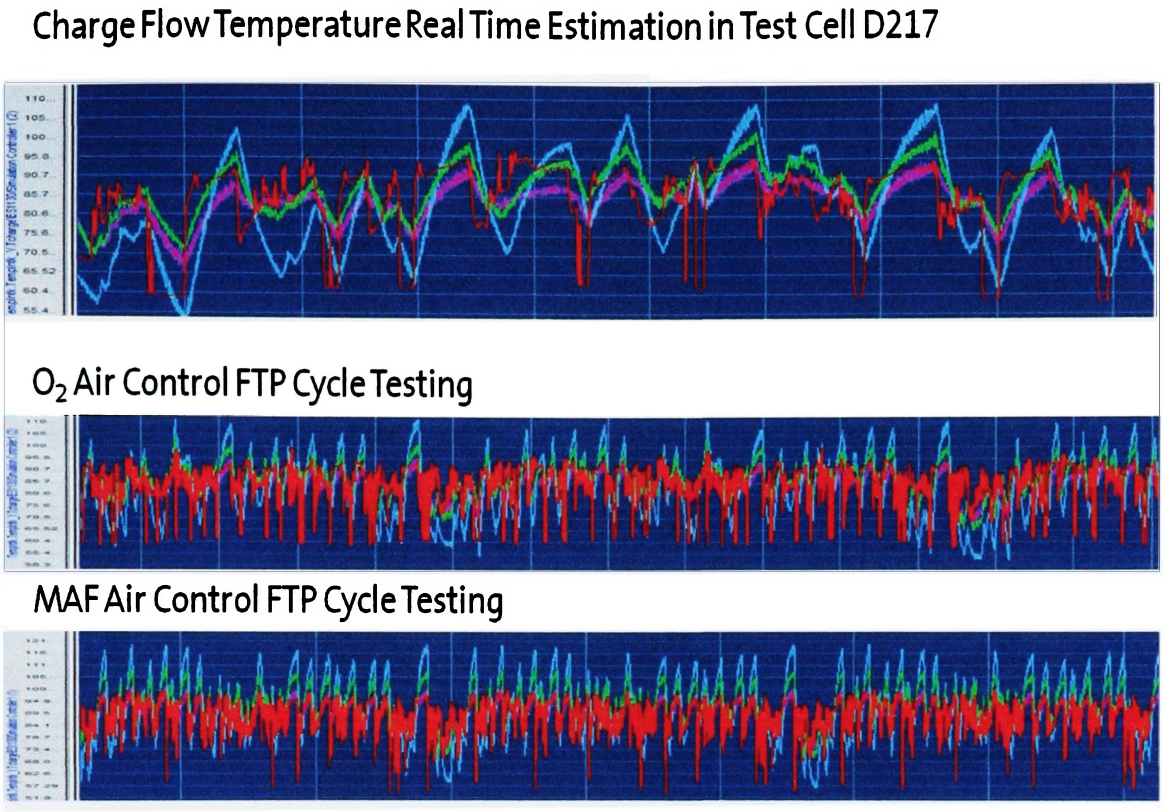

Figure 26: FTP Cycle Validation

Figure 26 above shows several cycle tests for the charge flow temperature estimate. The red line indicates the estimate, while the blue, green, and pink are the auxiliary sensor measurements. It can be seen in the top graph that with the estimate it is possible to estimate temperature spikes/steps that would otherwise be filtered out by the thermocouples.

See APPENDIX B for continued discussion on the tests performed.

CHAPTER 4: CONCLUSION AND RECOMMENDATIONS

As shown early on, heat transfer in the intake manifold can greatly affect the estimated temperature of the charge flow mixture. No calibration has been done for a moving vehicle, but it is expected to be a large factor in the final model as seen in (37). In the test cell, the ambient temperature exposure of the manifold is for all practical purposes a constant after the engine has warmed to operating temperature. In addition, the engine's charge air cooler is being artificially conditioned since, it is not in a moving vehicle, and as such, the CAC Outlet temperature remains mostly constant (see Figure 38 in Appendix B). Additionally, for this model, only three thermocouples were observed in the intake manifold, it might be beneficial to study individual intake manifold port temperatures to gain a more developed estimate of the temperature distribution across the manifold. Installing a secondary thermocouples very close to the existing as described in (32) would aid in validating the thermocouple estimation strategies beyond what was explored in this paper.

It has also been observed that the effects of some of the corrections are small in relation to the overall estimate. Namely the variation in R as a result of EGR recirculation, and the delay caused by the location of the MAF sensor relative to where

the actual mixing occurs. A possible reason may be the time involved in the charge mass transport is relatively small between the MAF and mixing location when compared to the overall thermocouple time constant. Enhancing the thermocouple response mathematically has noise limitations, so it is difficult to verify model the model accuracy over very short periods. Based on the cycle analysis performed, it has been shown that under the conditions tested, there is good repeatability in the temperature estimate with and without these corrections applied.

Another seemingly obvious discovery was the importance of the EGR charge temperature sensor location for engines with by-pass cooling valves. Early Duramax engines equipped with EGR by-pass cooling valves have diagnostic thermocouples mounted out of range of the non-cooled flow. When by-passed the thermocouple in these instances provides readings that do not indicate the flow moving into the intake. Therefore, this model is not recommend for application on these early engines. It is critical that the sensor be located in a position that can measure both the EGR Cooler outlet gas temperature and the EGR Cooler By-Pass outlet gas temperature. In addition, the EGR fraction estimation is a recursive calculation, so it is a possible location for instability in the model. This may occur in such a situation, when the reading varies significantly from the actual flow into the intake.

From PSR-173 (38) (eq. 20) we can see that it is difficult to estimate the EGR gas temperature over a range of operating conditions, but it would be beneficial to test the

enhanced temperature estimates from the sensors against a more developed model of the EGR charge temperature. A theoretical model of both the CAC Outlet temperature and the EGR Outlet Temperature would allow for a more accurate calibration of the transfer function being used in the sensor enhancement estimates. Current implementation focused on the use of minimum controller resources, for implementation, but this does not preclude future validation with MVEM.

Overall, the temperature estimate described by GM R&D and the model seen here both show a similar capability of reliably calculating an estimate for the intake manifold temperature. Unfortunately, a high degree of calibration may be necessary, depending on the accuracy desired in the estimate. A theoretical model of the heat transfer along the Duramax LML intake manifold would alleviate some of this calibration need, but given the complexity of the external intake manifold flow conditions, this would be difficult to implement. In addition, future design changes to the manifold would lead to offsets in the external heat transfer model, again necessitating calibration.

As mentioned at the time of this report, there are several conditions that remain to be tested, mainly those relating to actual on vehicle testing. Based on the extent of research and testing performed to date, there is a high degree of confidence that calculating a consistent estimate of the intake manifold charge flow temperature without the explicit use of a directly mounted intake manifold temperature sensor is achievable. It is still necessary to calibrate the estimate for specific applications, and

locations on the manifold. Further on vehicle testing is required to fully validate the model created, specifically, the impact of extreme variations in CAC Outlet temperature should be tested on the vehicle.

Since future implementation of this model is directly applicable to the control of engine air charge flow estimation, checks have been implemented, such as the input of actual EGR valve position, and saturation limiters, to minimize the impact of out-of-range values, but these should not be consider fully robust at this point. The sensitivity of the overall intake cylinder charge flow oxygen estimate and MAF model of cylinder charge mass flow to the intake charge flow temperature algorithm developed in this model has been observed to be low, but should also be studied further before implementation.

If it is possible to place one or multiple temperature sensors on the production engine to measure the intake charge flow temperature, it may still be desirable to implement the above algorithm as a diagnostic. Alternatively, where faster temperature response is needed, the model may be used as the primary estimate, where as the sensors become diagnostic/drift monitors to correct deviations over time due to EGR cooler fouling (31) or out-of-range algorithm estimates.

In summary, the state estimation model of the intake manifold charge flow temperature using the fusion of existing production sensors on the Duramax LML Diesel engine was tested using model based design techniques in conjunction with rapid prototyping

systems. Validation was performed using test cell instrumentation at General Motors Global Powertrain Headquarters in Pontiac, MI and the final model was presented and approved by the Diesel Combustion and Emissions Control group, with oversight by the Powertrain Product Development group, and recommended for production in the 2015 MY vehicle controllers.

(15)

REFERENCES

1. *Coordinated EGR-VGT Control for Diesel Engines: an Experimental Comparison.* **van Nieuwstadt, M. J., Kolmanovsky, I. V. and Moraal, P. E.** Detroit, MI : SAE International, 2000. 2000-01-0266.

2. *Boost and EGR System for the Highly Premixed Diesel Combustion.* **Buchwald, Ralf, et al.** Detroit, MI : SAE International, 2006. 2006-01-0204.

3. *Comparison of Different Transient Air Charge Models.* **Knaak, Mirko, Schoop, Ulrike and Roepke, Karsten.** Detroit, MI : SAE International, 2005. 2005-01-0051.

4. *Airpath Modelling and Control for a Turbocharged Diesel Engine.* **Bhushan Das, Himadri and Jabez Dhinagar, Samraj.** Detroit, MI : SAE International, 2008. 2008-01-0999.

5. *Measured Intake Temperature, BDC Temperature, and Combustion Phasing for Premixed and DI HCCI Engines.* **Sjöberg, Magnus and Dec, John.** Detroit, MI : SAE International, 2004. 2004-01-1900.

6. *The Effect of Intake Charge Temperature on Combustion and Emissions in an Optically Accessible DI Diesel Engine with and without Swirl.* **Solbrig, Charles E. and Litzinger, Thomas A.** Tulsa, OK : SAE International, 1990. 902060.

7. *Development and Validation of a 1D Model of a Turbocharged V6 Diesel Engine Operating Under Turbocharged V6 Diesel Engine Operating Under.* **He, Yongsheng.** Detroit, MI : SAE International, 2005. 2005-01-3857.

8. *Efficiency & Stability Improvements of Diesel Low Temperature Combustion through Tightened Intake Oxygen Control.* **Asad, Usman and Zheng, Ming.** Detroit, MI : SAE International, 2010. 2010-01-1118.

9. *Investigation of Mixing and Temperature Effects on HC/CO Emissions for Highly Dilute Low Temperature Combustion in a Light Duty Diesel Engine.* **Opat, Richard, et al.** Detroit, MI : SAE International, 2007. 2007-01-0193.

10. *Modeling of Sensor Performance During Engine Testing.* **Vávra, Jirí, et al.** Detroit, MI : SAE International, 2007. 2007-01-1299.

11. *Pneumatic and Thermal State Estimators for Production Engine Control and Diagnostics.* **Maloney, Peter J. and Olin, Peter M.** Detriot,MI : SAE International, 1998. 980517.

12. *Air Path Estimation on Diesel HCCI Engine.* **Chauvin, J., et al.** Detroit, MI : SAE International, 2006. 2006-01-1085.

13. *Low-Cost Air Estimation.* **Turin, Raymond, Dagci, Oguz and Chang, Man-Feng.** Detroit, MI : SAE International, 2009. 2009-01-0590.

14. *Reduction of Steady State NOx Levels from an Automotive Diesel Engine Using Optimised VGT/EGR Schedules.* **Hawley, J. G., et al.** Detroit, MI : SAE International, 1999. 1999-01-0835.

15. *Model-Based Control of the VGT and EGR in a Turbocharged Common-Rail Diesel Engine: Theory and Passenger Car Implementation.* **Ammann, M., et al.** Detroit, MI : SAE International, 2003. 2003-01-0357.

16. *Modelling Diesel Engine Combustion and NOx Formation for Model Based Control and Simulation of Engine and Exhaust Aftertreatment Systems.* **Ericson, Claes, et al.** Detroit : SAE International, 2006. 2006-01-0687.

17. *The Effects on Diesel Combustion and Emissions of Reducing Inlet Charge Mass Due to Thermal Throttling with Hot EGR.* **Ladommatos, N., et al.** Detroit, MI : SAE International, 1998. 980185.

18. *The Dilution, Chemical, and Thermal Effects of Exhaust Gas Recirculation on Diesel Engine Emissions Part 1: Effect of Reducing Inlet Charge Oxygen.* **Ladommatos, N, et al.** Detriot, MI : SAE International, 1996. 961165.

19. *Advanced EGR Control Concept for HD-Truck-Engines.* **Broda, Andreas, Rieping, Marcus and Eilts, Peter.** Detroit, MI : SAE International, 2008. 2008-01-1200.

20. *Modelling of the Intake Manifold Filling Dynamics.* **Hendricks, Elbert, et al.** Detroit, MI : SAE International, 1996. 960037.

21. *The Design and Concept of the Duramax 6600 Diesel Engine.* **Kerekes, Jim, Ohoka, Shinichi and Horada, Osamu.** Detroit, MI : SAE International, 2001. 2001-01-2703.

22. *Physics based diesel turbocharger model for control purposes.* **MARTIN, Guillaume, et al.** s.l. : SAE International, 2009. 2009-24-0123.

23. **Stolz, Michael.** Time- and Cost- Efficient Development with INTECRIO. *ETAS Group Automotive Life Cycle Solutions.* [Online] http://www.etas.com/data/RealTimes_2008/rt_2008_1_26_en.pdf.

24. *Air System and Diesel Combustion Model for a 4 Cylinder Engine in Real Time Computing Conditions: Application on a EU5 Personal Car with Diesel Particulate Filter.* **Millet, Jean-Baptiste, et al.** s.l. : SAE International, 2009. 2009-24-0136.

25. **GM Powertrain Electronics Integration and Software.** *Algorithm Changing Document for the Intake Temperatures Ring.* s.l. : GM Powertrain, 2009.

26. **Julien, Howard.** *Estimation of Thermocouple Error During Transient Gas Temperature Measurement: The Development of an Energy Exchange Model for Thermocouples in Gas Turbine Applications.* Gas Turbine Research Department, General Motors Corporation. Warren, MI : Research Labratories General Motors Corporation, 1972. GT-108.

27. *A Mean-Value Model for Estimating Exhaust Manifold Pressure in Production Engine Applications.* **Olin, Peter M.** Detroit, MI : SAE International, 2008. 2008-01-1004.

28. *Dynamic EGR Estimation for Production Engine Control.* **Müller, Martin, Olin, Peter M. and Schreurs, Bart.** Detroit, MI : SAE International, 2001. 2001-01-0553.

29. *Air Charge Estimation in Camless Engines.* **van Nieuwstadt, M. J., et al.** Detroit, MI : SAE International, 2001. 2001-01-0581.

30. *A Model for EGR Mass Flow Rate Estimation.* **Azzoni, P. M., et al.** Detroit, MI : SAE International, 1997. 970030.

31. *Direct Measurement of EGR Cooler Deposit Thermal Properties for Improved Understanding of Cooler Fouling.* **Lance, Michael J., et al.** Detroit, MI : SAE International, 2009. 2009-01-1461.

32. *Instantaneous Exhaust Temperature Measurements Using Thermocouple Compensation Techniques.* **Kar, Kenneth, et al.** Detroit, MI : SAE International, 2004. SAE World Congress. SAE 2004-01-1418.

33. *Estimating Actual Exhaust Gas Temperature from Raw Thermocouple Measurements Acquired During Transient and Steady State Engine Dynamometer Tests.* **Son, Seha and Kolasa, Arthur E.** Detriot, MI : SAE International, 2007. 2007 World Congress. SAE 2007-01-0335.

34. *Measurement of Exhaust Gas Temperatures in a High Performance Two-Stroke Engine.* **Kee, Robert J, et al.** Dearborn, Michigan : SAE, 1998. Motorsports Engineering Conference Proceedings. SAE 983072.

35. *Heat Transfer Model to Calculate Turbocharged HSDI Diesel Engines Performance.* **Luján, J. M., et al.** Detroit, MI : SAE International, 2003. 2003-01-1066.

36. *Cylinder Air Charge Estimator in Turbocharged SI-Engines.* **Andersson, Per and Eriksson, Lars.** Detroit, MI : SAE International, 2004. 2004-01-1366.

37. *Analysis of Thermocouple Temperature Response under Actual Vehicle Test Conditions.* **El-Sharkawy, Alaa E.** Detroit, MI : SAE International, 2008. 2008 SAE World Congress. SAE 2008-01-1175.

38. **Gangopadhyay, Anupam, Vennettilli, Nando and Maira, Massimiliano.** *Modification of GM R&D Diesel Intake Oxygen Model for D1 Product Implementation.* Powertrain Systems Research Lab. s.l. : GM Research and Development Center, 2007. PSR-173.

39. *A New Dynamic Combustion Control Method Based on Charge Oxygen Concentration for Diesel Engines.* **Nakayama, Shigeki, et al.** s.l. : SAE International, 2003. SAE International. SAE 2003-01-3181.

40. *Study of the Potential of Intake Air Heating in Automotive DI Diesel Engines.* **Payri, F, et al.** Detroit, MI : SAE International, 2006. 2006-01-1233.

41. *The Dilution, Chemical, and Thermal Effects of Exhaust Gas Recirculation on Diesel Engine Emissions - Part 4: Effects of Carbon Dioxide and Water Vapour.* **Ladommatos, N., et al.** Dearborn, MI : SAE International. International Spring Fuels & Lubricants Meeting. SAE 971660.

42. **GM Powertrain Electronics Integration and Software.** *Algorithm Description For Intake Charge Temperature Prediction.* s.l. : GM Powertrain, 2009.

APPENDIX A

DEVELOPMENT MODEL INPUTS:

AFS_dmSens - Mass Air Flow

VeEPSR_n_Lores - Engine Speed

VeFULC_V_FuelReq – Fuel Request

Airp_pIntkVUs – Intake Manifold Air Pressure

Air_tCACDs - Charge Air Cooler Outlet Temperature

Air_tEGRClr2Ds - EGR Cooler Outlet Temperature

Eng_Cool_temp - Engine Coolant Temperature

ECU_EGRVPOST_PCT EGR Valve Position

AirflowCorr - Vehicle Speed*

AirflowCorr2 - Cooling Fan Speed/Mode of Operation*

*Integrated but not currently being utilized

PRIMARY DEVELOPMENT MODEL OUTPUTS:

Tcharge – Intake Manifold Charge Flow Temperature (°C)

TchargeK – Intake Manifold Charge Flow Temperature (K)

VeEITR_r_Airfrac – Estimated intake air charge fraction

VeEITR_r_EGRFrac – Estimated intake EGR charge fraction

VeEITR_dm_Intaketotal – Estimated Total Mass Charge Flow

DEVELOPMENT MODEL CALIBRATION PARAMETERS:

Act_Sens_Time_Cnst1 = Charge Air Cooler Temperature Sensor Time Constant

Act_Sens_Time_Cnst2 = EGR Cooler Temperature Sensor Time Constant

CAC_TC - Vector for CAC Temperature sensor Time Constant Variation with Flow

EGR_TC – Vector for EGR Temperature sensor Time Constant Variation with flow

V_disp – Engine Displacement (L)

R – Ideal Gas Constant

EGRFracV – Vector for EGR Fraction Range

RVarV – Ideal Gas Constant 1-D Lookup Table Based on EGR Fraction

KnEITC_V_VolMetricCalBY – Volumetric Efficiency Fuel Flow Vector

KnEITC_n_VolMetricCalBX – Volumetric Efficiency Engine Speed Vector

KtEITC_r_VolMetricCall – 2-D Volumetric Efficiency Table based on Fuel and Speed

FuelSpeed – 2-D Table Used for Temperature Correction Based on Fuel and Speed

Mass_Flow = Vector for Mass Flow Range

First_Order_Lag_Coeff - 1-D Lookup Table for First Order Lag Filter based on Mass Flow

Veh_Speed – Vehicle Speed Correction Vector

Cool_Temp_Coef_1D – 1-D Lookup Table for Coolant Temperature Correction based on Mass Flow

Coolant_Temperature_Coefficient – 2-D Lookup Table Utilizing Mass Flow and Vehicle Speed for coolant correction

APPENDIX B

ADDITIONAL EVALUATION AND TESTING

The figures below represent some of the variability in testing and estimating the temperature as discovered over the course of the charge flow temperature model development.

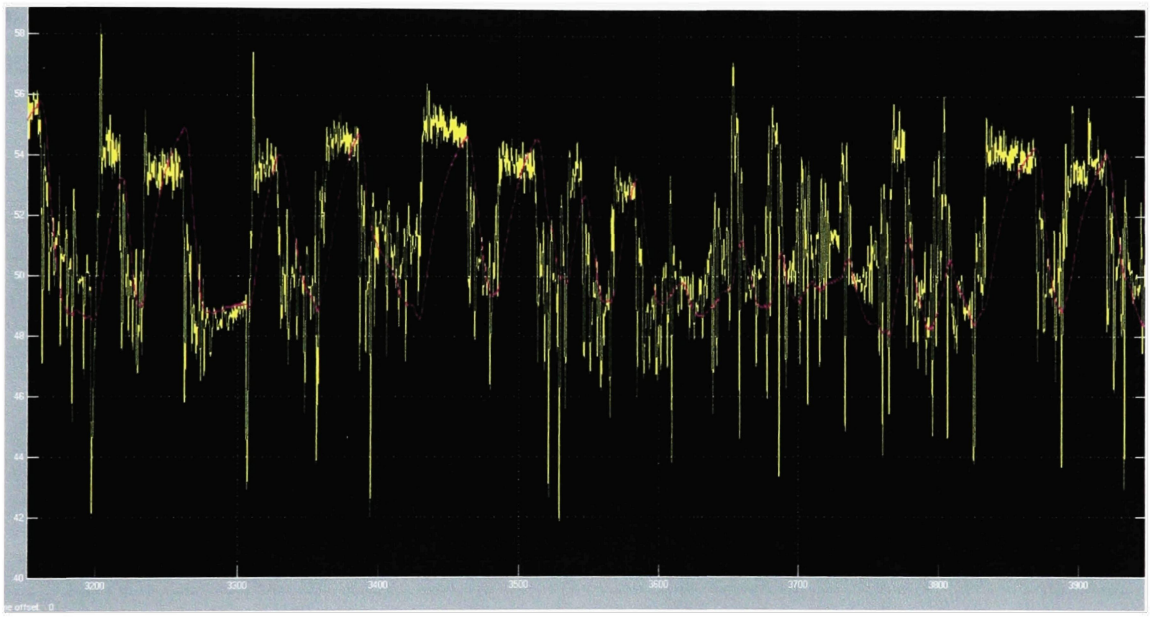

Figure 27: Measured Right Bank Intake manifold Temperature (Purple) vs. Time and Corrected Estimated Intake Manifold Temperature (Yellow)

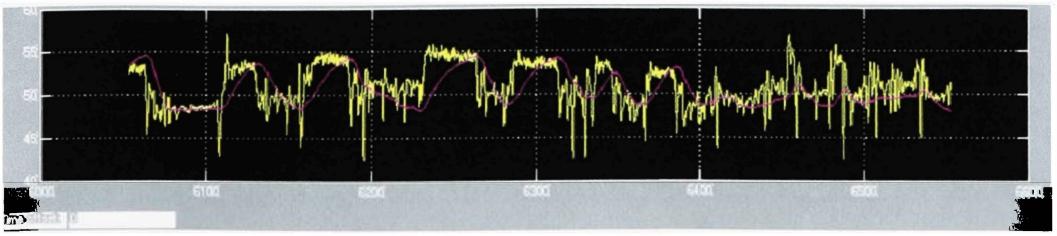

Figure 28: Calculated Temperature vs. Measured Temperature with Changing R

Figure 29: Calculated Temperature vs. Measured Temperature with Fixed R (287)

Figure 28 and Figure 29 show calculated temperatures for the Intake manifold temperature as compared to the measured. For both figures, there was zero EGR recirculation.

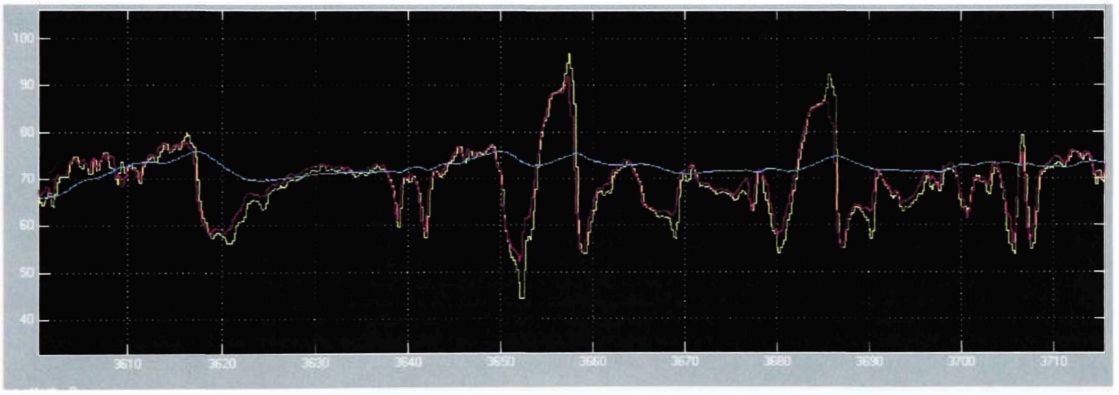

Figure 30: Tmix Temperature Estimation

Figure 30 shows the measured left bank intake temperature measurement (blue) as compared to the original (pink) and enhanced (yellow) temperature estimations. In Figure 31: Tcharge Temperature Estimation, the corrected value is shown after a correction for cooling and a lag filter. The unfiltered Tmix is being used for the recursive calculation.

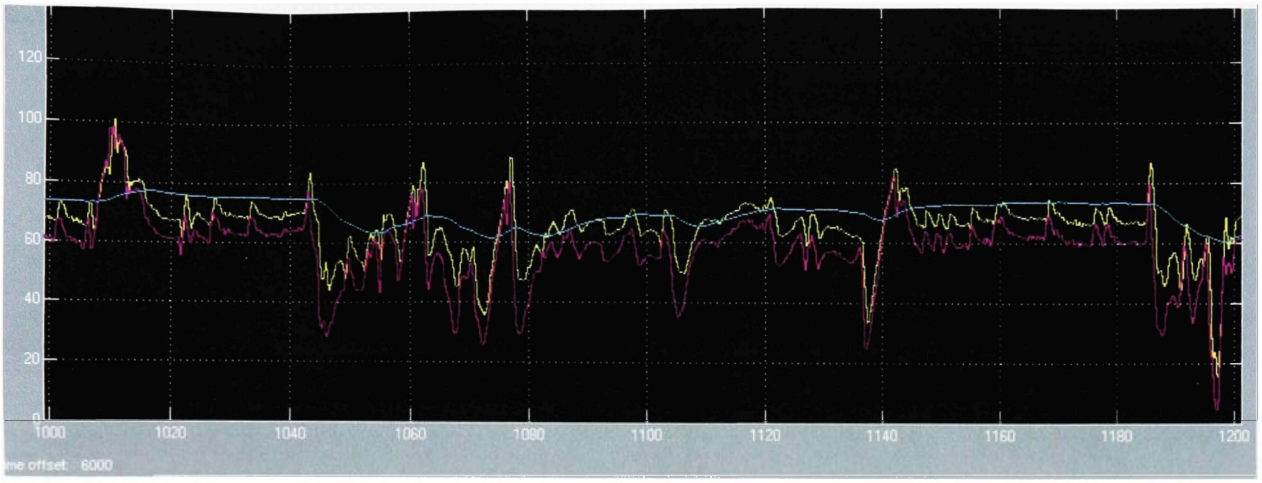

Figure 31: Tcharge Temperature Estimation

Figure 31 shows the measured left bank intake temperature measurement (blue) as compared to the original estimate of Tmix (pink) and the corrected calculated Tcharge estimate(yellow) . In this case, the Tcharge component is being used for the recursive calculation. From this point, the model was further developed by the following criteria:

- Find Temperature time constants from step response (~7-8 seconds on EGR)
- Develop Lead-Lag Filter coefficients
- Sensitivity Analysis –Effects of Drift on P,M,T, gamma
- Intake Mass Flow – volumetric flow rates (estimate volume) vs. speed
- Fan operation set points
- EGR off Operation Flag (Sanity Check)

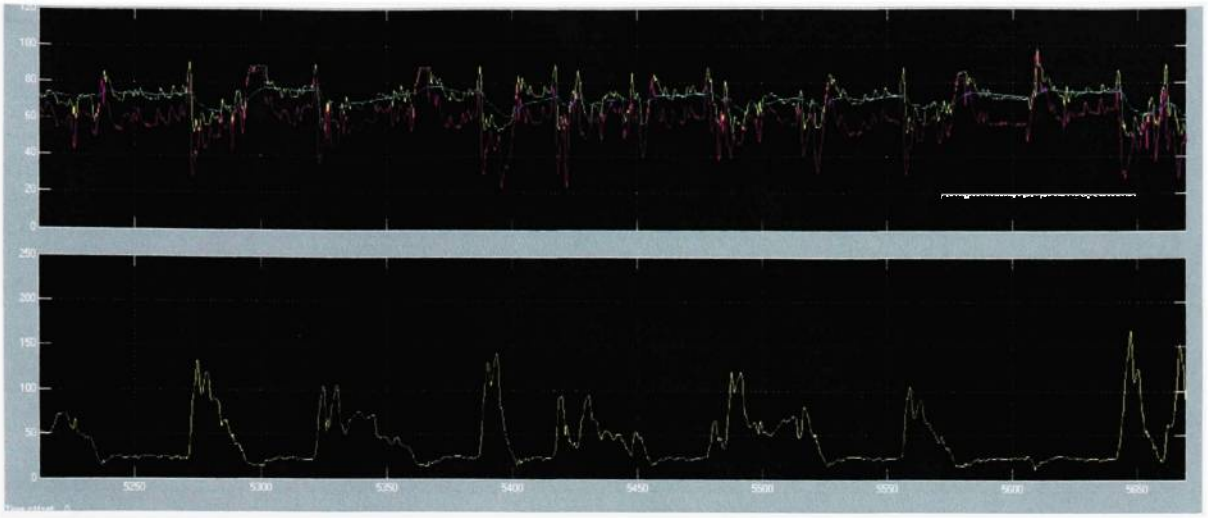

Figure 32: Comparison of Charge Temperature and MAF

Figure 32 shows a comparison of Intake Charge Temperature with correction (yellow) and the original charge temperature estimate (pink) and the measured charge temperature (blue). The lower graph of Figure 32 shows the MAF as read from the sensor.

MANIFOLD PRESSURE

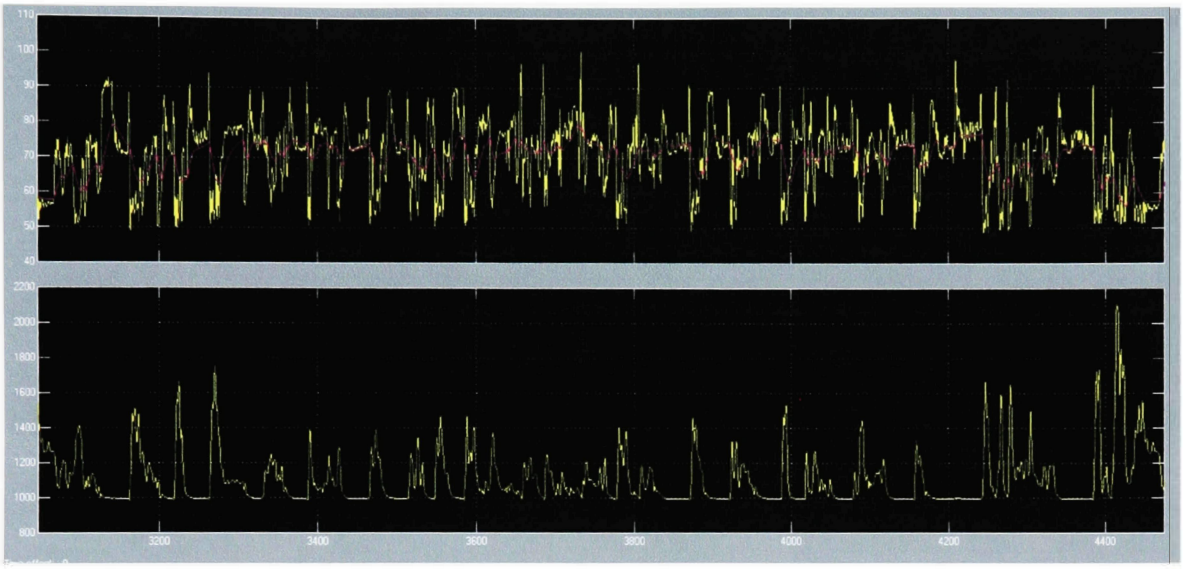

Figure 33: Estimated Charge Temperature and Intake Manifold Pressure

Figure 33 shows the coolant corrected intake charge temperature (Top Yellow) and the measured intake charge flow (Top Pink) over the Intake Manifold Pressure (Bottom Yellow)

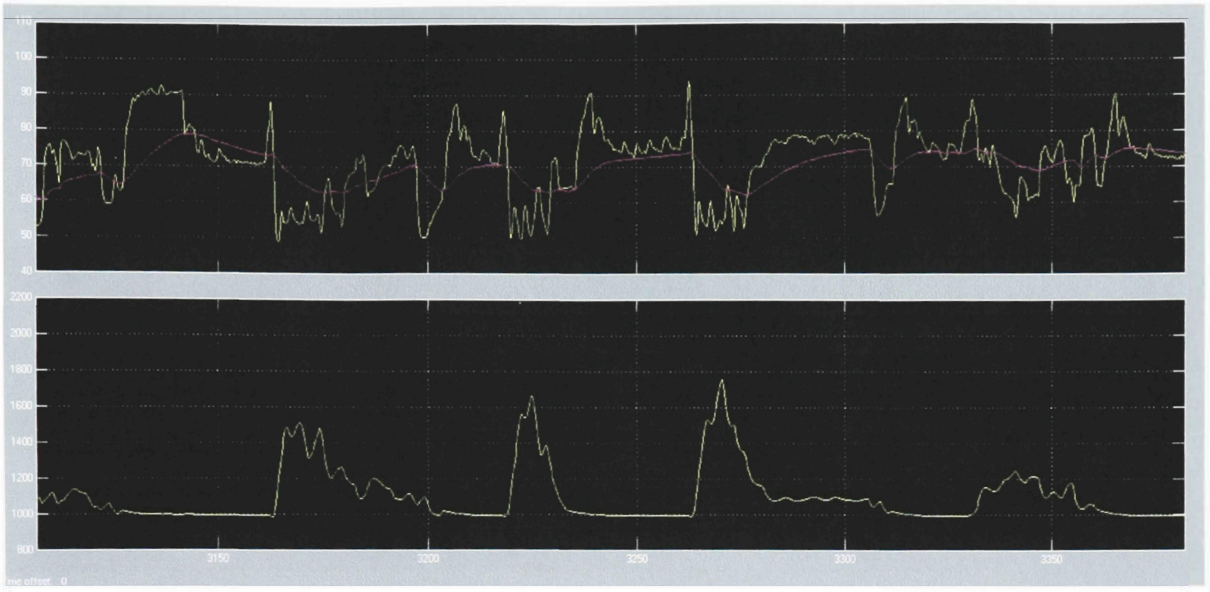

Figure 34: Zoomed ECT and MAP

Figure 34 is similar to Figure 33, however it has been zoomed to a smaller period to better illustrate the relationship between estimate and measurement.

MAF

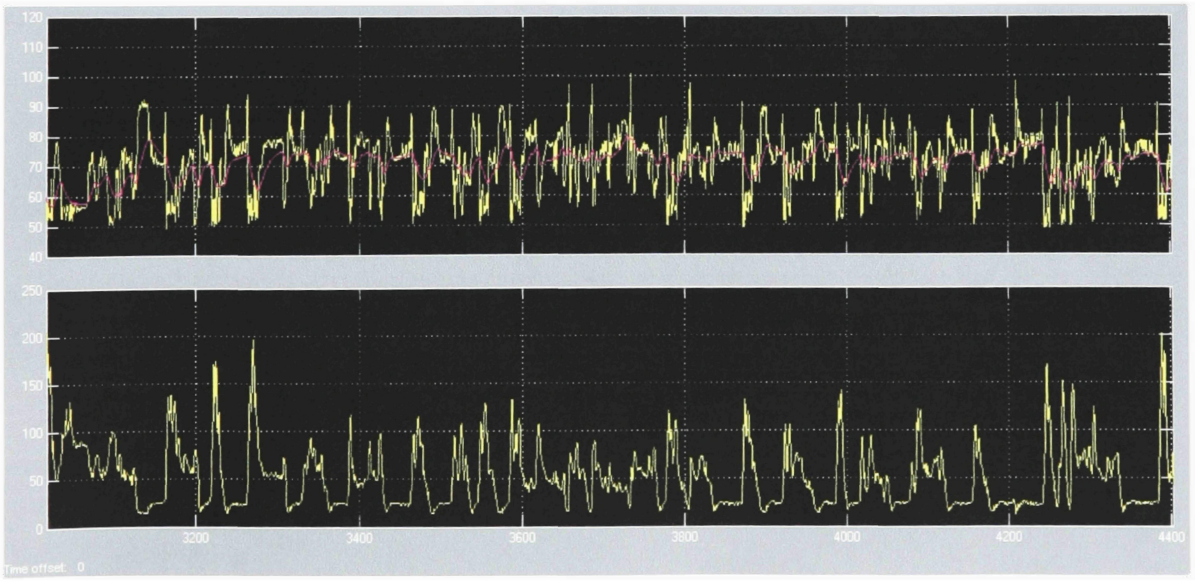

Figure 35: Estimated Charge Temperature and Mass Air Flow

Figure 35 shows the coolant corrected intake charge temperature (Top Yellow) and the measured intake charge flow (Top Pink) over the Mass Air Flow (Bottom Yellow)

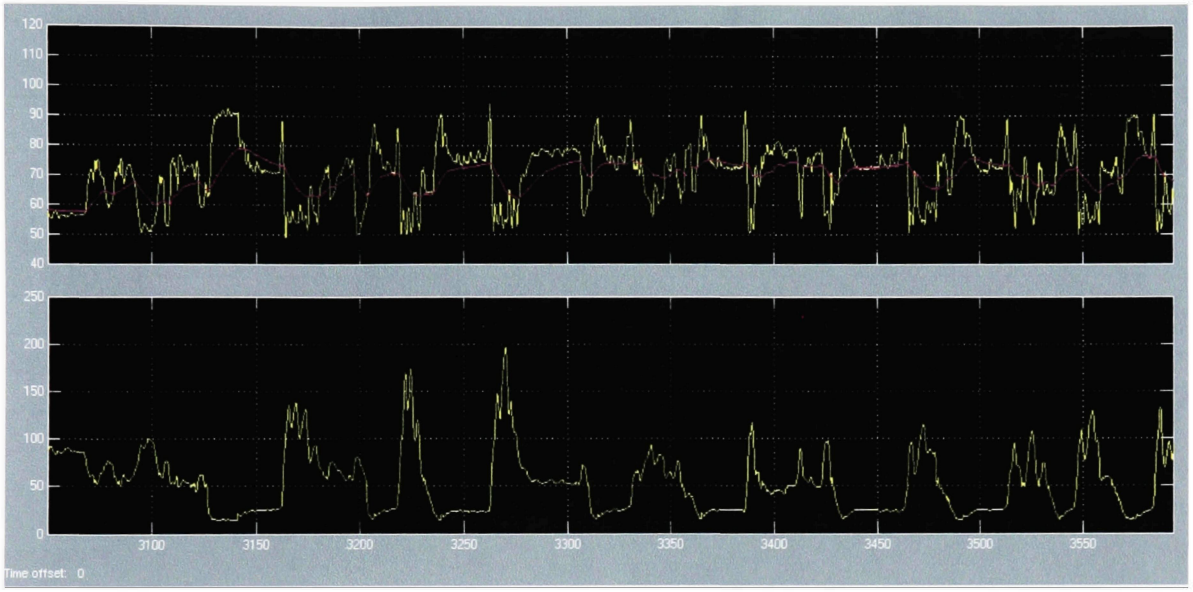

Figure 36: Estimated Charge Temperature and Mass Air Flow

Figure 36 is similar to Figure 35, however it has been zoomed to a smaller period to better illustrate the relationships.

EGR TEMPERATURE

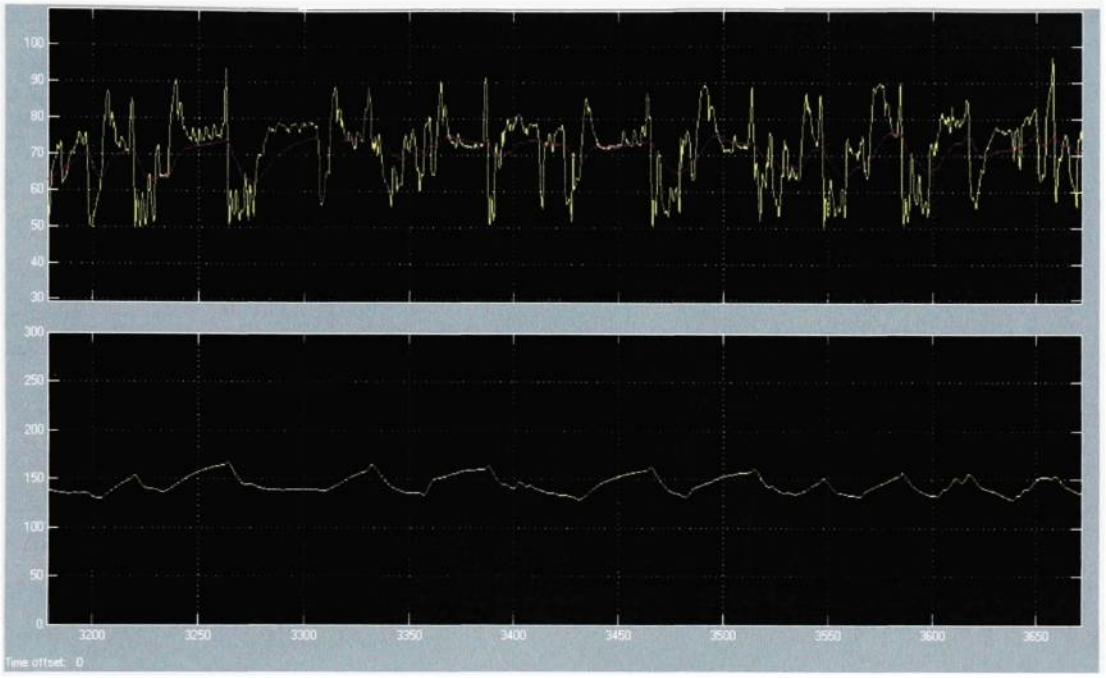

Figure 37: Calculated Charge Flow Temperature (Top Yellow), overlaid onto Measured Charge Flow Temperature (Top Pink) and EGR Temperature (Bottom Yellow)

Figure 37 shows an estimate of the actual charge flow temperature vs. the measured intake manifold charge flow temperature over a portion of a test cycle. In this instance, the measured EGR temperature is shown on a second chart for reference.

AIR TEMPERATURE

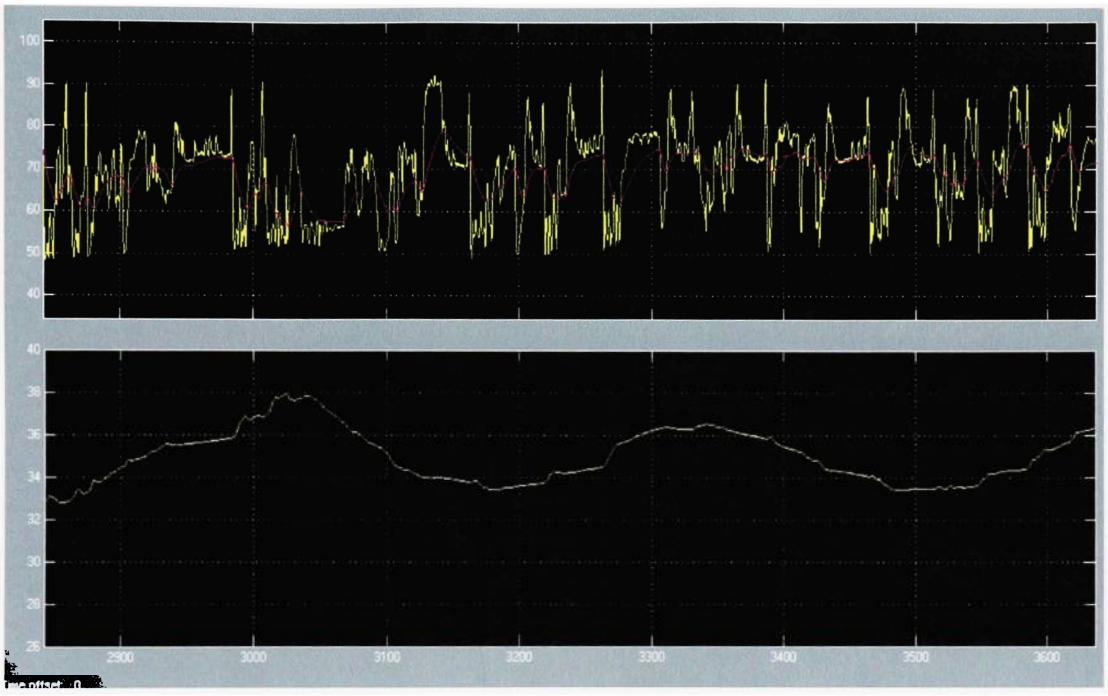

Figure 38: Calculated Charge Flow Temperature (Top Yellow), overlaid onto Measured Charge Flow Temperature (Top Pink) and CAC Out Temperature (Bottom Yellow)

Figure 38 is similar to Figure 37 but shows the relatively constant outlet temperature from the charge air cooler.

REGENERATION RESULTS

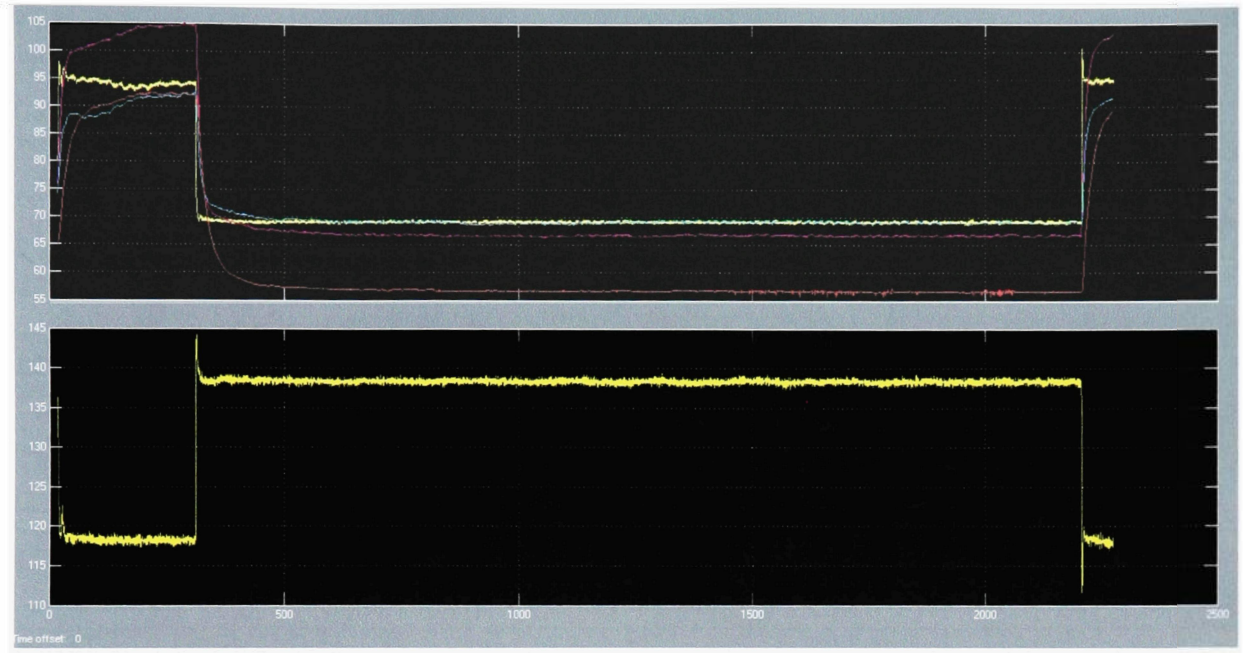

Figure 39: Calculated Temp (Top Yellow), Measured LB and RBTemp (Top Blue, Top Purple), Measured Intake Temp (Top Red), and MAF (Bottom Yellow) vs. Time

The estimation algorithm was compared to data gathered from a long steady state regen cycle. Figure 39 shows good agreement in the steady state condition at a MAF of approximately 137 g/s using a MAF vs. coolant correction table of:

Mass_Flow =

[0 10 20 30 40 50 60 70 80 90 100 110 120 130 140 150 160 170 250 300];

Cool_Temp_Coef_1D=

[0.3,0.3,0.3,0.3,1.0,1.0,1.0,0.7,0.5,0.5,0.4,1.4,1.4,0.5,0.5,0.5,0.6,0.5,0.3,0.3];

There is poor agreement at the beginning of the cycle, but also poor agreement between the measured values as well.

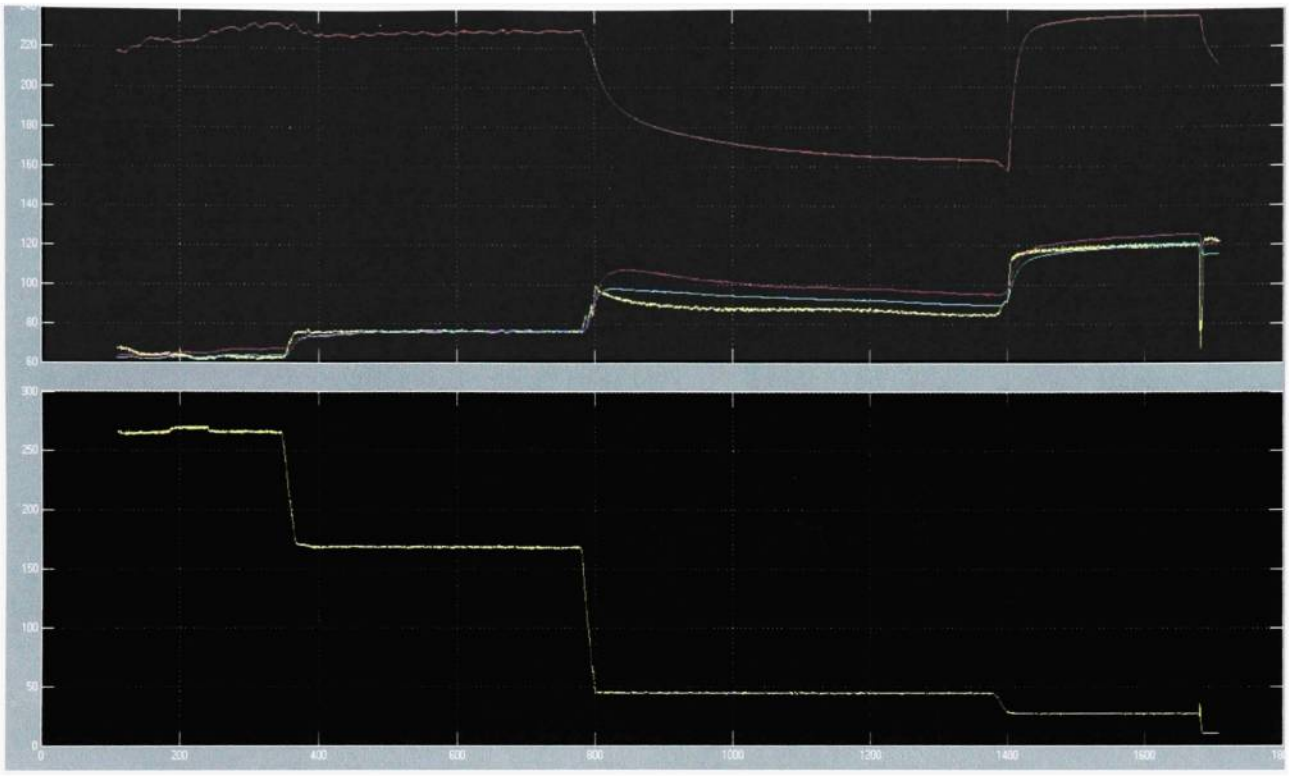

Figure 40: Estimated Charge Flow temperature (Top Yellow), Measured Intake Temperature (Top Purple and Blue), and EGR Outlet Temp (Top Red) vs. Time and MAF vs. Time (Bottom Yellow)

As seen in Figure 40 above, there is good agreement in the models until the EGR temperature falls of unexpectedly. The temperature underestimates, even with flow and cooling corrections.

Figure 40 comes from the 10_0519_TranSeq_E1T6F4_4AP_53346 EGR Step Run. The inconsistency occurs when the EGR is at 35-45% open.

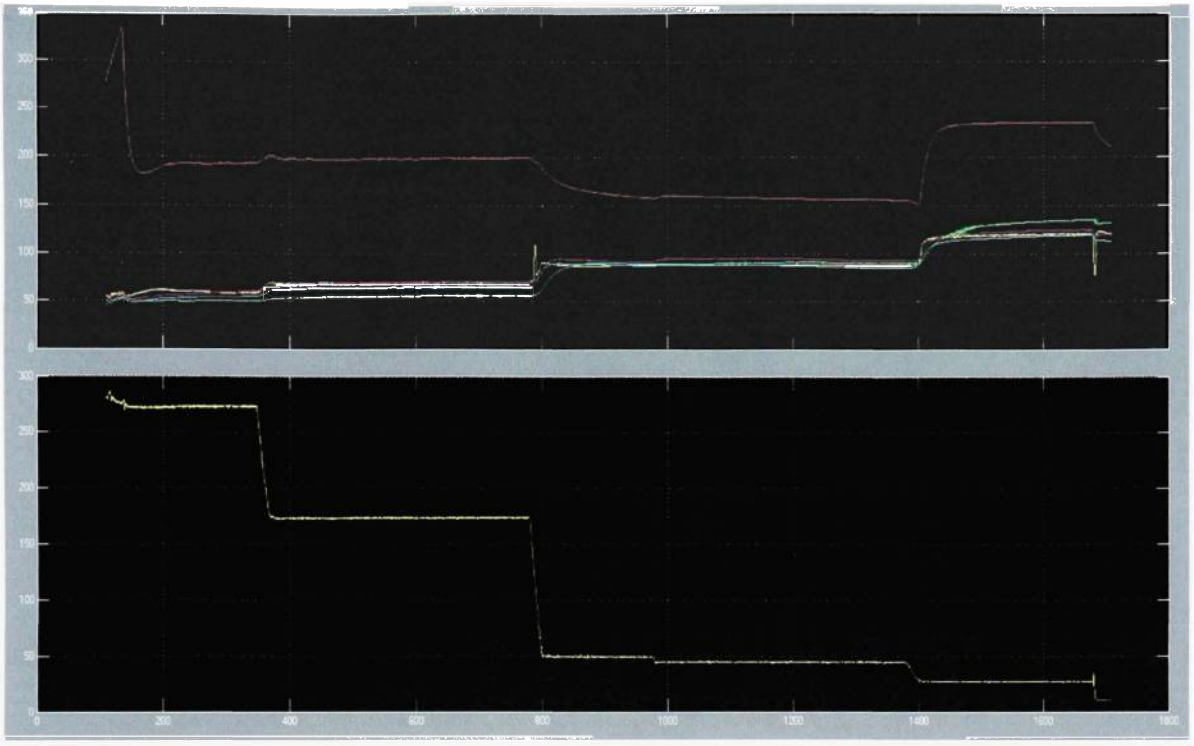

Figure 41: Estimated Charge Flow temperature (Top Yellow), Measured Intake Temperature (Top Purple and Blue), and EGR Outlet Temp (Top Red) vs. Time and MAF vs. Time (Bottom Yellow)

Figure 41 is similar to Figure 40; however, the data set is from 10_0519_TranSeq_E1T6F4_4AP_53346 EGR step run. The inconsistency seen in Figure 40 does not occur in this run; however, a small spike is still visible. This spike is corrected later as seen in Figure 53and Figure 55.

STEP INPUT TESTING

A small section of steady state input data was extracted from the engine test cycle recording: 10_0519_TranSeq_E1T6F4_4AP_53346. A snapshot in time was taken when the cycle was operating in a stable steady state condition. The data points were then

duplicated for a sufficient interval to evaluate a step input. The results of these tests are seen on the next page.

MAF Step Input:

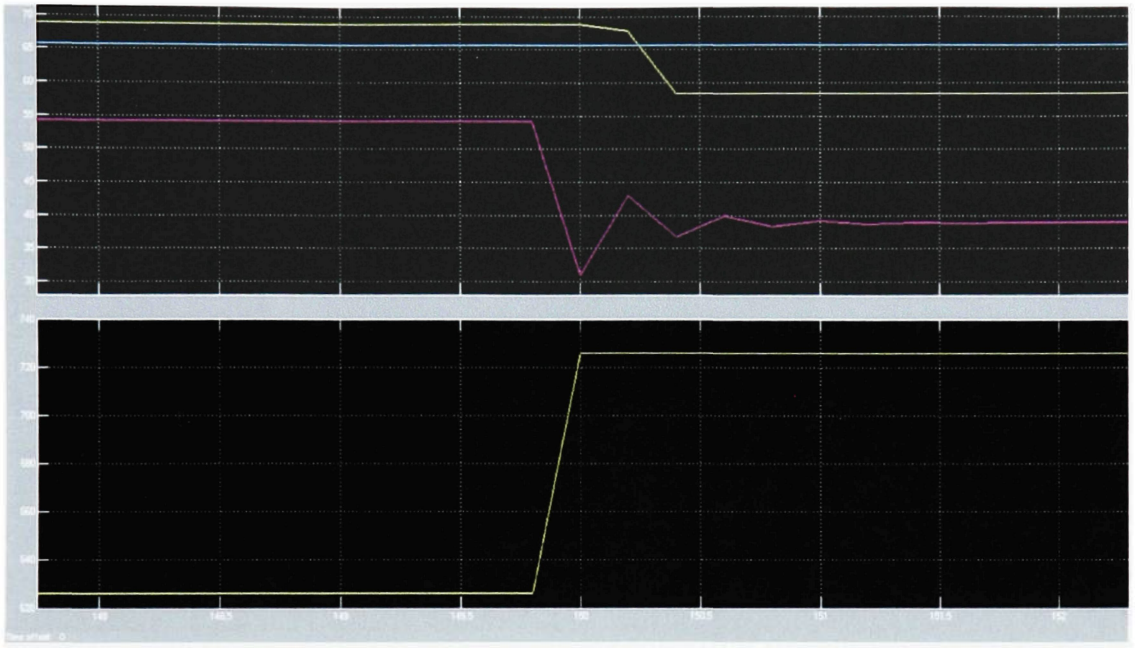

Figure 42: 100 kg/hr MAF Step Input

Figure 42 shows a step input for the MAF, holding all other signals constant. The figure shows the Estimated Intake Temperature (Top Yellow), the original estimate (Top Purple) and the constant measurement (Top Blue) for reference. The bottom chart shows the MAF response (bottom yellow).

An offset in the MAF will yield a constant shift in the estimated temperature, assuming no change in other parameters. In this instance, an increase in airflow yields a decrease in estimated temperature.

Engine Speed Step Input:

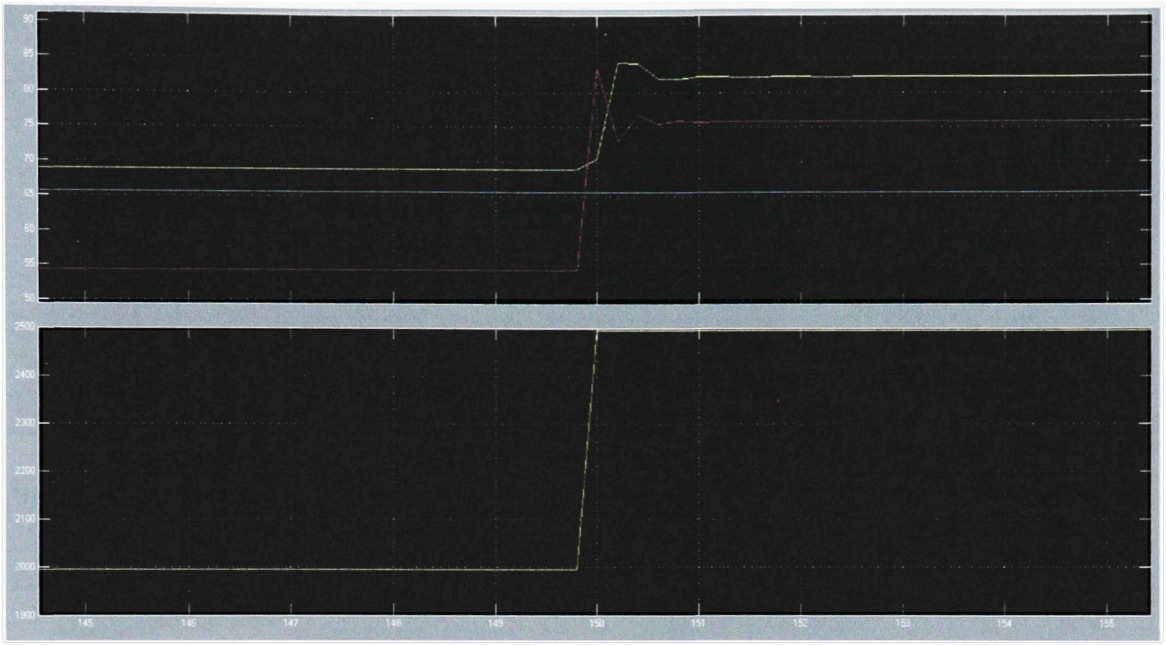

Figure 43: 500 RPM Step Input

Figure 43 shows a step input for the engine speed, holding all other signals constant. The figure shows the Estimated Intake Temperature (Top Yellow), the original estimate (Top Purple) and the constant measurement (Top Blue) for reference. The bottom chart shows the RPM response from 2000 to 2500 (bottom yellow).

An offset in the RPM will yield a constant shift in the estimated temperature, assuming no change in other parameters. In this instance, an increase in engine speed yields an increase in estimated temperature. This is expected, since no other variables are being changed. In an actual test, the engine speed would yield an increase in MAF, which would have a lowering effect on the temperature as seen in Figure 42.

Fuel Step Input:

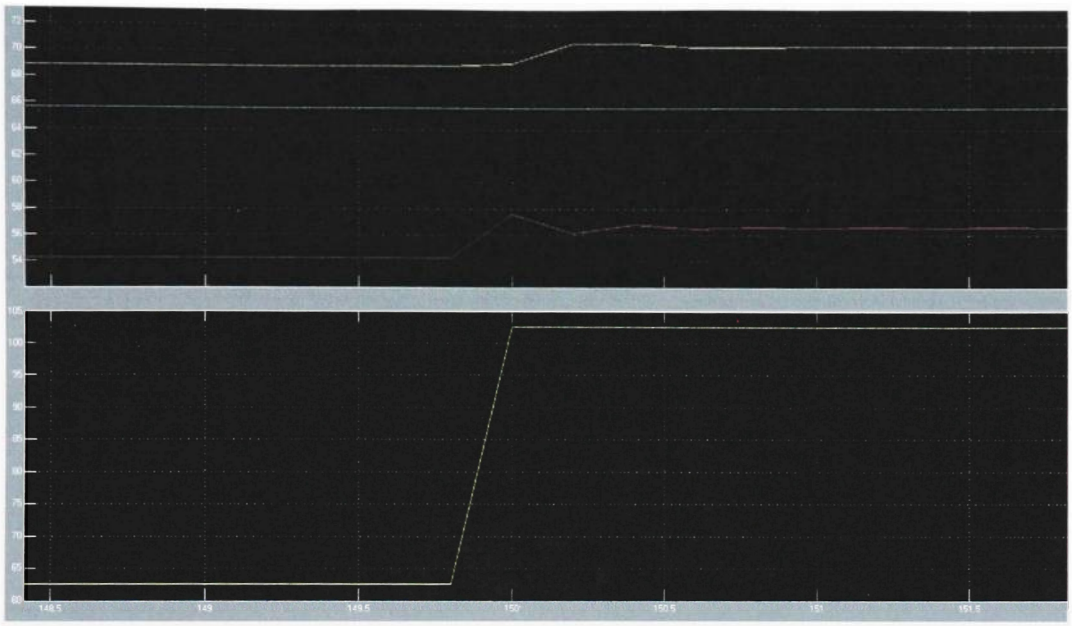

Figure 44: 40mm3 Fuel Step Input

Figure 44 shows a step input for fuel, holding all other signals constant. The figure shows the Estimated Intake Temperature (Top Yellow), the original estimate (Top Purple) and the constant measurement (Top Blue) for reference. The bottom chart shows the fuel response from 62.5 to 102.5 (bottom yellow).

An offset in the Fuel will yield a constant shift in the estimated temperature, assuming no change in other parameters. In this instance, an increase in fuel increases the estimated temperature.

MAP Step Input:

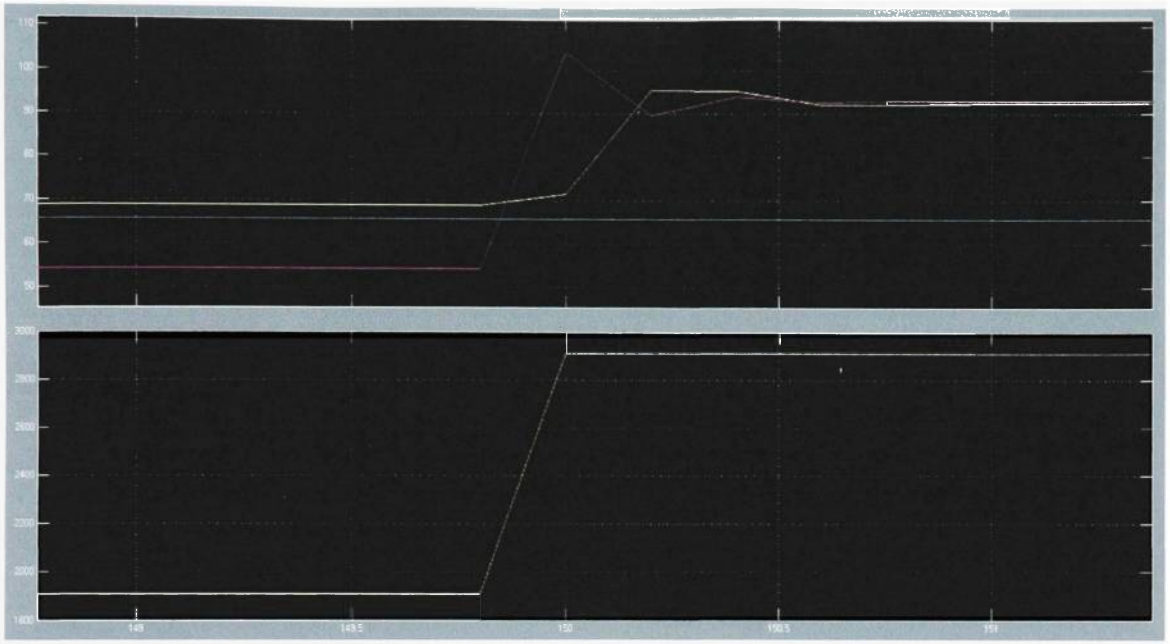

Figure 45: 1000hPa MAP Step Input

Figure 45 shows a step input for MAP, holding all other signals constant. The figure shows the Estimated Intake Temperature (Top Yellow), the original estimate (Top Purple) and the constant measurement (Top Blue) for reference. The bottom chart shows the MAP response from 1911 hPa to 2911 hPa (bottom yellow).

An offset in the MAP will yield a constant shift in the estimated temperature, assuming no change in other parameters. In this instance, an increase in MAP increases the temperature estimates to near identical levels.

CAC Outlet Air Temperature Step Input:

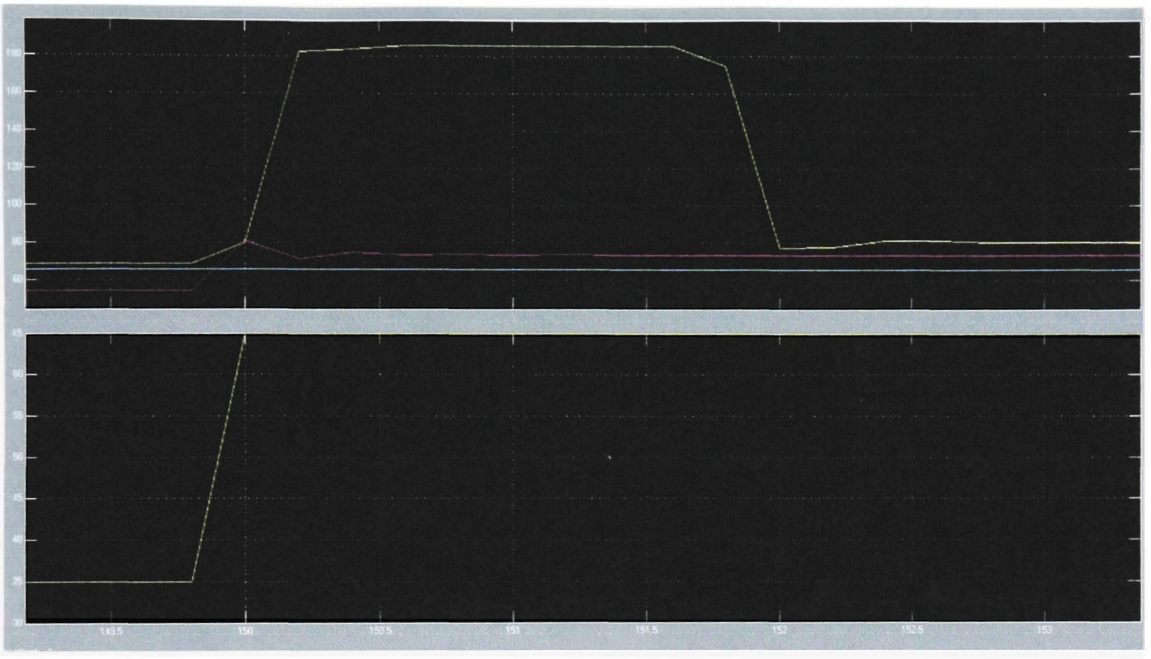

Figure 46: 30°C CAC Outlet Air Temperature Step Input

Figure 46 shows a step input for CAC Outlet Air Temperature, holding all other signals constant. The figure shows the Estimated Intake Temperature (Top Yellow), the original estimate (Top Purple) and the constant measurement (Top Blue) for reference. The bottom chart shows the CAC Outlet Air Temperature Step Input response from 35°C to 65 °C (bottom yellow).

An offset in the CAC Outlet Air Temperature yields a large temporary offset in the estimated temperature, followed by a return to a small constant offset.

In the original estimate, the offset is smaller initially, and takes less time to stabilize. In this instance, an increase in CAC Outlet Air Temperature yields an increase in the estimated charge flow temperature.

EGR Cooler Outlet Air Temperature Step Input:

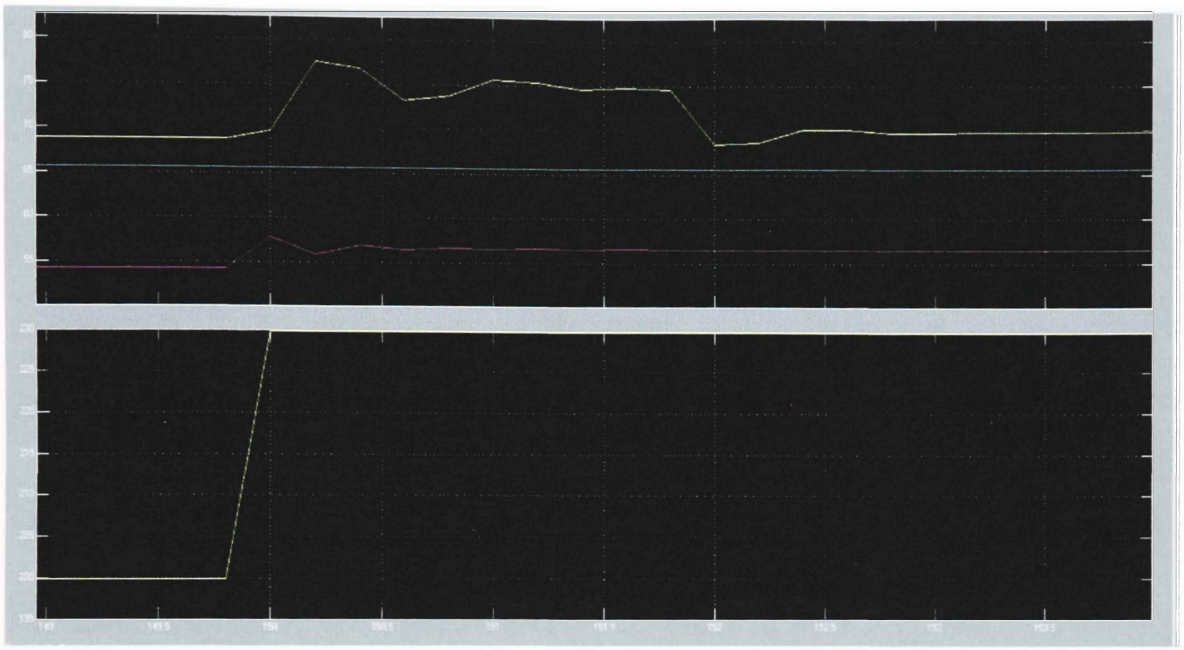

Figure 47: 30°C EGR Cooler Outlet Air Temperature Step Input

Figure 47 shows a step input for EGR Cooler Outlet Air Temperature, holding all other signals constant. The figure shows the Estimated Intake Temperature (Top Yellow), the original estimate (Top Purple) and the constant measurement (Top Blue) for reference. The bottom chart shows the EGR Cooler Outlet Air Temperature Step Input response from 200°C to 230 °C (bottom yellow).

Similar to the CAC Cooler Outlet Step Input response, the EGR Cooler Outlet Step Input response yields a large temporary offset followed by a small constant offset overtime. The original estimate is quicker to stabilize. In this instance, an increase of 20°C yields a slight increase in the charge flow temperature estimation.

Engine Coolant Temperature Step Input:

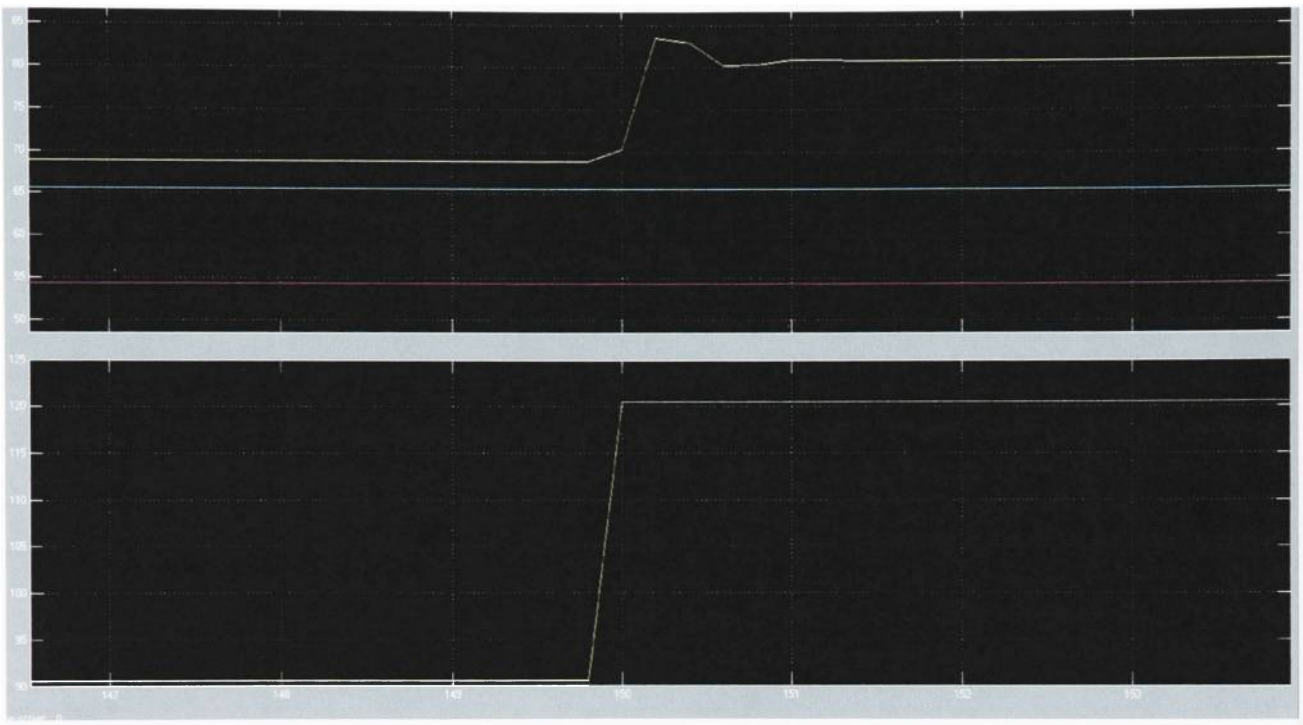

Figure 48: 30°C Engine Coolant Temperature Step Input

Figure 48 shows a step input for Engine Coolant Temperature, holding all other signals constant. The figure shows the Estimated Intake Temperature (Top Yellow), the original estimate (Top Purple) and the constant measurement (Top Blue) for reference. The bottom chart shows the Engine Coolant Temperature Step Input response from 90.55°C to 120.55 °C (bottom yellow).

There is a constant offset because of the engine coolant temperature step input, as expected in the new estimate, but no change in the old estimate. This is expected, since the original estimate does not include a factor for coolant temperature effects on intake

charge temperature. In this instance, an increase of 30°C in coolant temperature yields a rise from 68°C to 82°C in the estimated intake charge flow temperature.

FTP72 Cycle and Steady State Analysis

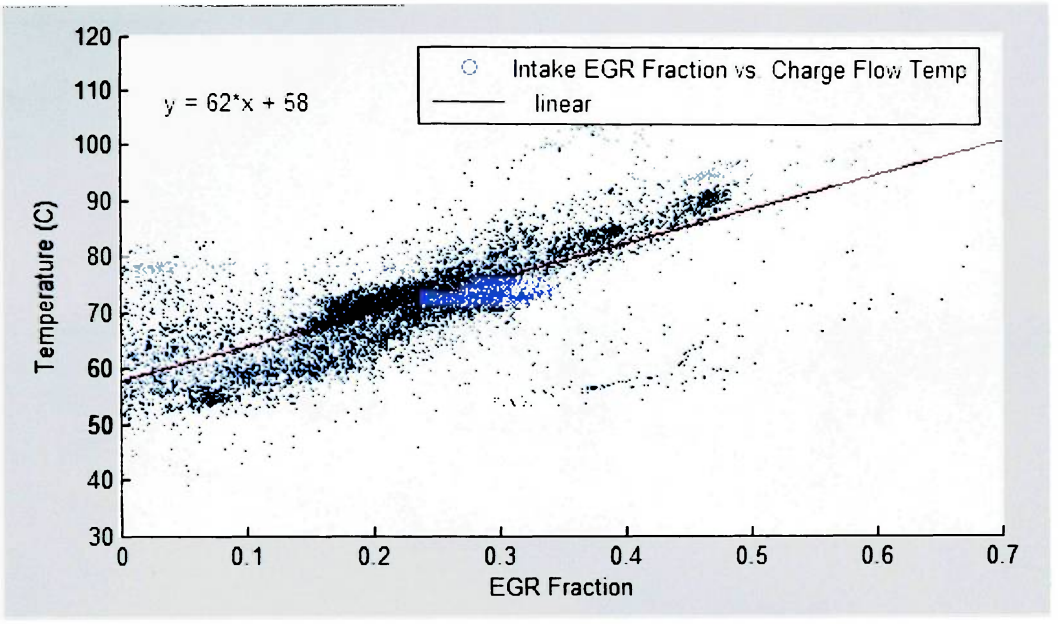

Figure 49: FTP Cycle Analysis of EGR Fraction vs. Charge Flow Temperature

Figure 49 shows a rough correlation between the intake manifold EGR charge fraction and the overall temperature in the intake manifold over a typical FTP cycle. In general, as the EGR flow rate increases, the total combustion flame temperature goes down due to a decrease in available oxygen. (39) The intake manifold temperature goes up however, as the EGR temperature remains higher than the fresh air charge.

EGR Air Fraction vs. Temperature

y = p1*x^1 + p2

Coefficients:

p1 = 62.118

p2 = 57.745

Norm of residuals =

676.33

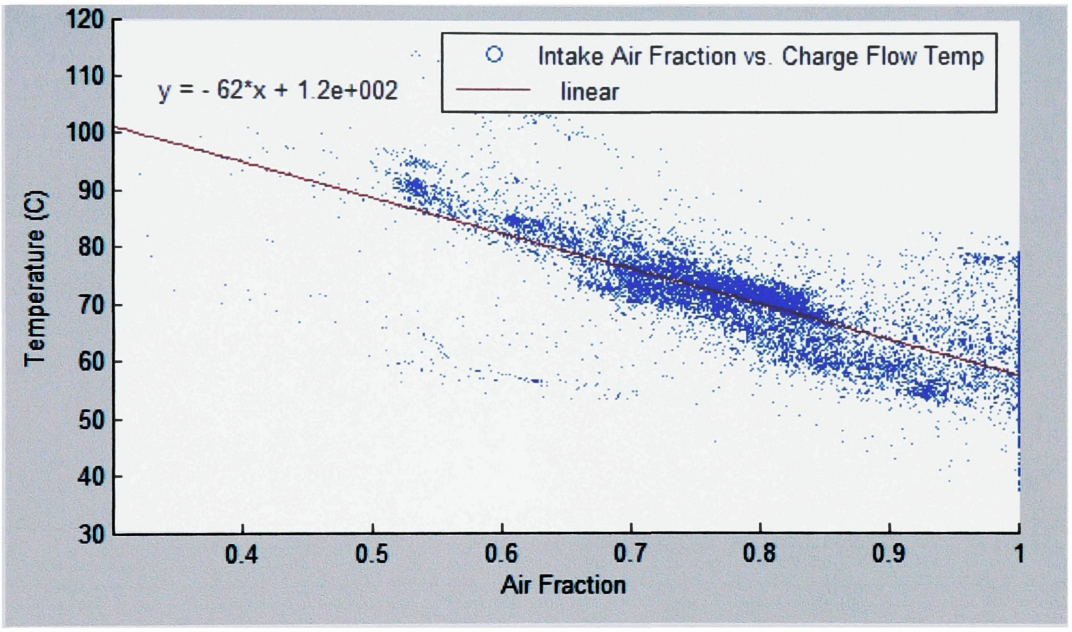

Figure 50: FTP Cycle Analysis of Air Fraction vs. Charge Flow Temperature

Figure 50 shows a rough correlation between the decrease in overall intake manifold temperature and the increase in overall fresh air charge flow.

Air Fraction vs. Temperature

y = p1*x^2 + p2*x^1 +

p3

Coefficients:

p1 = 32.812

p2 = -113.53

p3 = 139.49

Norm of residuals =

672.79

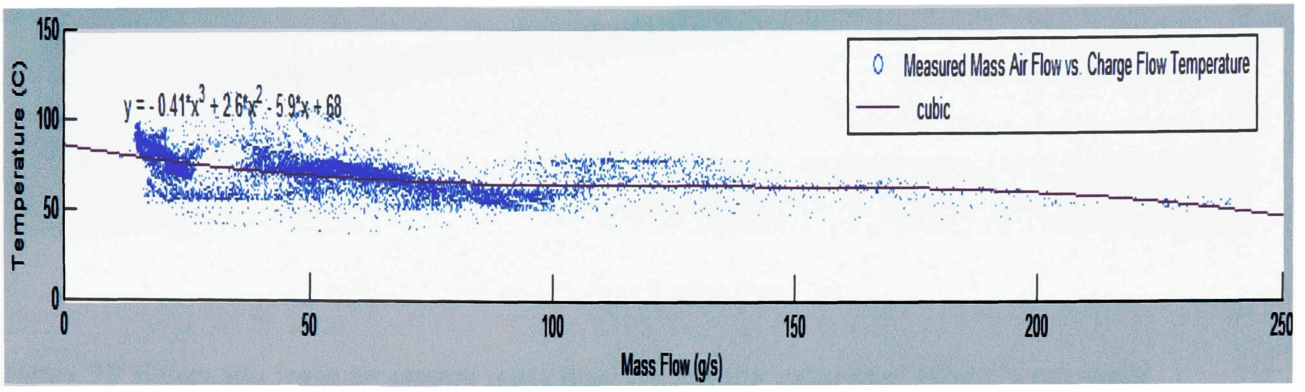

Figure 51: Measured Mass Flow vs. Estimated Charge Flow Temperature

Measured Mass Flow vs. Estimated Charge Flow Temperature (X data has been scaled and centered)

y = p1*x^3 + p2*x^2 +

p3*x^1 + p4

Coefficients:

p1 = -0.40514

p2 = 2.6419

p3 = -5.9274

p4 = 68.399

Norm of residuals =

918.01

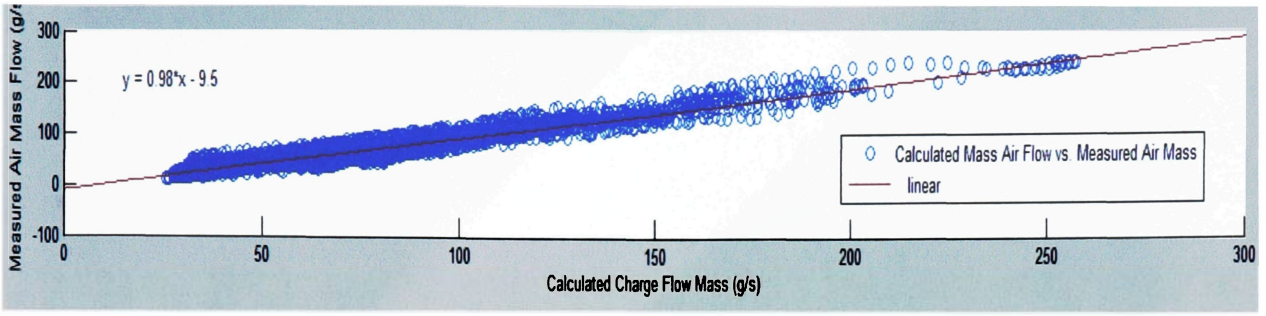

Figure 52: MAF vs. Calculated Charge Flow Mass

Figure 52 shows the fresh air charge mass flow against the calculated total charge mass flow over a standard FTP cycle. The lack of outlying points indicates that the model is stable in calculating the estimated charge mass flow, and thus the EGR fraction during the cycle.

y = p1*x^1 + p2

Coefficients:

p1 = 0.98115

p2 = -9.4822

Norm of residuals =

865.4

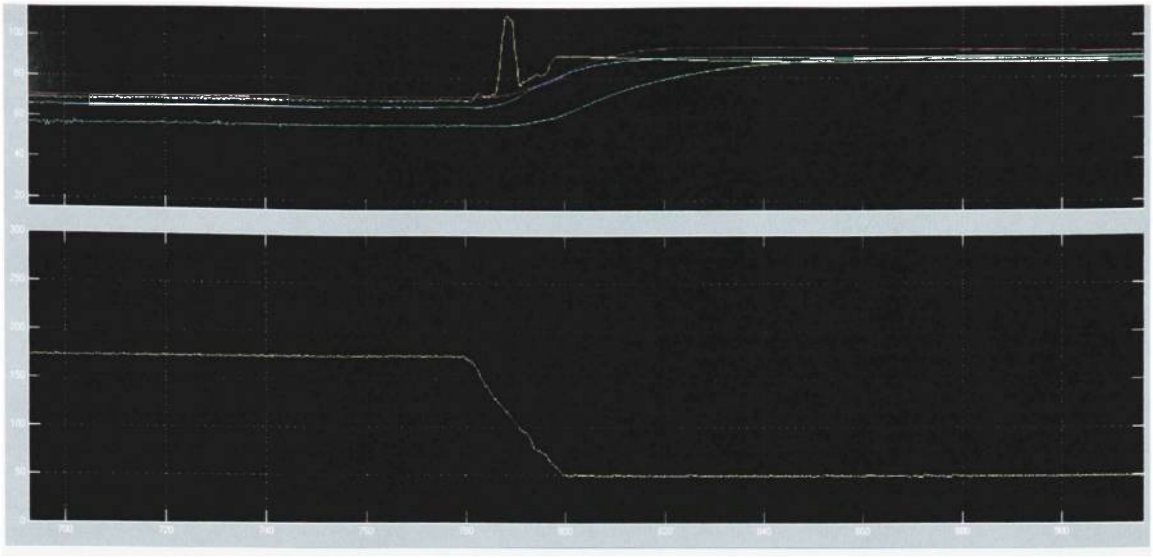

Figure 53: Spike in Estimated Temperature Graph vs. Measured Temperatures

Figure 53 shows the result of a poorly calibrated coolant temperature vs. MAF table; smoothing the table eliminated the spike.

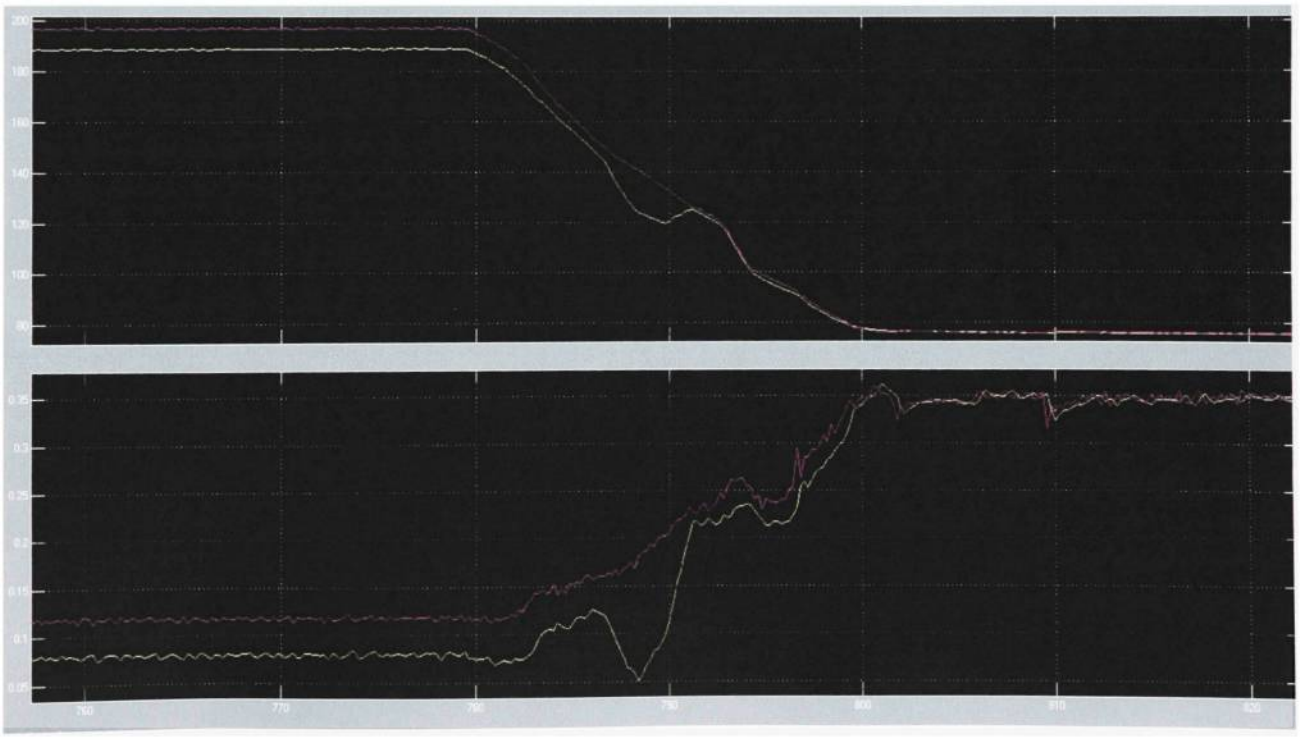

Figure 54: 'mdottmix' vs. time and EGR Fraction vs. time for EGR Step Run 2

Figure 54 shows an observed point of inflection on the enhanced temperature model (top yellow) for the 'mdottmix' signal output and the lack of a pronounced inflection for the original (top purple). The bottom graph shows the effect on the EGR air fraction for both the original (bottom purple) and the enhanced (bottom yellow).

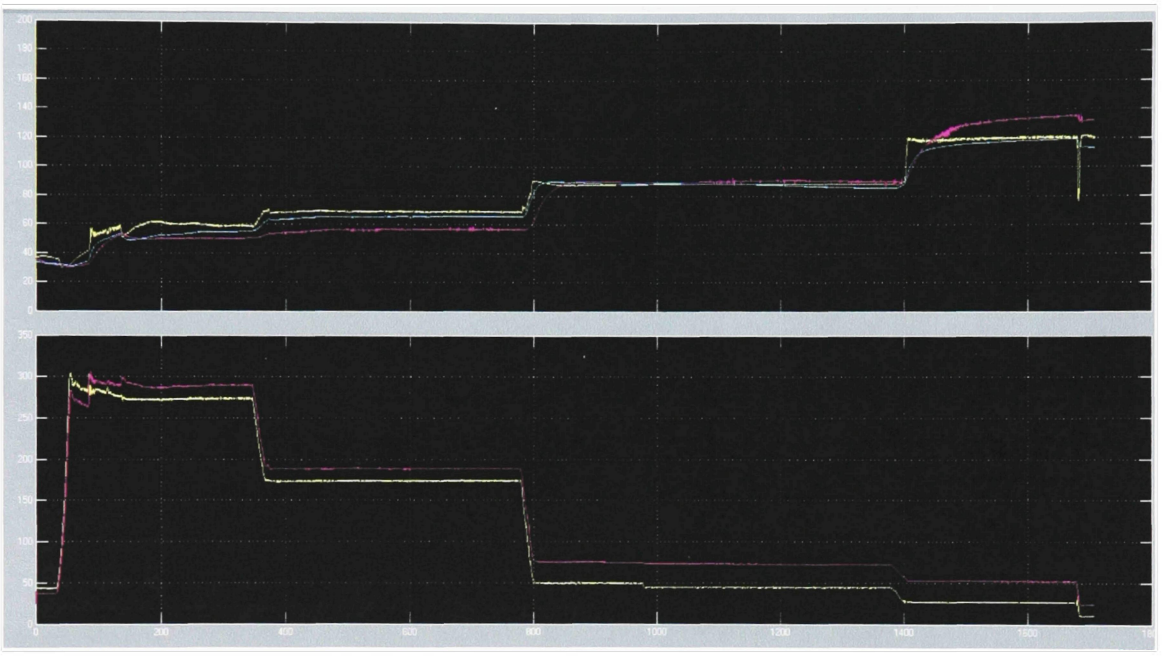

Figure 55: EGR Step without Spike

Figure 55 shows a test run without the spike, or inflection seen in Figure 41. The top chart shows the three measured temperatures and the estimated temperature (yellow) over a steady state test.

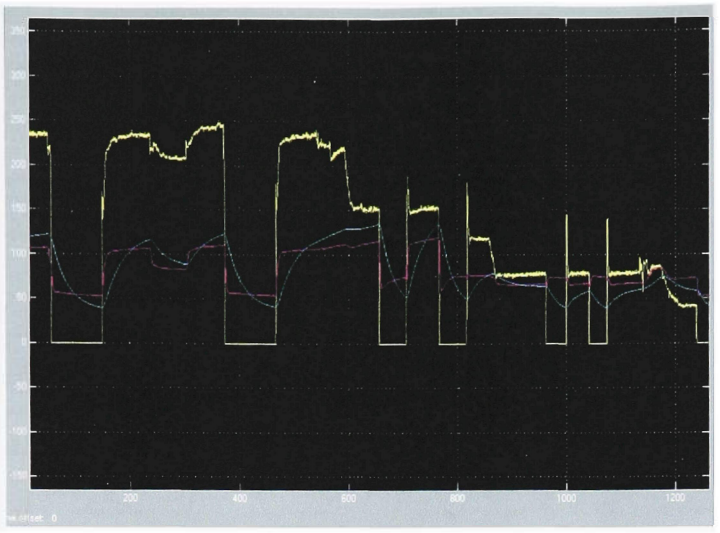

Figure 56: Steady State Step Input Analysis

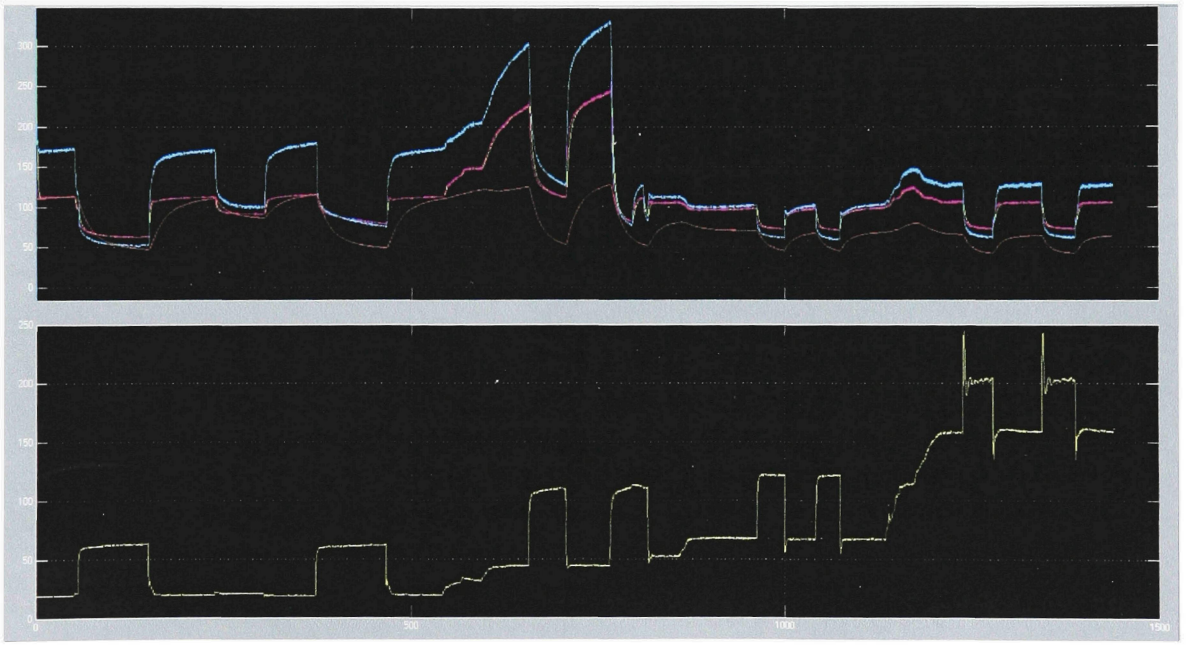

Figure 57: Comparison of Estimates and Mass Flow

Figure 57 above shows a preliminary calibration for the temperature estimate, plotted against the mass flow. The primary estimate is the yellow line seen in the top chart. It is calibrated first with the coolant temperature and mass flow rate.

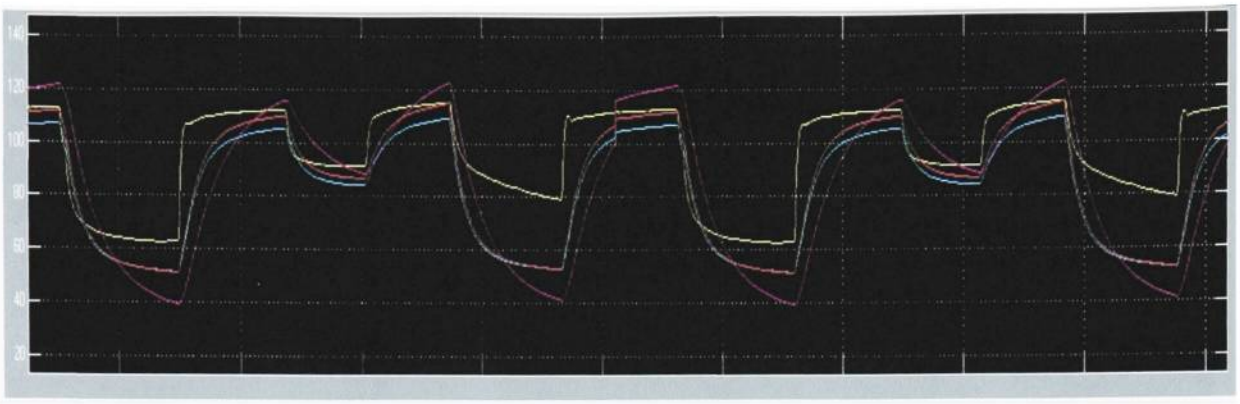

Figure 58: Estimated Charge Temperature and Measured Intake Manifold Temperature in Three Positions

Figure 58 above shows the estimated Charge Temperature (Yellow) and the measured temperatures (Red, Light blue, and Purple) plotted over two identical intervals. The plot shows good convergence and repeatability for the first and repeated third step. At the second and fourth steps the repeatability response is similar, however temperature is being overestimated compared to one and three.

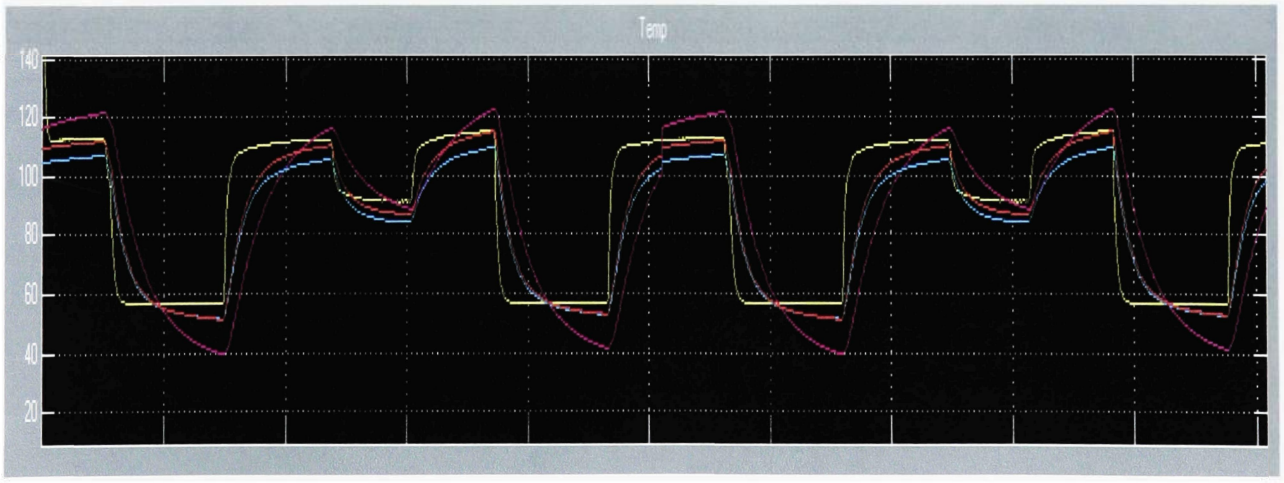

Figure 59: EGR Valve Position Check Correction of Temperature

Figure 59 shows the result of implementing the EGR valve actual position correction, to reset the EGR fraction on a simple test code.

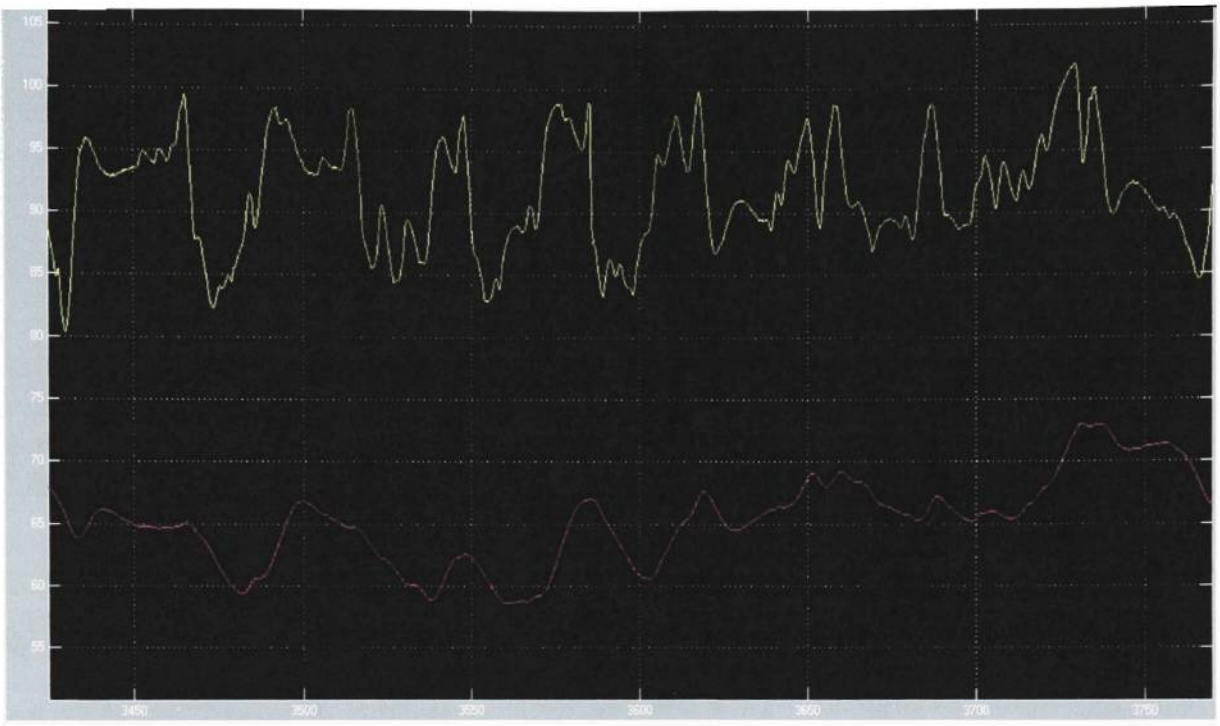

Figure 60: Estimated Temperature and Measured Temperature over section of FTP72

Figure 60 shows the same calibration used in Figure 59 but over a different run cycle. Over this cycle, there is a positive offset in the calibration over the baseline test. The yellow line is the estimate, while the purple indicates the measured intake manifold temperature. The offset is nearly 20°C for this case.

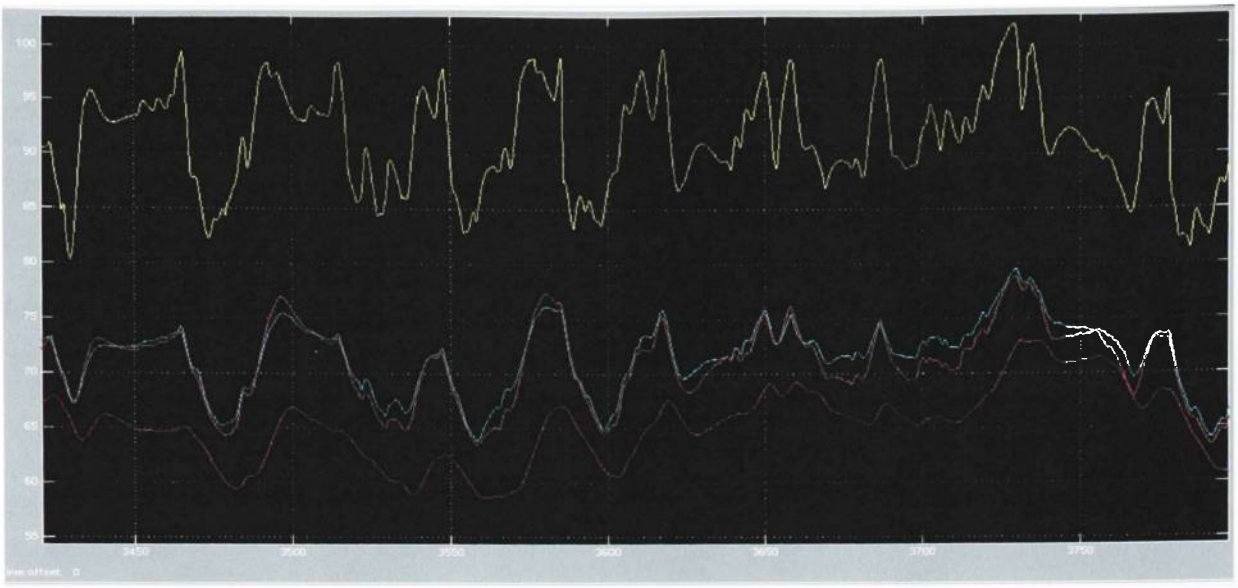

Figure 61: Estimated and Measured Temperatures including Left and Right Bank Sensors

Figure 61 is similar to Figure 60 however; it includes the additional measurements taken in the left and right banks of the intake manifold.

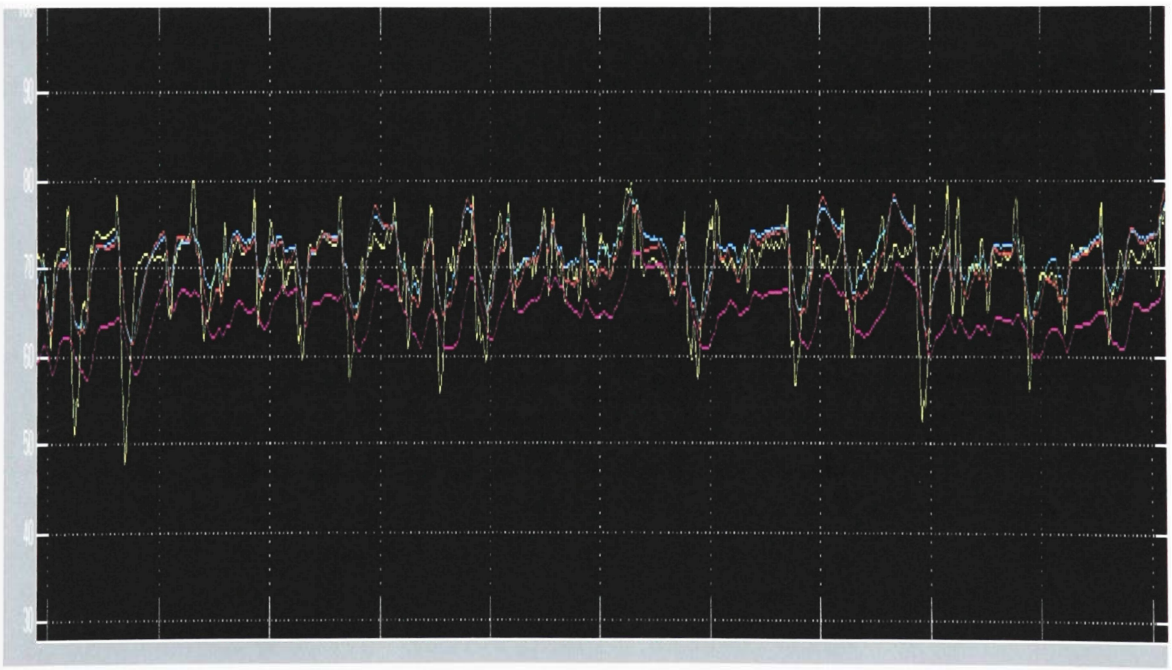

Figure 62: FTP72 Corrected Charge Air Temperature Estimation

Figure 62 shows a section of the FTP cycle for charge air temperature estimation after applying a correction for engine speed and fuel request.

The standard deviation of the Enhanced Temperature Difference of measured sensors and estimated temperature can be seen in the highlighted sample output below for various cycle runs.

Calibration: TempIntData_080510_Init
Model: tempintk_080510

With updated simulation calibration:

For MAF Run 1:
>> std(yout)
ans =
 Columns 1 through 11
 57.1255 0.1294 0.1465 25.2087 14.6590 6.8010 8.6978 14.4388 17.3777 19.0252 56.5060
 Columns 12 through 20
 0.5707 0.1889 4.7311 17.5583 25.4710 14.4388 10.7535 10.0691 9.4520

For O2 Run 1:
>> std(yout)
ans =
 Columns 1 through 11
 62.6165 0.0931 0.0931 17.5084 14.0247 5.7642 7.2912 5.1818 6.2645 8.4623 61.7701
 Columns 12 through 20
 0.1462 0.1845 2.8572 15.6099 18.0173 5.1818 5.1408 5.8850 10.8937

For O2 Run 2:
>> std(yout)
ans =
 Columns 1 through 10
 61.8684 0.0929 0.0929 17.0817 14.1435 5.9944 7.4500 5.0542 6.1064 7.7861
 Columns 11 through 20
 61.0494 0.1422 0.2154 2.9272 15.4124 17.6183 5.0542 5.6883 5.9646 11.2595

For MAF Run 2
>> std(yout)
ans =
 Columns 1 through 10

71.0332 0.1225 0.1419 22.4274 14.0425 6.8108 8.8039 7.5421 8.6066 17.8814

Columns 11 through 20

70.1413 0.5647 0.2621 3.0499 16.9357 22.4274 7.5421 6.3884 7.1079 10.6646

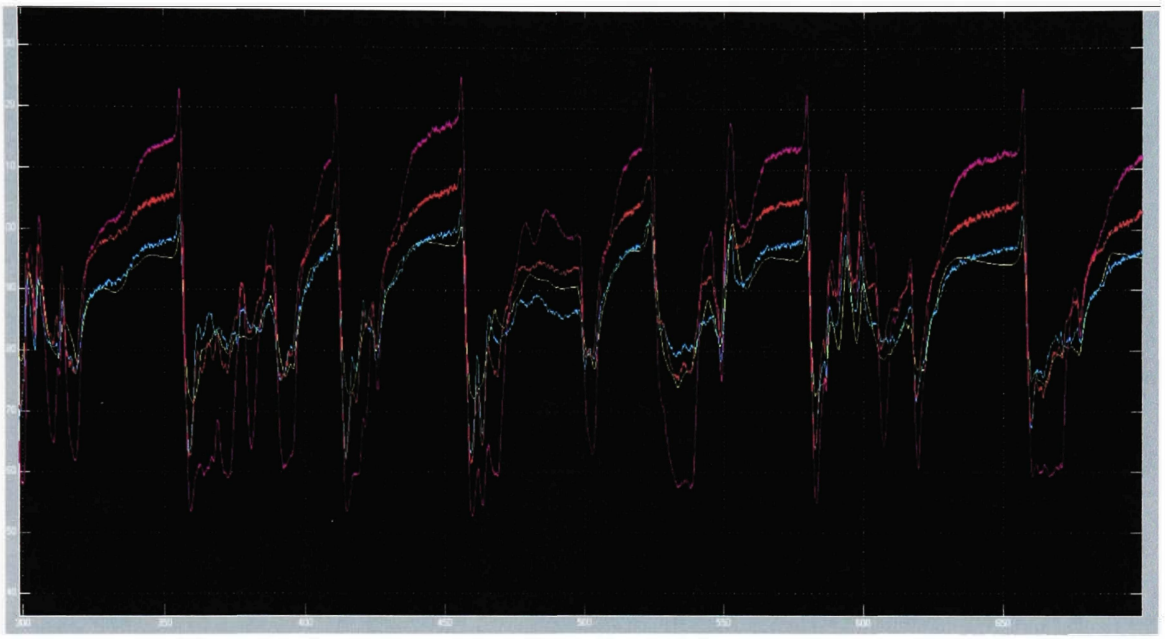

Figure 63: Charge Temperature Estimation with Enhanced Sensor Readings

Figure 63 shows the estimate of the charge flow temperature with overlays for the enhanced sensor measurements from the three temperature sensors outfitted on the test engine. This late test showed very good estimation.

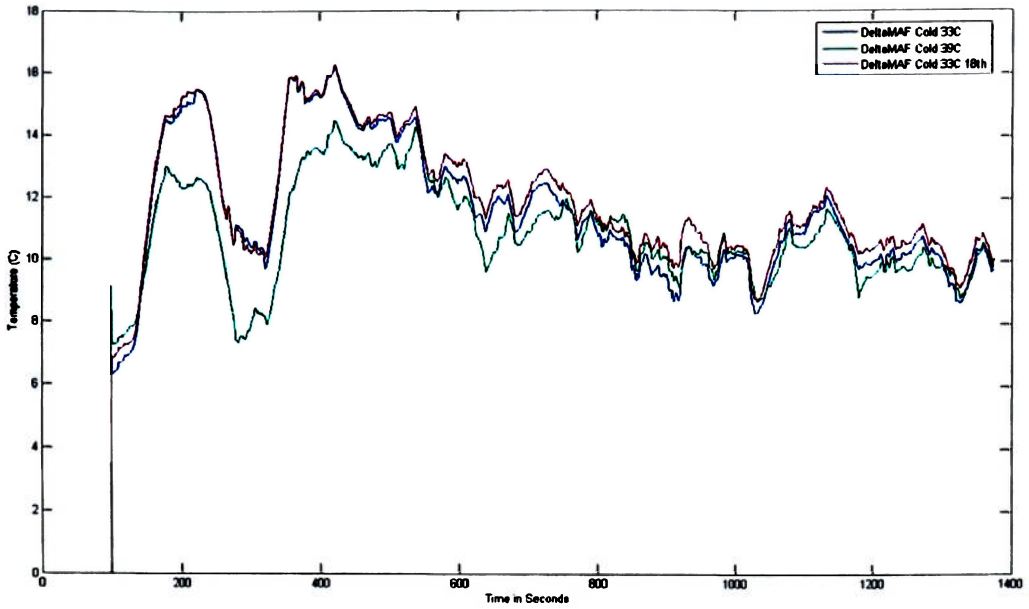

Figure 64: Measured Thermocouple RMS Difference at Various Cold Start Conditions

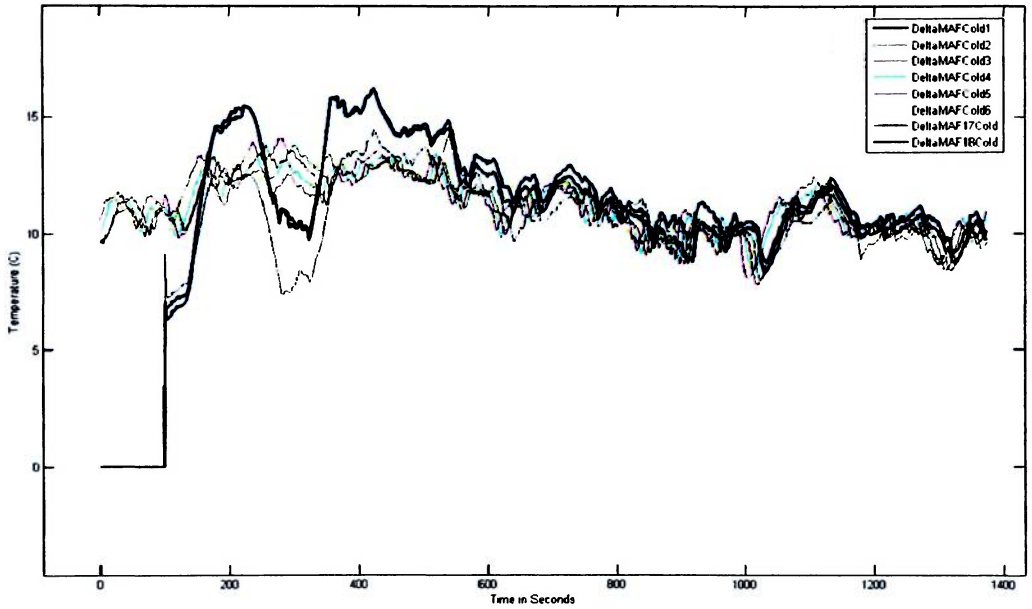

Figure 65: Variation in RMS of Measured Thermocouple Difference over repeated FTP Cycles

Figure 64 and Figure 65 show the root mean square (RMS) of the difference between the intake manifold temperature sensor, and the average of the left and right bank intake manifold temperature sensors. In Figure 64, the RMS is taken over three separate cold start tests, two with a measured engine coolant inlet temperature of 33°C and one with a measured inlet coolant temperature of 39°C. In Figure 65 the RMS of six

repeated FTP cycles is overlaid onto the three separate cold start cycles. The offsets seen between the cycles are minimal, and most of the lag observed is apparent due to the method of display above, not because of actual physical offsets. It can be seen that as the engine coolant temperature rises, the variation in the intake manifold RMS becomes less. Cold Start emissions form a very important part of total vehicle emissions, one study on these emissions, particularly for Diesel engines and the effect of intake air charge temperature is seen in (40).

APPENDIX C

LITERATURE RESOURCE REVIEW

Fig.(3): The increase in inlet charge heat capacities at various mass percent of EGR for the temperature range of diesel combustion

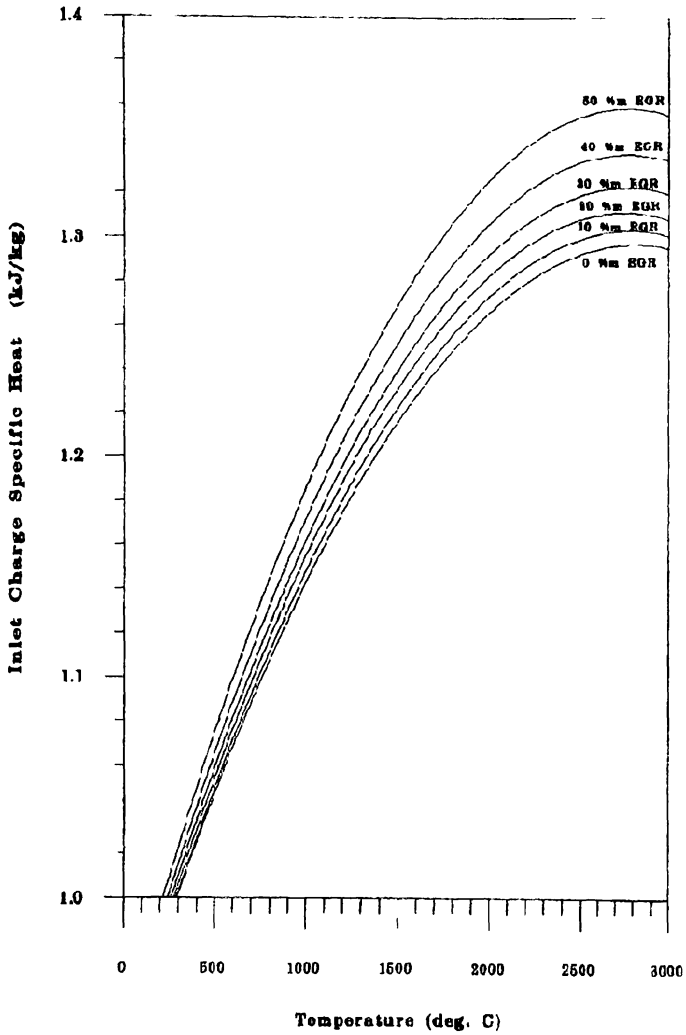

Figure 66: Inlet Charge Specific Heat from SAE 971660 (41)

Figure 66 is reprinted here from SAE 971660 and shows the relatively close specific heat capacity of different EGR mixtures in the intake manifold charge flow.

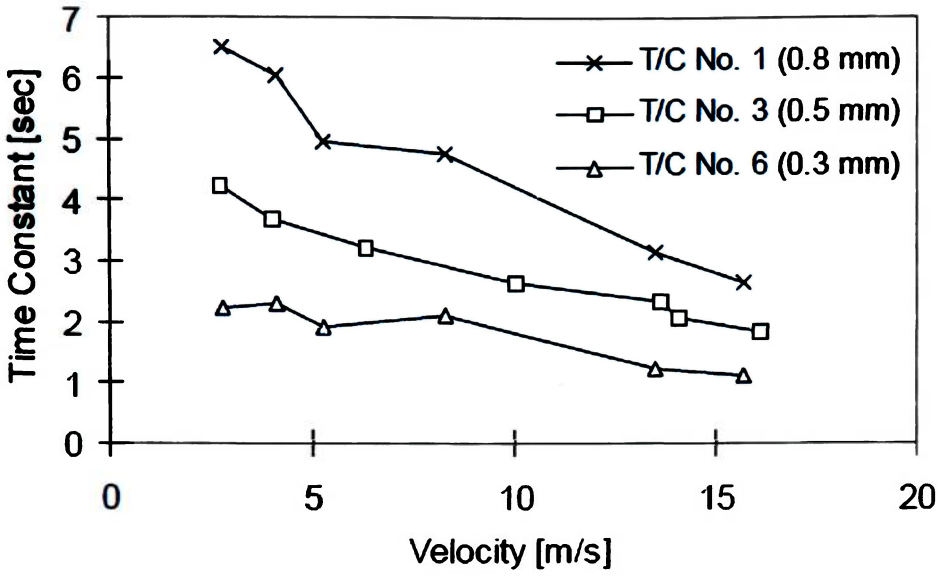

Figure 13. Variation of Time Constants with Velocity

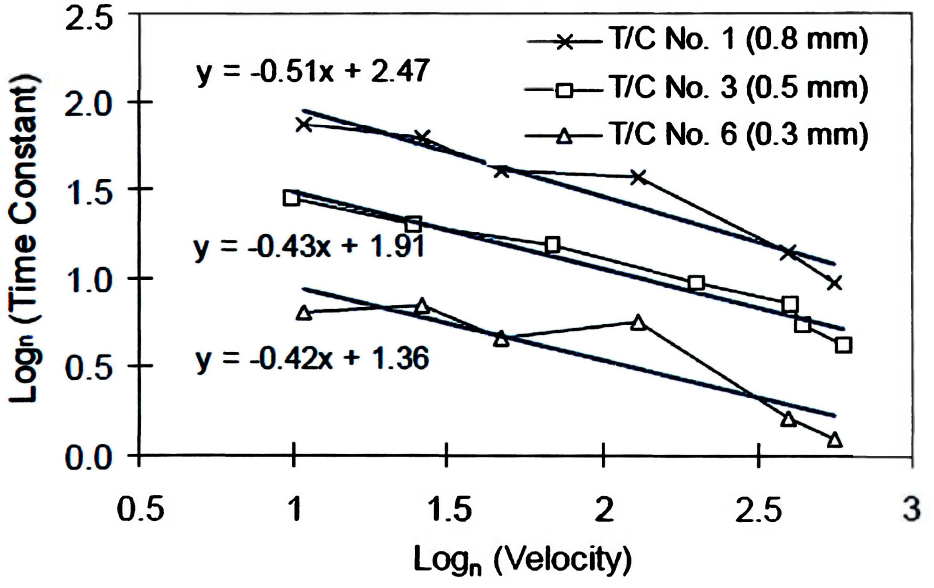

Figure 14. Logarithmic Relationship of Time Constant and Velocity

Figure 67: Variation of Sensor Time Constant with Flow Velocity from SAE983072 (34)

Figure 67 is reproduced here from SAE983072 for convenience and shows an example of how the time constant of a thermocouple can vary with the flow rate.

SENSOR TIME CONSTANT:

SAE2004-01-1418 (32)describes ways of calculating the time constants for the thermocouples, which allows for faster, more accurate temperature response measurement through sensor compensation. The paper focuses on a technique that requires two identical thermocouples to be placed in the same location. Since this is not the case for this study, an alternative method must be used. The paper does however, confirm that filtering methods must be employed during transients in order to distinguish real estimates from background noise. SAE2004-01-1418 (32) also makes the distinction that thermocouple time constants are dependent on the fluid flow characteristics, which are constantly changing in an ICE.

As stated in SAE2008-01-1175 (37): (Which pulls the equation below from Whitaker, S., AICHE Journal, Vol. 18, Page 361, 1972), reprinted here for convenience:

> The relationship between thermocouple relative error and the exhaust surface temperature and airflow rate is illustrated in figure 3. The convection heat transfer coefficient for air flow around a spherical thermocouple junction is calculated at different air stream velocities using the following equation by Whitaker [7]:

$$Nu = 2 + (0.4\,\mathrm{Re}^{1/2} + \mathrm{Re}^{2/3})(\mathrm{Pr})^{0.4}\left(\frac{\mu}{\mu_s}\right)^{1/4}$$

Calibration for the coolant correction tables can be performed as described in (42), again reprinted here for reference:

From EITIk_ICT.pdf –

Calibration Information

The following engine dynamometer tests should be run to calibrate the coolant temperature influence coefficient function

Measure the exhaust gas temperature, intake air temperature, and engine coolant temperature during steady state operation at several air and EGR mass flows After the data is collected, it can be used to

calibrate KtEITI_K_ICT_CoolTempInfluence Perform transient tests by changing air and EGR mass flows to determine the filter coefficient KtEITI_k_ICT_ChargeTempFilt This will be used to calibrate the correct transient response

APPENDIX D

REFERENCE CALIBRATION TABLES

The tables below are for reference when evaluating the initial model. They are not implied to be the actual correction values for any particular parameter, merely example tables that may be used for basic calibration and simulation.

V_disp = 6.6; % Engine displacement volume = 6.6 liter
R = 287; % Gas constant
EGRFracV = [-1, 0, 0.10, 0.20, 0.30, 0.40, 0.5, 0.6]; %EGR R Estimator Vector
RVarV = [288, 287.323, 286.490, 285.506, 284.722, 283.651, 283.184, 283.067]; %Variable R Range

% Volumetric Efficiency
KnEITC_V_VolMetricCalBY = [0 10 15 20 25 30 35 40 45 50 60 70 80 90 100 110];
KnEITC_n_VolMetricCalBX = [600 800 1000 1200 1400 1600 1800 2000 2200 2400 2600 2800 3000 3200 3400 3600 3800];
KtEITC_r_VolMetricCall = [
0.843 0.843 0.849 0.860 0.920 0.889 0.869 0.855 0.856 0.860 0.835 0.831 0.814 0.804 0.794 0.818 0.818
0.836 0.839 0.848 0.857 0.875 0.886 0.878 0.857 0.873 0.864 0.859 0.838 0.831 0.809 0.798 0.798 0.798
0.839 0.840 0.854 0.865 0.881 0.890 0.886 0.859 0.882 0.873 0.862 0.851 0.835 0.826 0.816 0.816 0.816
0.840 0.841 0.861 0.881 0.887 0.896 0.887 0.873 0.886 0.880 0.872 0.866 0.852 0.841 0.830 0.830 0.830
0.839 0.841 0.866 0.888 0.890 0.897 0.887 0.876 0.887 0.882 0.873 0.868 0.860 0.847 0.836 0.836 0.836
0.833 0.841 0.861 0.886 0.885 0.892 0.884 0.879 0.889 0.885 0.873 0.873 0.863 0.850 0.841 0.841 0.841
0.828 0.840 0.859 0.882 0.888 0.894 0.884 0.882 0.891 0.890 0.879 0.879 0.874 0.857 0.848 0.848 0.848
0.826 0.840 0.855 0.872 0.886 0.896 0.883 0.883 0.884 0.881 0.872 0.870 0.866 0.859 0.849 0.849 0.849
0.822 0.834 0.849 0.866 0.883 0.894 0.886 0.887 0.892 0.888 0.881 0.872 0.869 0.865 0.855 0.855 0.855
0.822 0.834 0.845 0.872 0.883 0.890 0.885 0.886 0.892 0.884 0.877 0.868 0.866 0.860 0.850 0.850 0.850
0.821 0.832 0.843 0.862 0.880 0.888 0.886 0.882 0.892 0.884 0.882 0.875 0.868 0.861 0.851 0.852 0.852
0.819 0.830 0.839 0.857 0.877 0.886 0.887 0.882 0.888 0.881 0.877 0.874 0.866 0.856 0.848 0.848 0.848
0.819 0.830 0.855 0.872 0.881 0.899 0.900 0.896 0.891 0.887 0.892 0.882 0.881 0.873 0.862 0.863 0.863
0.819 0.830 0.855 0.871 0.881 0.899 0.900 0.900 0.887 0.886 0.878 0.877 0.872 0.864 0.854 0.855 0.855
0.819 0.830 0.855 0.871 0.881 0.899 0.900 0.902 0.887 0.896 0.885 0.874 0.867 0.864 0.854 0.855 0.855
0.819 0.830 0.855 0.871 0.880 0.899 0.900 0.904 0.884 0.882 0.885 0.880 0.868 0.873 0.863 0.855 0.855];

%Correction for Engine Speed and Fuel
%KnEITC_V_VolMetricCalBY = [0 10 15 20 25 30 35 40 45 50 60 70 80 90 100 110];
%KnEITC_n_VolMetricCalBX = [600 800 1000 1200 1400 1600 1800 2000 2200 2400 2600 2800 3000 3200 3400 3600 3800];

% Row: KnEITC_V_VolMetricCalBY
% Column: KnEITC_n_VolMetricCalBX

FuelSpeed =[
0.700 0.700 0.700 0.700 0.700 0.700 0.700 0.700 0.700 0.700 0.700 0.700 0.700 0.700 0.700 0.700 0.700
0.800 0.800 0.700 0.700 0.700 0.700 0.700 0.700 0.700 0.700 0.700 0.700 0.700 0.700 0.700 0.700 0.700
0.700 0.780 0.700 0.700 0.850 0.850 0.700 0.700 0.700 0.700 0.700 0.700 0.700 0.700 0.700 0.700 0.700
0.700 0.700 0.700 0.700 0.800 0.800 0.700 0.700 0.700 0.700 0.700 0.700 0.700 0.700 0.700 0.700 0.700
0.700 0.700 0.700 0.700 0.700 0.700 0.700 0.700 0.700 0.700 0.700 0.700 0.700 0.700 0.700 0.700 0.700
0.700 0.700 0.700 0.700 0.700 0.700 0.700 0.700 0.700 0.700 0.700 0.700 0.700 0.700 0.700 0.700 0.700
0.700 0.700 0.700 0.700 0.700 0.700 0.700 0.700 0.700 0.700 0.700 0.700 0.700 0.700 0.700 0.700 0.700
0.700 0.700 0.700 0.700 0.900 0.900 0.700 0.700 0.700 0.700 0.700 0.700 0.700 0.700 0.700 0.700 0.700
0.700 0.700 0.700 0.700 0.700 0.700 0.700 0.700 0.700 0.700 0.700 0.700 0.700 0.700 0.700 0.700 0.700
0.700 0.700 0.700 0.700 0.700 0.700 0.700 0.700 0.700 0.700 0.700 0.700 0.700 0.700 0.700 0.700 0.700
0.700 0.700 0.700 0.700 0.700 0.700 0.700 0.700 0.700 0.700 0.700 0.700 0.700 0.700 0.700 0.700 0.700
0.700 0.700 0.700 0.700 0.700 0.700 0.700 0.700 0.700 0.700 0.700 0.700 0.700 0.700 0.700 0.700 0.700
0.900 0.900 0.900 0.900 0.900 0.900 0.900 0.900 0.900 0.900 0.900 0.900 0.900 0.900 0.900 0.900 0.900

```
0.900 0.900 0.900 0.900 0.900 0.900 0.900 0.900 0.900 0.900 0.900 0.900 0.900 0.900 0.900 0.900 0.900
1.000 1.000 1.000 1.000 1.000 1.000 1.000 1.000 1.000 1.000 1.000 1.000 1.000 0.900 0.900 0.900 0.900
1.000 1.000 1.000 1.000 1.000 1.000 1.000 1.000 1.000 1.000 1.000 1.000 1.000 1.000 0.900 0.900 0.900
];

%Vectors for Mass Flow and Vehicle Speed Corrections
Mass_Flow =[0 10 20 30 40 50 60 70 80 90 100 110 120 130 140 150 160 170 250 300 ];
%First_Order_Lag_Coeff
First_Order_Lag_Coeff =
[0.1,0.1,0.1,0.1,0.05,0.05,0.05,0.05,0.05,0.05,0.05,0.05,0.05,0.05,0.05,0.05,0.05,0.05,0.05,0.05];

% Temperature Sensor Time Constant Correction
CAC_TC =[1.9 1.8 1.7 1.7 1.6 1.5 1.4 1.3 1.2 1.1 1 1 1 1 1 1 1 1 1 1 ];
EGR_TC =[1.3 1.3 1.3 1.3 1.3 1.0 1.0 1.0 1.0 1.0 1 1 1 1 1 1 1 1 1 1 ];


%Cool_Temp_Coef_1D
Cool_Temp_Coef_1D =[0.6,0.6,0.5,0.5,0.5,0.5,0.5,0.5,0.4,0.4,0.4,0.4,0.4,0.4,0.4,0.4,0.4,0.4,0.4,0.4];

% Cooling Losses Correction Table -2D Table Used for on Vehicle Calibration Not Used in Cell
];
Veh_Speed = [0 5  10 15 20 25 30 35 40 45 50 55 60 65  70 80 90 100 110 120];

% Row Index: Veh_Speed
% Column Index: Mass_Flow

%*NOTE TABLE MUCH LARGER THAN NEEDED AT PRESENT!
Coolant_Temperature_Coefficient = [
0.6 0.6 0.5 0.5 0.5 0.5 0.5 0.5 0.4 0.4 0.4 0.4 0.4 0.4 0.4 0.4 0.4 0.4 0.4 0.4
0.6 0.6 0.5 0.5 0.5 0.5 0.5 0.5 0.4 0.4 0.4 0.4 0.4 0.4 0.4 0.4 0.4 0.4 0.4 0.4
0.6 0.6 0.5 0.5 0.5 0.5 0.5 0.5 0.4 0.4 0.4 0.4 0.4 0.4 0.4 0.4 0.4 0.4 0.4 0.4
0.6 0.6 0.5 0.5 0.5 0.5 0.5 0.5 0.4 0.4 0.4 0.4 0.4 0.4 0.4 0.4 0.4 0.4 0.4 0.4
0.6 0.6 0.5 0.5 0.5 0.5 0.5 0.5 0.4 0.4 0.4 0.4 0.4 0.4 0.4 0.4 0.4 0.4 0.4 0.4
0.6 0.6 0.5 0.5 0.5 0.5 0.5 0.5 0.4 0.4 0.4 0.4 0.4 0.4 0.4 0.4 0.4 0.4 0.4 0.4
0.6 0.6 0.5 0.5 0.5 0.5 0.5 0.5 0.4 0.4 0.4 0.4 0.4 0.4 0.4 0.4 0.4 0.4 0.4 0.4
0.6 0.6 0.5 0.5 0.5 0.5 0.5 0.5 0.4 0.4 0.4 0.4 0.4 0.4 0.4 0.4 0.4 0.4 0.4 0.4
0.6 0.6 0.5 0.5 0.5 0.5 0.5 0.5 0.4 0.4 0.4 0.4 0.4 0.4 0.4 0.4 0.4 0.4 0.4 0.4
0.6 0.6 0.5 0.5 0.5 0.5 0.5 0.5 0.4 0.4 0.4 0.4 0.4 0.4 0.4 0.4 0.4 0.4 0.4 0.4
0.6 0.6 0.5 0.5 0.5 0.5 0.5 0.5 0.4 0.4 0.4 0.4 0.4 0.4 0.4 0.4 0.4 0.4 0.4 0.4
0.6 0.6 0.5 0.5 0.5 0.5 0.5 0.5 0.4 0.4 0.4 0.4 0.4 0.4 0.4 0.4 0.4 0.4 0.4 0.4
0.6 0.6 0.5 0.5 0.5 0.5 0.5 0.5 0.4 0.4 0.4 0.4 0.4 0.4 0.4 0.4 0.4 0.4 0.4 0.4
0.6 0.6 0.5 0.5 0.5 0.5 0.5 0.5 0.4 0.4 0.4 0.4 0.4 0.4 0.4 0.4 0.4 0.4 0.4 0.4
0.6 0.6 0.5 0.5 0.5 0.5 0.5 0.5 0.4 0.4 0.4 0.4 0.4 0.4 0.4 0.4 0.4 0.4 0.4 0.4
0.6 0.6 0.5 0.5 0.5 0.5 0.5 0.5 0.4 0.4 0.4 0.4 0.4 0.4 0.4 0.4 0.4 0.4 0.4 0.4
0.6 0.6 0.5 0.5 0.5 0.5 0.5 0.5 0.4 0.4 0.4 0.4 0.4 0.4 0.4 0.4 0.4 0.4 0.4 0.4
0.6 0.6 0.5 0.5 0.5 0.5 0.5 0.5 0.4 0.4 0.4 0.4 0.4 0.4 0.4 0.4 0.4 0.4 0.4 0.4
0.6 0.6 0.5 0.5 0.5 0.5 0.5 0.5 0.4 0.4 0.4 0.4 0.4 0.4 0.4 0.4 0.4 0.4 0.4 0.4
0.6 0.6 0.5 0.5 0.5 0.5 0.5 0.5 0.4 0.4 0.4 0.4 0.4 0.4 0.4 0.4 0.4 0.4 0.4 0.4
0.6 0.6 0.5 0.5 0.5 0.5 0.5 0.5 0.4 0.4 0.4 0.4 0.4 0.4 0.4 0.4 0.4 0.4 0.4 0.4
0.6 0.6 0.5 0.5 0.5 0.5 0.5 0.5 0.4 0.4 0.4 0.4 0.4 0.4 0.4 0.4 0.4 0.4 0.4 0.4
0.6 0.6 0.5 0.5 0.5 0.5 0.5 0.5 0.4 0.4 0.4 0.4 0.4 0.4 0.4 0.4 0.4 0.4 0.4 0.4
0.6 0.6 0.5 0.5 0.5 0.5 0.5 0.5 0.4 0.4 0.4 0.4 0.4 0.4 0.4 0.4 0.4 0.4 0.4 0.4
0.6 0.6 0.5 0.5 0.5 0.5 0.5 0.5 0.4 0.4 0.4 0.4 0.4 0.4 0.4 0.4 0.4 0.4 0.4 0.4
0.6 0.6 0.5 0.5 0.5 0.5 0.5 0.5 0.4 0.4 0.4 0.4 0.4 0.4 0.4 0.4 0.4 0.4 0.4 0.4];
```

APPENDIX E

ADDITIONAL PUBLICATIONS AND REPORTS BY THESIS AUTHOR

ASME ES2010-90411

Proceedings of the ASME 2010 4th International Conference on Energy Sustainability
ES2010
May 17-22, 2010, Phoenix, Arizona, USA

ES2010-90411

DESIGN AND ASSEMBLY OF AN EXTENDED RANGE ELECTRIC VEHICLE AS A UNIVERSITY CAPSTONE PROJECT

Vincent J. Sabatini — Ryle Maxson
William Haupfear — Sean Carter
Darris White — J. E. McKisson

Embry-Riddle EcoEagles
Embry-Riddle Aeronautical University Daytona Beach, Florida 32114

ABSTRACT

The Embry-Riddle HyREV system is an innovative combination of power-split Hybrid and Extended-Range Electric Vehicle technologies, designed to reduce petroleum energy consumption and improve vehicle efficiency across a range of operating conditions on a captured GM fleet vehicle. The HyREV system was developed for the EcoCAR Challenge and features a high degree of vehicle electrification including all electric accessories plug-in charging and electric all-wheel-drive through the integration of three electric motors. The proper packaging and integration of components used in the EcoCAR vehicle development process required a comprehensive understanding of element interaction from both a static (space claim) and dynamic (feasibility) standpoint.

The research conducted in this competition is used as a capstone project for a wide array of majors, as well as being integrated extensively in several courses in the form of projects and lectures. The overall vehicle design requires expertise in mechanical, electrical, aerospace, computer software and controls engineering as well as incorporating human factors students into the failure modes and effects analysis. The team is split into the different majors for organizational hierarchy however, there are many tasks that require multidisciplinary ideas and experiences to properly design.

The first year of EcoCAR incorporated an entirely virtual design, with the teams receiving hardware in year two. The team is currently in year two, and is assembling the physical components of the vehicle, along with the controls architecture that will drive the vehicle's power systems. This 65% "mule" vehicle will be tested May 2010 at GM's Desert Proving Grounds, located in Yuma, Arizona.

INTRODUCTION

Each of 17 teams in EcoCAR were given the same base platform GM Crossover SUV to redesign to be more fuel efficient and achieve better emissions while maintaining or improving upon the stock performance of the vehicle. All desired powertrain and chassis modification must be within the confines of this base vehicle.

Design of the HyREV system is based on the detailed analysis of a team of students supervised by both university faculty advisors and a combination of support from the Argonne National Laboratory (ANL) organizers and competition sponsors. Each team is also assigned industry mentors from several of the sponsors including GM, The Mathworks, and National Instruments. The program is supported over a three year design cycle that emphasizes separate major goals in each of the individual years.

The first year provided the basis for the architecture selection and vehicle platform via extensive simulation and CAD design. The second year is primarily an assembly and powertrain control and development testing stage. The third year will focus on control and aerodynamic optimization, and weight reduction.

The competition is a student driven one with a focus on not only vehicle design, but on preparing students to enter the automotive and automotive support industries. Industry standard tools, software and design practices are all employed to allow for an easy transition into the workplace, where the sponsors benefit from have new employees already trained and familiar with their operations. In addition, sponsor mentors from GM, NI etc. allow for unparalleled access to expert advice on component use, system-level design and software troubleshooting.

VEHICLE DESIGN

The HyREV design differs from many of the current offerings in production hybrid vehicles. However, it should be noted that this is a prototype design, and as such, some of the manufacturing techniques, materials used, and hardware integrated are not currently cost effective, and therefore would have to be substantially reduced before such a vehicle could go into production. Some of this would be covered by an economy of scale, but the major focus of the competition is not to develop a production vehicle for GM, but rather to prove that several hybrid vehicle powertrain concepts would be feasible, both from a fuel economy standpoint and a utility standpoint, and to educate students in the hardware and industry practices.

Table 1: HyREV Vehicle Technical Specifications

Accel 0-60	8.7
Accel 50-70	5.3
Fuel Economy Gasoline Equivalent	37.7 mpg
Electric Range	20 miles
Full Tank Charge Range	320 miles
Towing Capacity	680 kg
Cargo Capacity	20.5 ft^3

Table 1 lists some of the vehicle technical specifications for the HyREV vehicle. The design goals of the competition focus on a design that obtains higher fuel economy and lower emissions, while maintaining the utility and performance of a conventional vehicle. This means that while the vehicle has an electric range of 20 miles and a significantly higher fuel economy (38.3 mpg stock) it also still seats 5 passengers can tow, accelerate rapidly, fit a significant amount of cargo, and drive 300+ miles on a full tank unlike many current hybrid and electric vehicle model on the market.

CAPSTONE DESIGN

The EcoCAR project represents the definitive final design, or "capstone", project for student engineers. It incorporates numerous learned disciplines over the academic career of the students in order to safely and correctly design the various vehicle subsystems. The project requires not only mechanical design but also electrical, controls, human factors, and aerodynamic design as well, and is thus suitable for many of the majors to use the project for their respective degree requirements.

The project is as close to a "real-world" project as can be expected with many of the unexpected problems, delays, personnel issues that are found in any engineering industry. The competition sets deliverable deadlines which determine the team's milestones, and subsequently the success or failure of the students' work. As in the real world, failing to meet necessary milestones can have severe consequences. The team also has to deal with the logistics of component procurement and delivery. Dealing with out of stock or delayed components is a common but real challenge that must be overcome.

Unlike most of the current capstone projects at the university, this project goes beyond simple design and documentation. Not only is there a rigorous design component, but the design has to suit a third party of judges with a specified design report format. This design then needs to be implemented, with the various subsystems being physically built, integrated, and tested. This test vehicle will then need to be refined and optimized to maximize the performance of the vehicle. This will happen over the course of three years with various design teams changing people over the course of the competition as people graduate. This necessitates high-quality documentation, which allows for the easy transition from one year to the next.

As stated, the project would require numerous majors working on the project, which is another significant departure from other projects. Instead of a capstone that only use one discipline, EcoCAR makes use of numerous students working together, relying on one another, and solving the problems that play to their respective strengths. This forces the team to approach problems from multiple angles to ensure that problems aren't overlooked from a particular discipline.

TEAM ORGANIZATION

The Team is split into 3 main design tracks, as shown in Figure 1. Each of these groups has a leader that is responsible for the decisions and progress made under him or her. There is also an Outreach and Business aspect to the project, which involves community involvement and education, which also has its own group leader. Finally, there is a Team Leader and Co-Team Leader, who are the final word in all design decisions able to even override the group leads. These leaders are usually senior or graduate level students with the most experience in the project. This ensures that no one group can make design decisions that can hinder the other divisions for their own gain.

This checks and balances system is furthered by the inclusion of a faculty advisory board that meets with the team and group leaders often. This board is composed of a faculty member from mechanical, electrical, aerospace, software, and computer engineering, as well as an engineering physicist. Any decisions that affect more than one group are reviewed to determine the level of the effects, and whether another, more mutual solution can be found. This allows all groups to voice their concerns, as well as having the opinions of the experienced faculty.

This checks and balances system is furthered by the inclusion of a faculty advisory board that meets with the team and group leaders often. This board is composed of a faculty member from mechanical, electrical, aerospace, software, and computer engineering, as well as an engineering physicist. Any decisions that affect more than one group are reviewed to determine the level of the effects, and whether another, more mutual solution can be found. This allows all groups to voice their concerns, as well as having the opinions of the experienced faculty.

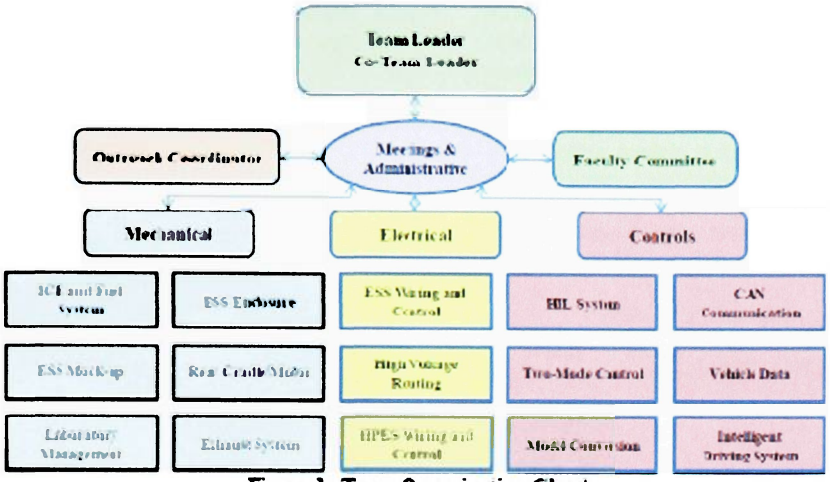

Figure 1: Team Organization Chart

The Mechanical Group is primarily in charge of the physical modeling of the vehicle, both dynamically and geometrically, as well as the eventual assembly and integration of the vehicle. The mechanical team works with a human factors group that is helping with ergonomics and hazard mitigation. In addition, powertrain integration and refinement, as well as weight reduction and aerodynamic optimization, will all be handled by the mechanical team. This represents the largest percentage of the team, but it is also responsible for the largest portion of the work to be done.

The Electrical Group is primarily in charge of the modeling of the high voltage system in the vehicle, and are responsible for the assembly and wiring of the battery pack for the vehicle, which is easily the single most complex, expensive, and dangerous component on the vehicle. The modules being used are donated; however the enclosure, wiring schematics, and safety systems are all being custom designed by the team. Also, the extremely high voltage represents a huge danger, both to the vehicle and its systems, as well as any students or potential drivers. So while this group seems to have the least assigned to them, the danger, and therefore required safe hazard mitigation and redundancy, makes this an equally critical component of the team.

The Controls Group is in charge of arguably the most difficult aspect of the project, which is the vehicle control system. This task requires not only logic that must be designed and endlessly refined, but also requires the ability to safely, accurately, and rapidly communicate with all of the components of the vehicle. Due to the complexity of the system, coupled with the necessary electrical and mechanical backgrounds required to properly interpret the system inputs and outputs, this group has the most trouble finding and retaining members to work on it. New students to the project cannot immediately start working on the control system because of this, as well as the sensitivity of the control logic to even slight changes, which can make uneducated changes turn into huge time losses in order to find and correct the mistake.

Each of these groups has their own respective tasks assigned to them the most important of which are shown in Figure 1. This hierarchy is reviewed and updated as the project progresses, with new people entering leadership roles as necessary, along with task being added or removed based on design and assembly progress. This overall hierarchy allows for both independent leadership and progress for each of the groups, while ensuring that the overall focus and goal of the competition is not lost, which fits with the desire to use system engineering techniques to manage the project.

One of the goals of the EcoCAR competition is to adapt the Road-to-Lab-to-Math mentality. Industry vehicle design is moving away from building expensive and time consuming prototypes to just test to perfection, and moving towards developing more lab and math based designs. For this reason, the first year of the competition is all design, with a focus on software and hardware-in-the-loop (SIL, HIL). Using this design philosophy vehicle design time can be taken from decades to years.

The team consists of students of varying levels of involvement. Some students are working on the project for fun and the experience that comes with it, while some are using the project for engineering elective credits. For use as a capstone project, this paper will focus on those students that are working on their respective senior design projects, which represent more complex tasks than those that are assigned to other students.

MECHANICAL GROUP

The Mechanical Group seniors are predominately tasked with designing components that have critical requirements that much be met. All components, especially

those that are replacing structures on the stock vehicle, must meet strict design criteria (1.5 FS). This forces the students to not only perform FEA on any parts they design, but to also document their design for the purposes of design waivers and competition design reports. An excerpt from the team's rear cradle waiver is shown in Figure 2.

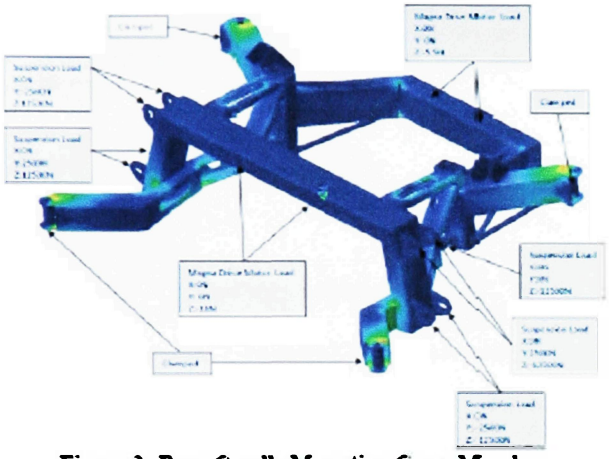

Figure 2: Rear Cradle Mounting Cross Member Preliminary FEA with Loading Conditions

The students are also assembling the entire vehicle in CAD to ensure that all components will have an appropriate space claim, taking into account clearances and work space. This is important, as it allows the different design groups to look at the "completed" vehicle while making design changes, reducing the chances of invalid redesign. This virtual vehicle is constantly referenced for alternative designs, especially as design flaws come to light as the project progresses. The Electrical Storage System (ESS) assembly CAD can be seen in Figure 3.

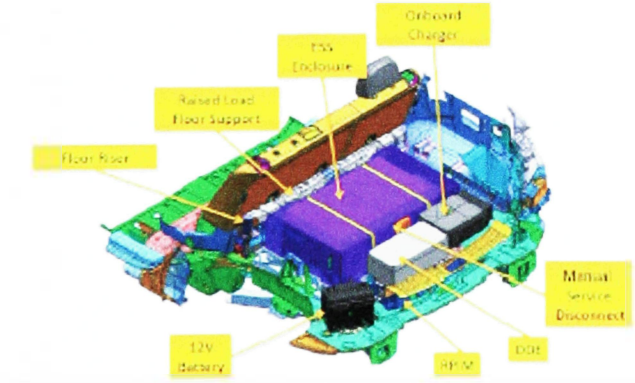

Figure 3: ESS Assembly

The vehicle was virtually modeled during the first year of the competition using the Powertrain Systems Analysis Toolkit (PSAT), which required extensive experience with MATLAB and Simulink. Using this tool, the team was able to rapidly prototype several possible powertrain architectures. These analyses provided potential performance specifications, such as top speed, 0-60 time, energy use, and fuel economy. Very coarse models were developed for all possible design configurations, determined by the donated components, competition rules and requirements, and the team's estimated budget. These designs were then ranked based on several of the performance aspects that competition scoring would be based on.

Table 2: Architecture Decision Matrix

Option	Performance	Fuel Economy	WTW GHG	Tailpipe Emissions	WTW PEU	Norm Score	Rank
2.4L Production Vue	3.7	2	2	2	2	0	
1.3L B20 2-mode AWD HEV	2	2	5.8	9.2	2	3.5	
1.3L B20 2-mode AWD PHEV10	2	6.3	8.2	9.7	2.5	6.4	
1.3L B20 2-mode AWD PHEV20	3	10	10	10	5.2	10	1
1.3L B20 2-mode FWD HEV	2	2	5.6	9.2	2	3.4	
1.3L B20 2-mode FWD PHEV10	2	6.2	8	9.7	2.4	6.3	
1.3L B20 2-mode FWD PHEV20	3	10	9.9	10	5.2	9.9	2
2.4L E85 BAS-AWD HEV	5.6	2	2	2	6.6	2.5	
2.4L E85 BAS-AWD PHEV10	7.5	4.8	2	2.2	8.6	5	
2.4L E85 BAS-AWD PHEV20	10	4.8	2	4.2	10	9.3	3

The three most promising architectures were then refined in PSAT to be more accurate, along with testing different control algorithms, battery sizes, and driving conditions. The architectures were also run through ANL's GREET model to estimate the Well-To-Wheels (WTW) greenhouse gas (GHG) emissions and petroleum energy usage (PEU). These detailed analyses were more complex, and required more time to both develop and analyze, with the result being much more accurate performance specifications. These models were then ranked again using the same decision matrix to determine the team's desired architecture, as shown in Table 1. It should be noted that the architecture chosen in year one is set and unable to be changed for the remainder of the competition.

ELECTRICAL GROUP

The Electrical Group seniors are primarily in charge of designing the High Power Electrical System (HPES), including the ESS design. They also help advise the mechanical and controls groups on the operation and performance characteristics of the electrical systems.

The HPES design maximizes safety and serviceability while optimizing wiring geometry for the GM 2-Mode Transmission (TRANS) and the electric Rear Wheel Drive system (eRWD). The HPES consists of the ESS, a Manual Isolation Switch (MIS), a Disconnect and Distribution

Enclosure (DDE), a Plug-In Charge Controller (PCC), DC/DC converter (DCDC), and the Emergency Disconnect System (EDSYS).

With exception of the contactors in the ESS, the HPES design encloses all HV switching and safety components in the DDE. This simplifies wiring topology and helps assure safety. The geometry of DDE placement eliminates exposed wiring to the ePWT controller and minimizes other exposed wiring runs. Figure 4 shows the simplified wiring schematic for the HPES, encompassing the energy storage system and disconnect enclosure.

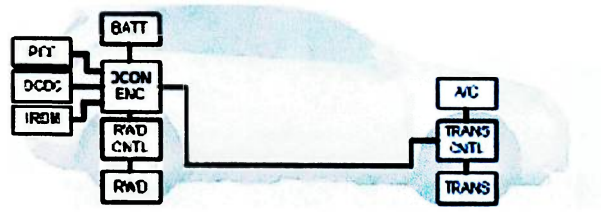

Figure 4. HPES Simplified Wiring Schematic

The HPES system combines selection of components with a design that implements a rule-compliant, safe, reliable and highly functional system for transferring electrical energy between electrical drivetrain and energy storage elements. Safety is assured through careful matching of wire, fuses, switching components and materials and by applying a wiring topology that eliminates unnecessarily exposed HV conductors. Component selection has taken into account thermal and electromagnetic compatibility issues to minimize or eliminate problems with the high power system integration and control. The design concept selected also takes into account the specialized safety considerations of the emergency disconnect and manual isolation systems.

Development of the ESS is a large part of the project plan for the vehicle. The tasks required to realize the ESS include developing a design, building a high voltage work area, developing safety procedures, training, manufacturing, assembly and testing. The ESS design for the vehicle integrates 4 of the A123 2?S2P modules in series to yield a 12.9kWh energy storage capacity at 330V nominal. The pack is water cooled through an integrated cooling/mounting plate connected to a dedicated radiator and coolant loop. The ESS enclosure is sealed and vented to the exterior of the vehicle though a check valve.

The cooling system is an integral part of the ESS design and development. These tasks include the design, manufacture and testing of the cooling system. This process will include manufacturing the enclosure, integrating the cooling system, and constructing the battery pack. The ESS will be subjected to a range of bench tests to ensure communication with the BMS and controller, temperature management and performance.

Persons working on the high voltage system are required receive training on proper operating and safety procedures. A list of safety procedures has been prepared and a safety short course has been developed by the University's Environmental, Health and Safety department. Assembly of the ESS may not begin until the new HV workroom has been inspected by the University's Director of Environmental, Health and Safety.

CONTROLS GROUP

The Controls Group seniors are predominately tasked developing the control architecture of the vehicle, following a V-diagram strategy for verification and validation (Figure 5). This required developing system models of all of the vehicle components that would require active control, which were modified versions of those used in the mechanical powertrain simulations. However, the control would be coming from the team's Supervisory Control Unit (SCU) rather than the more generic ones in PSAT.

The SCU controls the vehicles operations using Controller-Area Network (CAN) signals. This requires mechanical, electrical, and software backgrounds to understand and program. The signals themselves control a variety of electro-mechanical mechanisms, which requires a mechanical background to understand and obtain the desired physical output of the mechanisms. However, CAN is a digital signal, which requires extensive wiring, as shown in Figure 6, and an electrical and software background to decipher and program the multitude of different possible signals.

The system models were converted to National Instruments' (NI) Labview models, as team is using all NI software and hardware for the control system. These models were modified to make CAN the inputs and outputs of the systems, so that each of the systems could "talk" to one another, as well as with the SCU. This allows for the safe testing of the SCU control logic by communicating with each system individually using pre-recorded vehicle data, which will bring problems to light before they can damage actual hardware.

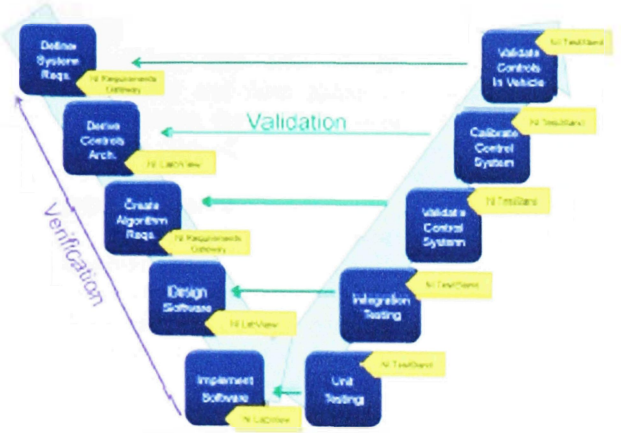

Figure 5: Software V-Diagram

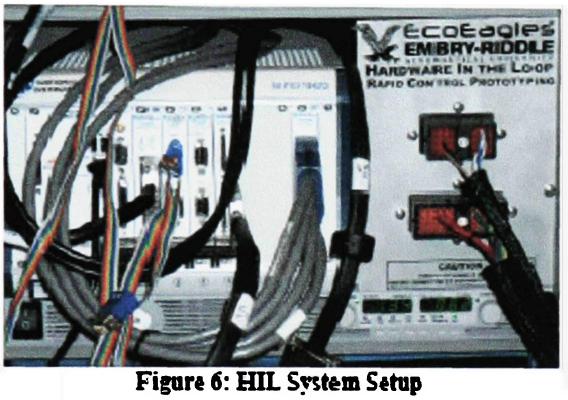

Figure 6: HIL System Setup

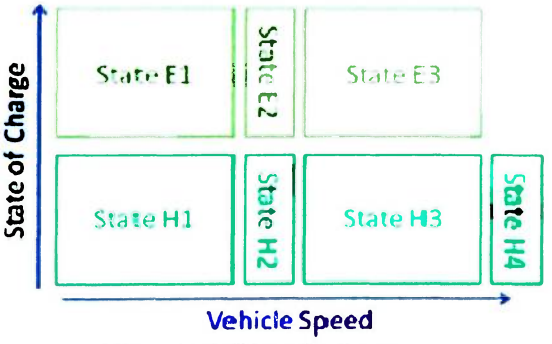

Figure 7: SCU Control Strategy

The control strategy developed had to optimize performance characteristics, especially fuel economy, for a variety of driving conditions. The SCU overall strategy developed is shown in Figure 7. This state diagram determines the optimum driving mode, which determines which powertrain components are supplying power to the wheels. These driving modes are primarily determined by the current vehicle speed (driver power demand) and the current battery state-of-charge (SOC). At a higher SOC, the vehicle will drive in an all electric (charge depleting) mode, while driving in a hybrid (charge sustaining) mode when the SOC drops below desirable limits.

The Intelligent Driving Efficiency Assistant (IDEA) group is an offshoot of the controls team, comprised of software and computer engineers. The IDEA system, diagramed in Figure 8, will gather external data, such as the GPS position, current and predicted traffic, and road elevations, and compare this information to historical driving profiles. The IDEA system will determine the most efficient driveline configuration(s) for the estimated remaining driving schedule and submit the selection to the SCU. The SCU will consider the recommendation from the IDEA system and determine if the recommendation is feasible and safe for the real-time operating conditions. The IDEA system does not communicate directly with the component control modules, but rather is a factor that the SCU takes into consideration.

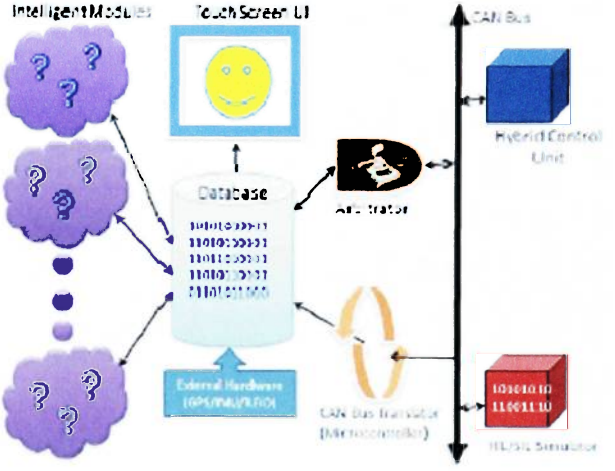

Figure 8: IDEA System

MENTORSHIP

Each team in the EcoCAR competition is given a GM team mentor, someone who has significant vehicle design experience, and is usually in charge of their own team at GM. The mentors give feedback on the designs and team reports, offering suggestions for improvement, or pointing out flaws in the designs. Acting as a private contact at GM, they have the ability to track down answers to technical questions and part locations that would otherwise be difficult or impossible to obtain otherwise. They also make personal visits to the campuses to help in person as well, make sure the labs and teams are adequately equipped for the project, as well as helping to recruit the most talented students to work for GM.

There are also similar forms of mentoring from some of the other sponsors, and especially the ANL organizers. Company reps from Snap-On, The Mathworks, NI, and A123 have all made visits to teams to help with installation and troubleshooting of various components. Technical phone conferences were arranged any time there were significant

developments or difficulty regarding a particular sponsored component. The ESS design actually required both a preliminary and final phone conference design review with A123 before the designs would be approved and have the batteries shipped.

CONCLUSION

This project has had an amazing effect on the students involved. Many of the seniors and graduate students involved have already secured jobs because of their involvement with the EcoCAR project, as well as making numerous industry contacts. In addition, the students have learned about team dynamics, industry standard tools and practices, and the communication skills required to be well rounded engineers, which is and should be the goal of a capstone project.

ACKNOWLEDGEMENTS

The authors would like to acknowledge the support provided by the EcoCAR competition organizers, the Department of Energy, General Motors, Natural Resources Canada and the many sponsors that make this program a success.

ERAU ECOEAGLES FINAL TECHNICAL REPORT FOR YEAR 2

ERAU EcoEagles' HyREV: EcoCAR Year Two Final Technical Report

Vincent J. Sabatini, Ryle Maxson, William Haupfear, Sean Carter, Darris White, and J. E. McKisson
Embry-Riddle Aeronautical University

Scott Miller
General Motors

ABSTRACT

EcoCAR: The NeXt Challenge is a three-year collegiate advanced vehicle technology competition (AVTC) established by the United States Department of Energy (DOE) and General Motors (GM). Argonne National Laboratory (ANL) has managed the AVTC series for 20 years.

The competition challenges 16 North American universities to reduce the environmental impact of a Chevrolet EcoCAR by minimizing its fuel consumption and reducing emissions while retaining the vehicle's performance, safety and consumer appeal. Sponsors of the competition provide teams with the engineering tools, equipment and technical assistance required to execute this realistic vehicle design project. Using these tools the ERAU team, the EcoEagles, have devised a Plug-In Hybrid Electric Vehicle propulsion system. The team has built a prototype vehicle that will be tested at GM's Desert Proving Grounds in Yuma, Arizona.

Vehicle electrification and the use of biodiesel fuel are center themes of the EcoEagles' strategy for improving fuel economy and tailpipe emissions. The EcoEagles selected an electric range of approximately 40 km. The median commuter drives less than 40 km per day, which means that most of the vehicle operation will be conducted using either fully electric or electric-assisted propulsion. When driving conditions required high tractive forces or long distances, an efficient biodiesel engine will couple with two electric motors through an innovative electrically variable transmission, known as the 2-mode transmission. The EcoEagles design will reduce petroleum energy consumption by 78%, improve fuel economy by 66% and reduce well-to-wheel greenhouse gas emissions by 30%.

The Year Two Final Technical Report focuses on the implementation of the Year One design and performance validation of VTS produced through modeling and HIL development. The report presents the vehicle's architecture and background information to help the reader understand why this given architecture was chosen and how it might compare to the base Chevrolet EcoCAR. Major subsections focus on powertrain integration, control, and ESS design. Performance predictions made from simulations are contrasted against those from HIL development and finally on-road testing, with the goal of showing why the model-based, HIL-enhanced, and vehicle-tested VTS did or did not agree.

INTRODUCTION

The EcoCAR Challenge is an effort by the US Department of Energy, GM, and National Resources Canada to promote the development of cleaner, more efficient vehicles as part of a comprehensive educational program. The EcoEagles team represents Embry-Riddle Aeronautical University (ERAU) in this three year competition. The design goals for this competition are to reduce petroleum energy consumption and reduce well-to-wheel (WTW) emissions, while maintaining consumer acceptability. Because of the availability and efficiency of electricity and electric power systems, vehicle electrification was identified as a key technology for this project.

The modern automotive is the result of over a century of evolution. A wide range of propulsion systems have been attempted with electric, hybrid-electric and plug-in hybrid vehicles having been developed as starting in the late 1800s. GM developed an experimental plug-in hybrid vehicle, called the XP-883, in 1969 (1). Despite notable efforts to increase the degree of vehicle electrification, the cost, weight, and complexity of these systems has prevented widespread market acceptance. Recent advances in battery, and control system technologies, along with increased awareness of the environmental impact of petroleum energy use, have resulted in new opportunities for vehicle electrification. The EcoEagles' HyREV system features a high degree of vehicle electrification including; an all-electric driving range of 40 km, all electric accessories, plug-in charging and electric all-wheel-drive and the integration of three electric motors each with over 55kW of peak power. The competition requirements and EcoEagles' vehicle can be seen in Table 1.

Table 1: Vehicle Technical Specifications

Specification	Competition		EcoEagles
EcoCAR	Stock Chevrolet	Competition Requirement or Target	Projected
Accel 0-60	10.6 s	≤14 s	12 s
Accel 50-70	5.7 s	≤10 s	9 s
Towing Capacity	680 kg (1500 lb)	≥580 kg @ 3.5% 20 min @ 72 kph (45 mph)	680 kg
Cargo Capacity	.83 m^3	Height: 457mm (18") Depth 686mm (27") Width: 762mm (30")	Height: 630 mm (24.8") Depth: 920 mm (36.2") Width: 1000 mm (39.4")
Passenger Capacity	5	4	5
Braking 60 - 0	38 m- 43 m (123 -140 ft)	< 53.8 m (170 ft)	46m (151 ft)
Mass	1758 kg (3875 lb)	≤ 2268 kg (5000 lb)	1976 kg
Starting Time	≤ 2 s	≤ 15 s	10s
Ground Clearance	198 mm (7.8 in)	≥178 mm (7 in)	178 mm (7 in)
Range	> 580 km (360 mi)	≥ 320 km (200 mi)	563 km (350 mi)
Fuel Consumption, CAFE Unadjusted, Combined, Team	8.3 L/100km (28.3 mpgge)	7.4 L/100km (32 mpgge)	5.0 L/ 100km (0.43 UF) (47.0 mpgge)
Charge Depleting Fuel Consumption	N/A	N/A	2.07 L/100km (114.6 mpgge)
Charge Sustaining Fuel Consumption	N/A	N/A	7.4 L/100km (32 mpgge)
Charge Depleting Range	N/A	N/A	40 km (25 mi)
Petroleum Use	0.85 kWh/km	0.77 kWh/km	0.477 kWh/km
Emissions	Tier II Bin 5	Tier II Bin 5	Tier II Bin 5
WTW GHG Emissions	250 g/km	224 g/km	195 g/km

DEVELOPMENT OF THE HYREV SYSTEMS

The EcoEagles team has adhered to a simplified version of GM's Global Development plan. The development process can be divided in four phases; concept evaluation, design, prototype, and pre-production. At the project initialization, the EcoCAR organizers and GM provided a description of the project goals and a list of minimum requirements for the vehicle, representing the Document of Strategic Intent. Based on this information, the EcoEagles team organized into vehicle development groups and began the process of defining the requirements for our vehicle through research and evaluation of design concepts.

The team selected a conceptual powertrain configuration based on the competition requirements and vehicle technical specifications (VTS). The VTS was used to determine the engineering specifications for the vehicle and related components, which drove the selection of each component in the HyREV system. The selection of the powertrain configuration and components marked the completion of the conceptual evaluation phase of the project. The team is finished the design phase of the project, which concluded during the Fall 2009 term. The team is used a range of design tools to evaluate solutions to structural, thermal, and control system challenges. The team is in the midst of the third phase of the project, the prototype phase, where the mule vehicle is built and tested. The mule vehicle is a prototype test vehicle, with working, yet unrefined powertrain systems. The prototype phase concludes at the 65% design review, which is the Year Two competition in May 2010. The pre-production phase of the competition includes the refinement of the mule vehicle into a production ready vehicle. This phase will conclude at the 99% design review, which is the Year Three competition in Summer 2011. If the HyREV design was slated for production, there would be an additional production phase in the VDP to include manufacturing and final refinements.

The goal of the powertrain configuration process was to determine the optimal propulsion system configuration that could be built with the resources available to the ERAU team. Preliminary research indicated that fuel cell vehicle and electric vehicle technologies are not currently sufficient to meet the minimum range, weight, and volume requirements for this project. The remaining options allowed by the competition requirements include a range of hybrid and plug-in hybrid configurations, and fuel selections of B20, E85, and H_2.

To evaluate potential designs, the Powertrain Systems Analysis Toolkit (PSAT) was used. PSAT provides a graphical user interface to Simulink, predefined hybrid-electric vehicle configurations, and many preconfigured OEM component models, making it an ideal tool for the rapid development of vehicle models. The baseline model of the vehicle used the following parameters, which were provided to the team from GM and ANL:

- Vehicle Mass: 1742 kg
- Engine Power: 123 kW
- Mechanical Accessory Load: 0 Watt
- Electrical Accessory Load: 300 Watt
- Road Load Equation: $f = 112.85\ N - 4.60\ V + 0.542V2$

For plug-in hybrid vehicles, a Utility Factor (UF) is used to measure the percentage of travel that uses electrical energy and is one indication of the degree of vehicle electrification. To evaluate the influence of utility factor on vehicle performance, baseline PHEV models were created in PSAT.

Approximately 50% of daily travel distances are less than 40 km (3). The team originally selected a charge depleting range of 30 km, and the final distance of 40 km was selected based on battery constraints and consultation with the battery module manufacturer, A123 Systems.

A123 Systems produces an energy storage system that meets energy storage requirements, while meeting the packaging and weight requirements for the vehicle. The final configuration, consisting of four 25S2P battery modules, is capable of 40 km of all-electric operation.

B20 architectures have better fuel economies and lower greenhouse gas emissions, but higher petroleum energy use than E85 architectures. B20 was selected as the fuel source using a weighted average decision matrix. These effects were then ranked based on their importance in the EcoCAR competition with regard to scoring.

Another factor in the fuel selection was the list of supported engines, which included 1.3 L diesel, 2.0L diesel, 1.6L gas, and 1.8L gas engines. The 1.3 L diesel engine could be packaged with a wide range of hardware, including GM's front wheel drive two-mode transmission, without significant chassis modifications. Since all four engines met the minimum torque and power requirements determined for this project, the 1.3 L diesel engine was selected.

CONTROL SYSTEM DEVELOPMENT AND INTEGRATION

The control development process can be summarized in fives phases: requirements specification development, algorithm development, SIL HIL testing, vehicle integration and validation. The controller software and hardware will make use of various National Instruments software packages, such as LabVIEW and TestStand, and hardware platforms, such as the Single Board Rio (sbRio) for the vehicle supervisory control unit (SCU). These development phases have been further refined, emphasizing verification and validation at each stage, using the system design development V-diagram.

SIL HIL Testing

NI Test Stand will be used to automate tests, as the whole suite may take many hours to run. Any failed tests can be traced back to assert their requirements using NI Requirements Gateway, which assists in generating the traceability matrix, which traces each requirement forward to its corresponding design, implementation, and test artifacts. The focus of this testing is to provide system level requirement validation, tracing the original design to the finished, tested simulation.

The SIL and HIL testing promote the development of on-board diagnostics and detection. Using the Design Failure Mode Effects Analysis (DFMEA) process the team is identifying each failure mode, its likelihood and its severity. With that list, the critical items for failure detection including directly measured parameters such as vehicle ground speed and engine or motor speed, as well as several indirectly calculated quantities such as torque and energy exchange are determined, and provisions made in the controller software to smoothly manage the failure detection and maintain a safe shut-down if driving. The team is developing diagnostics tools to display important information during HIL and vehicle testing, as shown in Figure 1.

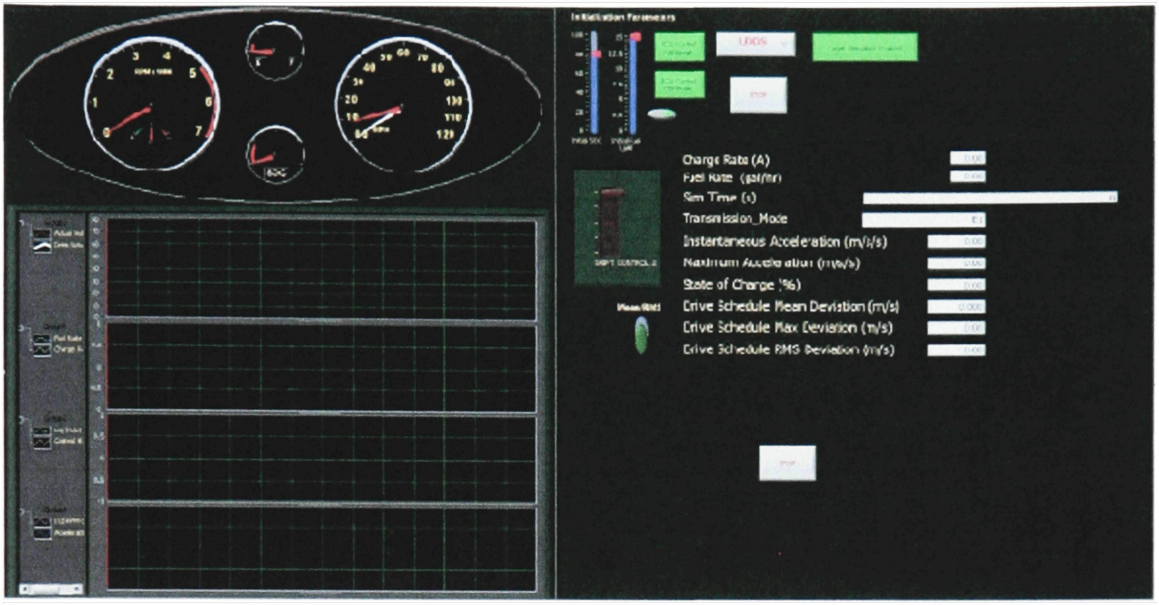

Figure 1. HIL Test Panel

More importantly, the DFMEA process has allowed the team to identify opportunities to remedy some of the identified failure modes. Some are simple; recognizing that connection reliability in the mule vehicle is more challenging than in a production vehicle, special attention has been paid to the selection of connectors and connection techniques to mitigate failures due to connection and connector fatigue. To mitigate temperature-related battery failures, it has been determined that at least one secondary independent temperature sensor will be integrated into the battery pack so that early detection of thermal excursions close to battery operational limits will be more reliably detected.

Integration Plan

Because the architecture relies primarily on serial digital communication over the CAN networks, the controllers can be integrated into the vehicle in an electrically simple manner but a well planned integration is required to ensure proper communication and performance. Validation and testing of the communication between the SCU, ECM, and TPIM controllers can take place partially in the HIL stage, but ultimately the final integration and testing will be performed on-vehicle. To facilitate those tests, the system has been designed to allow independent isolation of the electrical loads so that control for each of the drive train sub-systems can be at least partially verified before all-up testing occurs. The control strategies also anticipate this incremental integration and test process.

The initial integration step is the verification that the SCU can replicate the stock vehicle communication signals that are expected by the remaining vehicle systems after stock component removal. The intimate control coupling between the engine and the two-mode transmission implies the integration of these controls will be performed simultaneously. Charge control, including external voltage detection and charging hazard prevention controls are independent of the driving strategy, and can thus be integrated incrementally at almost any time

through the process. Additional control algorithms managing body control interactions can also be added independent of the powertrain controls in many cases.

Control System Architecture

The architecture is comprised of two high-speed and two low-speed controller area network (CAN) bus communication lines as well as several digital and analog input and output control signals. The majority of the communication takes place over the four CAN buses. The low-speed CAN bus network will be used for non-time-critical data, such as mode recommendations from the IDEA system. The high-speed CAN bus network will transfer time-critical data to and from the drivetrain components. These CAN buses are connected to the SCU. The controller roles and responsibilities are defined below.

- Supervisory Control Unit (SCU) – The SCU facilitates selection of operating modes to assure smooth and safe transitions between modes and torque requests. Primary inputs are the driver controls and the state of each driveline component. Secondary inputs come from the IDEA system in the form of recommended configurations. The SCU is responsible for maintaining torque safety and is the final authority on selecting the operating condition of all driveline components.
- Engine Control Module (ECM) – This controller will be provided as part of the 1.3 L SDE and is responsible for engine operation and monitoring and response to the SCU.
- Traction Power Inverter Module (TPIM) – This controller will be provided as part of the two-mode transmission, and controls the electric and mechanical power used in the transmission. It will respond to torque requests while assuring torque safety. The TPIM reports status of the transmission to the SCU.
- Emergency Disconnect Monitor (EDM) – This system monitors the state of the fault disconnect systems, and communicates that information to the PCC and the SCU to guide operation mode selection.
- Plug-in Charge Controller (PCC) – This system has the responsibility to ensure safe and effective charging of the battery pack during plug-in charging. It detects the power source and monitors the battery state of charge, temperature, and ventilation system. It also controls the battery-charging-supply voltage and current.

As shown in the communication map in Figure 2, the SCU communicates directly with the ECM from the 1.3 L diesel engine, the two-mode transmission control unit, the plug-in charge controller, and the emergency disconnect monitoring system. Communication occurs between the SCU and the data acquisition system via a local area network (LAN). The CAN cards each contain two bundled signal wires: a fast CAN, and a slow CAN. One CAN card corresponds to the ECM which will be initially installed in the Chevrolet EcoCAR and the other CAN card corresponds to the ECM and the TPIM, which will be added to control the new hardware configuration modified by the EcoEagles team. The analog and digital signals will originate from sensors connected to the SCU, which are transmitted over the CAN bus. The field programmable gate array (FPGA) is able to simulate sensor signals for use with a virtual vehicle, and will take care of all the low level CAN communication including scheduling of periodic messages and buffering received messages.

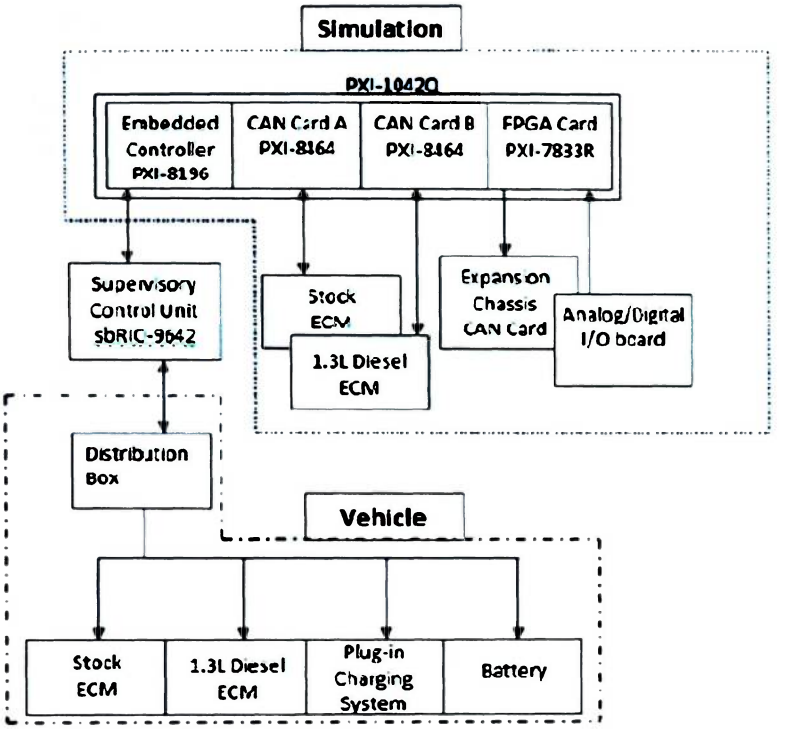

Figure 2: Component Communication Diagram

Control Strategy

The low level control strategy is designed to work with the selected powertrain configuration, which uses a two-mode transmission and 1.3 L diesel engine for front wheel propulsion. The assortment of powertrain hardware allows the HyREV system to operate in several different operating conditions. The drive modes can be grouped into a few categories: electric-only, hybrid-electric, and engine-only. Each of these categories includes multiple operating modes, which can further be divided into sub-modes that describe the operating conditions: propulsion, regenerative braking, friction braking, etc.

The control system will select an operating mode based on the current operating conditions, including: torque/power requests, throttle and brake pedal position, state of charge of the battery, and engine speed. Figure 3 shows the basic modes and the relationship of the basic propulsion modes to two of the vehicle parameters: state of charge and vehicle speed. The Ex and Hx modes refers to whether the vehicle is driving in Electric (Charge-Depleting) or Hybrid (Charge-Sustaining) mode, respectively. The lower modes are for lower (City) speeds, the middle modes act as transition states, and the higher modes are for higher (highway) speeds. The final transition points of SOC and vehicle speed will be determined after testing and optimizing the final vehicle.

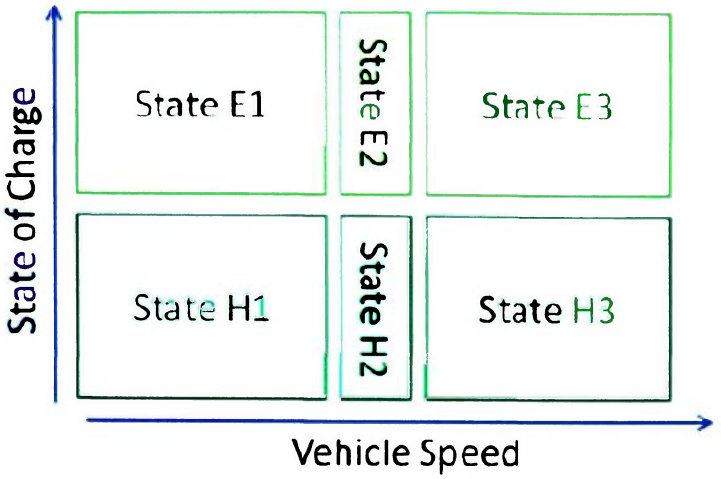

Figure 3: Basic Propulsion Modes

An overview of the propulsion modes starts with electric-only modes (E1, E2, and E3). When the battery state of charge is between 30% and 80%, the control strategy will attempt to operate in one of these three modes, based on the vehicles speed. The three electric modes correspond to states of the two-mode transmission. The two-mode transmission must be shifted into specific states as a function of vehicle speed for the electric motors to remain within their speed ratings. Since the powertrain is capable of full functionality in the electric-only modes, which are inherently more efficient than the hybrid-electric modes, the controller will remain in one of the electric only modes unless conditions require another mode.

There are three hybrid-electric modes (H1, H2, and H3). The vehicle will switch from an electric mode into a hybrid-electric mode if the battery state-of-charge (SOC) drops below 30% or the high level control system (IDEA) recommends the transition. The high level control system may recommend that the vehicle operate in one of the hybrid-electric modes if a blended control strategy has a high probably of reducing fuel consumption for a given driver, historical route or terrain.

Control Algorithm

The algorithm of the controller will be written using LabVIEW software and implemented as a state machine comprised of case structures, sequence structures, event structures, and loops to make each mode separate. A preliminary version of the control algorithm is shown in Figure 4.**Error! Reference source not found.** but it should be noted that the state chart diagram is only presented to convey the control concept. The National Instruments real-time development tools do not support the use of state charts. Event structures and case structures will make use of the inputs from the ECM and sensors to make a feasible mode selection; each mode will be in its own structure and have no direct connection to any other mode. CAN bus communication is handled in routines based on simple read and write functions for signal processing that are already contained in LabVIEW. The FPGA coding will also be based on simple codes already written in LabVIEW that make use of all of the functions of an FPGA interface such as analog and digital input and output and CAN messaging.

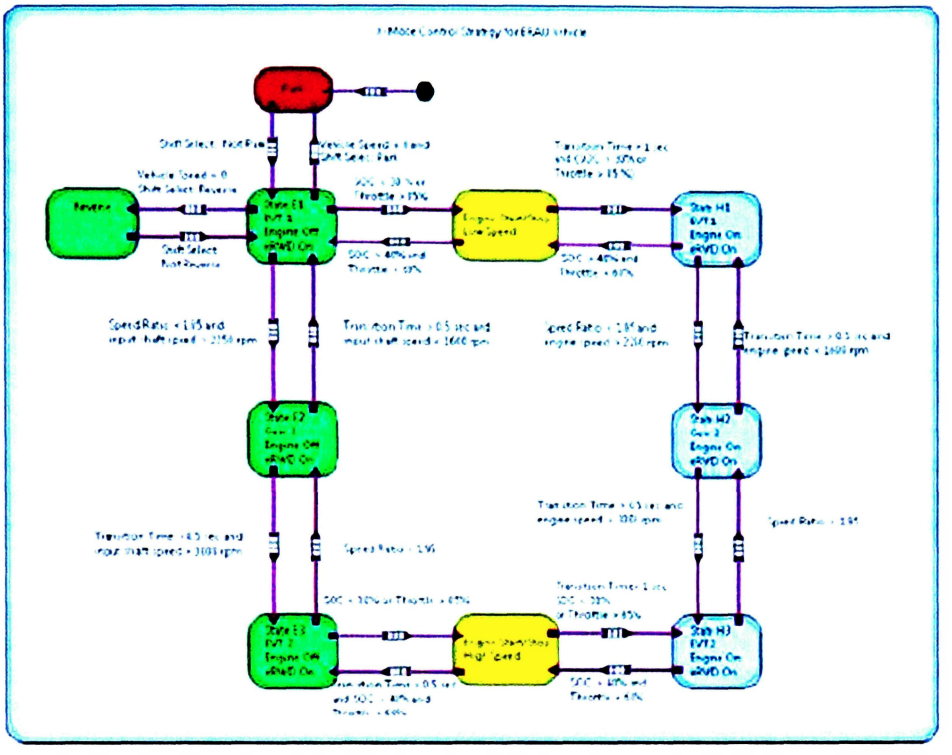

Figure 4: Control Algorithm State Chart

TESTING AND VALIDATION

The team developed a DFMEA in order to identify and design for potential problems before they can negatively impact the vehicle. The DFMEA establishes the potential causes and effects of these failure modes. These failure modes are then tested in the HIL to determine the actual effect they have on the vehicle and the control system. If any of these failure modes causes a fatal error in the system, then the control system is modified to account for that particular error potentially occurring.

In the DFMEA, each failure mode is given a Risk Priority Number (RPN), which represents the relative potential threat a failure poses, with a range of 1-1000. It is calculated based on the product of the severity (potential damage), occurrence (likeliness of occurrence) and detection (chance of detection), with the higher the number, the higher the threat. The RPN allows for the team to identify the most dangerous errors, and correct for them early.

An example error is an "Incorrect Accelerator Signal", which has an RPN of 96, representing a mid-to-high level error for the team. This error could be caused by poor electrical connection, or a mechanical connection failure (e.g., cut wire), and would result in erratic vehicle performance. This fault was included in the HIL testing to determine if the control safety features are sufficient. The EcoEagles controller system is designed to display a warning to the driver and perform a controlled shut down if an accelerator signal fault is detected. The results of the HIL testing indicate that these safety features are sufficient but the fault detection algorithm was modified to also monitor the brake pressure to improve fault detection.

The proper packaging and integration of components used in the EcoCAR vehicle development process required a comprehensive understanding of element interaction from both a static (space claim) and dynamic (feasibility) standpoint. Extensive computer aided design (CAD) analysis was performed for the anticipated vehicle architectures using both organizer provided component data and student designed elements. The engine and transmission models were adapted for use in the CAD environment, and then placed into the chassis to meet the safety and dimension requirements set out by the sponsors and organizers. Care was taken to ensure all components maintained adequate clearances for installation, maintenance and operation by examining areas of possible contact or interference as well as evaluating the mass balance of the vehicle with the proposed changes. The university's background in the aerospace industry also set standards for aerodynamic and mass reduction early in the design using innovative replacement materials.

Packaging large amounts of equipment into the Chevrolet while maintaining consumer acceptability and functionality required innovative approaches. The ERAU team has selection a powertrain configuration that has not been used in combination in a production vehicle. Siemens NX and vehicle models donated by GM were vital tools used to successfully package the 1.3 L engine and two-mode transmission into the Chevrolet engine compartment, along with the electric AC compressor, electric vacuum boost, and the Traction Power Inverter Module (TPIM). The accessory drive belt and accessory pulleys were removed from the engine, which improves packaging, efficiency, and noise vibration hardness. All of the accessories were converted to electric systems.

To satisfy the team's vehicle design goals, the starter motor was retained on the engine. This feature allows the control strategy to switch from electric-only modes to hybrid-electric modes at any vehicle speed but it also required a more complex adaptor plate between the engine and two-mode transmission and a more detailed packaging analysis.

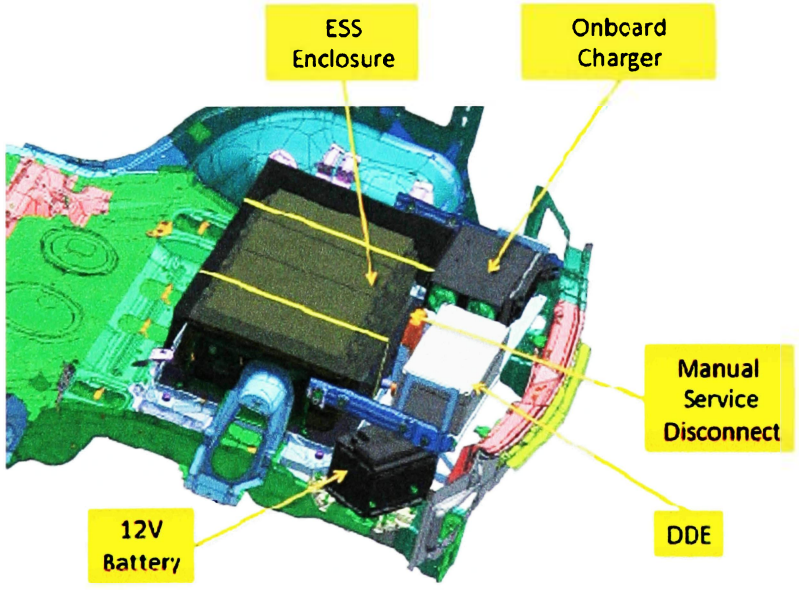

Figure 5: Rear Compartment Packaging

As shown in Figure 5Error! Reference source not found. the energy storage system plug-in charge controller and disconnect enclosure were packaged in the rear of the vehicle, predominately in the spare tire area. This system includes an on-board charge controller, which allows the vehicle to charge from any outlet.

The high voltage (HV) electrical cables, fuel system, cooling systems and exhaust system each required component routing to be run along the length of the vehicle. The exhaust system incorporates two new mufflers, a selective catalytic reduction (SCR) unit, and a diesel particular filter (DPF). The fuel system was replaced with biodiesel rated equipment The high voltage cables were routed to connect the two-mode transmission and energy storage system.

The parts of the vehicle must not only fit into the vehicle, but must also hold up to the rigors of testing and competition. Because the 1.3 L engine has not been paired with the front wheel drive two-mode transmission, the team designed a custom adaptor plate. The teams control strategy requires that the production starter remain on the 1.3 L SDE. The adapter plate must also permit access for attachment of the engines fly-wheel/flex plate to the transmission.

Using the 2 Mode transmission with the compact 1.3 L SDE allows the team to use the production transmission mounts, half-shafts and steering geometry, including the electric steering motor. The minimal weight change in the front of the vehicle allows for the use of the production shock absorbers and spring rates as well, which made for an easy front suspension and steering integration

To accommodate the selected vehicle architecture, many components are removed or replaced. Approximately 287 kg of components were removed from the baseline vehicle and approximately 578 kg of components were added to the vehicle. These values are still subject to change with proposed Year Three weight reductions The HyREV version has a projected vehicle mass of 1976 kg (curb) and 2303 (loaded), which is below the loaded competition requirement of 2450 kg. As shown in Table 2, the loaded front and rear axles are well below the maximum limits of 1210 kg and 1340 kg, respectively.

Table 2. Vehicle Mass, Not Including Proposed Mass Reductions

Vehicle	Stock Chevrolet	EcoEagles HyREV
Curb Weight (kg)	1689	1976
Loaded Weight (kg)	2098	2303
Front Axle Loading (kg)	980	1073
Rear Axle Loading (kg)	710	904

ESS Thermal Analysis

The thermal analysis of the ESS cooling system was done in three phases. In the first phase, the average heat generated by the ESS was analyzed for several driving scenarios to determine the heat transfer requirements for the cooling plate. In the second phase, the heat transfer requirements were translated into engineering specifications for the mass flow rate and a coolant pump was selected. In the third phase, the ESS current draw was calculated for the most demanding driving schedules in electric-only operation, which was used to calculate the heat flux out of the battery modules. A thermal system for the ESS was created using the fan and air flow rate selected above. Using the heat flux time history for the most demanding drive cycles and the ESS thermal model, the transient and steady state temperatures were simulated. Under the most severe operating conditions, the peak temperature of the HyREV ESS design never exceeds 46° Celsius, which is below the recommended limit of 50° Celsius.

YEAR 3 WORK TO BE PERFORMED

Year Three of the competition is intended to be the optimization and refinement year. With aerodynamic and controller modifications planned, year three will be a full year. The major projects will include: replacing all of the body panels to improve weight and aerodynamics, refinement of the SCU algorithm, implementation of the Magna eRDM (if the system meets requirements) and implementation of the IDEA advisory control system.

Vehicle Aerodynamics

Integrating aerodynamic improvements into a complex hybrid vehicle can improve the fuel economy through the direct reduction of drag forces during propulsion and also through the capture of more energy during regenerative braking. Reduced drag can also improve customer acceptability by reducing noise, increasing the charge-depleting range and improving vehicle acceleration. The team has currently evaluated a baseline CFD model of the Chevrolet EcoCAR using Fluent but the team has not evaluated the impact of potential aerodynamic improvements. The aerodynamic improvements that are under investigation include:

- Active Aerodynamics – The ERAU team considers the front fascia as ideal for the application of active aerodynamics. A variable air flow rate through the front grill and radiators will meet the cooling requirements for the various liquid cooled systems, which have fluctuating thermal requirements. Restricting the air flow rate through the front grill through the use of an active control system will reduce the parasitic drag of the vehicle.
- Passive Aerodynamics – The competition allows for changes to the vehicle's design profile, provided the vehicle still resembles the Chevrolet. The EcoEagles will pursue several passive aerodynamic opportunities to reduce drag. Each of the following concepts will be compared to the baseline aerodynamics models.

The team has proposed design changes to the rear spoiler, rear wheel well coverings, side view mirrors, front air dam, and underbody. The underbody airflow will change from the production Chevrolet due to changes in the driveline, particularly with the addition of a rear drive system and rear cradle.

Weight Reduction

The aerospace industry has long used composite materials for vehicles that are highly mass sensitive. For automotive production, the ability to implement labor and design intensive composite structures has been limited and is only now becoming a cost effective way of improving performance. All components replaced will be investigated to ensure that they are at least as safe as the original components, and meet all competition and DOT regulations. Proposed weight savings candidates include:

- Hood - A composite hood is being investigated, however care must be taken to make sure that in the event of a crash that the hood would buckle instead of shearing into the cabin.
- Roof - The roof of the vehicle could be replaced with a composite sheet, but analyses will be done to ensure the structural integrity of the vehicle in case of a rollover.
- Rear Windows - The rear windows could be replaced with thermoplastic substitutes.
- Rear Hatch - The rear hatch could be replaced with a combination of composites and thermoplastics.
- Doors - The doors could be replaced with composite or thermoplastic body panels
- Wheels - The vehicle wheels could be replaced with lighter rims. The rim size may change, though simulations still need to be performed in order to determine the potential performance benefit with a larger or smaller wheel diameter. In addition, lower rolling resistance tires could replace the current stock tires.

Rear Motor

The team originally had a Magna eRDM on the vehicle, which would have significantly increased the electrification of the vehicle and improved the overall fuel economy. However, the higher voltage of the donated A123 battery modules (330 V nominal, 360 V peak), is much higher than the stock GM battery pack (276 V nominal, 330 peak). The RPIM eRDM control module cannot accept these higher voltages, which makes the eRDM unusable currently. Due to this, the team has removed the rear drive motor for Year Two, as it would only be dead weight on the vehicle.

GM is currently working on a solution to allow the eRDM to run at this higher voltage, in which case the rear motor would be re-integrated onto the vehicle. This would allow the team to meet all of its original performance goals, including faster acceleration, improved fuel economy, and additional control strategies, without adding significant cost, time, or difficulty to the team's vehicle. The team already has the required hardware to mount and install the eRDM, and the control software was designed originally to make use of the rear motor. The only new components would be additional cooling and electrical lines, these lines are already established on the vehicle and could be easily spliced in.

SUMMARY/CONCLUSIONS

This paper provides an overview of the ERAU HyREV system design. The EcoEagles design team has taken advantage of numerous advanced development methods and tools as part of the development of the HyREV system, including model-based design, SIL, HIL, CAD, FEA, and project management. The project has passed the first phase, conceptual analysis, and is midway through the second phase, which is the design phase. A vehicle powertrain configuration has been selected that meets the project requirements and design goals of the team. As the project continues into the next phase, the design will continue to be refined towards the goal of building a production ready vehicle.

REFERENCES

1. Norbye, Jan P., Dunne, Jim. "GM Takes the Wraps Off its Steam Cars and a commuter Car with Hybrid Drive." Popular Science July 1969: 86-87. Print.
2. Rousseau, A., Deville, B., Kern, J., Duoba, M., Ng, H., "Honda Insight Using PSAT," (2001) SAE, Paper Number: 2001-01-2538.
3. Gonder, J., T. Markel, A. Simpson, M. Thornton. "Using GPS Travel Data to Assess the Real World Driving Energy Use of Plug-In Hybrid Electric Vehicles (PHEVs)." (2007). NREL Report Number: NREL CP-540-40858.

CONTACT INFORMATION

Vincent J. Sabatini

VJSabatini@gmail.com

ACKNOWLEDGMENTS

The authors would like to thank the EcoCAR organizers and the PSAT teams for their assistance in developing and debugging the PSAT models used in the analysis. They would also like to thank GM for providing models, data, and mentor-ship throughout the competition

ABBREVIATIONS

B20 - 20% Biodiesel, 80% Standard Diesel
CAN - Controller Area Network
DFMEA - Design Failure Mode Effects Analysis
DOT - Department of Transportation
E85 - 85% Ethanol, 15% Standard Gasoline
ECM - Engine Control Module
EDM - Emergency Disconnect Monitor
eRDM - Electric Rear Drive Module
EREV - Extended Range Electric Vehicle
FPGA - Field Programmable Gate Array
FWD - Front Wheel Drive
GHG - Green House Gasses
HEV - Hybrid Electric Vehicle
HIL – Hardware-In-the-Loop
HWFET - Highway Fuel Economy Test
MPGGE - Miles per Gallon Gasoline Equivalent
PCC - Plug-in Charge Controller
PEU - Petroleum Energy Usage
PHEV(XX) - Plug-in Hybrid Electric Vehicle (Charge Depleting Range in miles)
PSAT - Powertrain Systems Analysis Toolkit (Argonne National Laboratory)
PTW - Pump-to-Wheel
RPIM - Rear Power Inverter Module
RPN - Risk Priority Number
RWD - Rear Wheel Drive
SCU - Supervisory Control Unit
SIL – Software-In-the-Loop
SOC - State of Charge (Battery Percentage)
TPIM - Traction Power Inverter Module
UDDS - Urban Dynamometer Driving Schedule
UF - Utility Factor
US06 - Supplemental FTP Driving Schedule (Aggressive)
WTP - Well-to-Pump
WTW - Well-to-Wheel

SAE 2010-01-1446

SAE International

Road to Lab to Math: A Student-Designed B20 Power-Split Extended Range Electric Vehicle for the EcoCAR Challenge

2010-01-1446
Published
05/05/2010

Vincent J. Sabatini
Embry-Riddle Aeronautical Univ.

Ryle Maxson and William Haupfear
Embry-Riddle Aeronautical Univ

J. E. McKisson
Embry-Riddle Aeronautical University

Darris White
Embry-Riddle Aeronautical Univ

ABSTRACT

EcoCAR: The NeXt Challenge is a three-year collegiate advanced vehicle technology competition (AVTC) established by the United States Department of Energy (DOE) and General Motors (GM). Argonne National Laboratory (ANL) has managed the AVTC series for 20 years.

The competition challenges 17 North American universities to reduce the environmental impact of a captured GM fleet vehicle by minimizing its fuel consumption and reducing emissions while retaining the vehicle's performance, safety and consumer appeal. The competition requires teams to use GM's Global Development Process (GDP) to design a vehicle in a real-world atmosphere. Sponsors of the competition provide teams with the engineering tools and equipment needed to create a realistic vehicle design project. Using these tools the Embry-Riddle Aeronautical University (ERAU) team, the EcoEagles, have devised a Power-Split Extended Range Electric Vehicle (EREV) propulsion system.

The team designed around a 25-mile city/highway combined electric range, which would provide a significant benefit for most consumers. The average commuter (80%) drives less than 28 miles per day [1]. This means that a consumer using the EcoEagles vehicle almost never has to use the diesel engine, resulting in a reduction in total petroleum energy use by 40-50%.

The first year of competition is entirely done virtually, with all testing and analysis being done using software tools, including: PSAT, Matlab and Simulink, NX, and LabVIEW. This allowed the team to design, test, and optimize their powertrain and control system, without any vehicle hardware components. The designs of the teams are currently being implemented in Year Two of the competition, which will ultimately test these "virtual vehicles" against their real-world counterparts. This paper will also address some of the challenges associated with a soft design versus a hard design, including software approximation limitations.

INTRODUCTION

Designing a new vehicle, or redesigning an existing vehicle, is a time and resource consuming task. With that in mind, the automotive industry is moving towards the way of the aerospace industry when it comes to the system-level development process. The aerospace industry has established this practice due the difficulty and inherent danger in testing an unproven, dangerous prototype. UAV's are particularly researched as there is no human to take control in case of failure [2, 3]. By developing comprehensive models of

vehicles, virtual designs can be "driven" to determine platform viability, performance characteristics, and control algorithms. These virtual prototypes allow for a more rapid, cheaper and safer development process. Physical prototypes, which are expensive and potential dangerous, are being used for final verification, rather than a starting point. This can significantly reduce vehicle design time, greatly saving on long-term costs and profits for a company.

This paper will outline the virtual design of the EcoEagles vehicle, with an emphasis on the vehicle dynamics modeling. Design decisions based on the modeling will also be discussed. While extensive CAD modeling was performed to determine space claims of components, this is not deemed important for the scope of this paper.

VIRTUAL DESIGN

The goal of the architecture selection process was to determine the optimal driveline configuration that could be built with the resources available to the ERAU team. Since the EcoEagles team has minimal experience with fuel cell vehicles, hydrogen was not considered a viable fuel option. Electric vehicles were also not considered viable because of the competition range (320 km) and charge requirements (max. eight hours charge @ 110 V AC). The remaining options included a variety of hybrid and plug-in hybrid configurations with fuel selections of E85 and B20. The required performance requirements can be seen in Table 1.

(See Table 1 after last section of paper)

A literature review [4, 5] was conducted to determine the most promising hybrid architectures, which were analyzed in PSAT, Siemens NX (CAD), and using the GREET model. Powertrain Systems Analysis Toolkit (PSAT) [6] was developed by ANL as a way to quickly analyze various vehicle configurations and driving conditions to determine performance characteristics such as fuel economy and energy usage. Individual components such as engines, batteries, and vehicle bodies can be strung together to create an overall vehicle model, all of which is done using MATLAB and Simulink. Models of the various powertrain components were developed by the PSAT staff with data from GM. The development of these individual models is beyond the scope of this paper. GREET is a program, also developed by ANL, that estimates lifetime well-to-wheel (WTW) greenhouse gas emissions for a particular vehicle [7].

Based on the literature review and preliminary PSAT results, the most promising architectures were analyzed in more detail while the architecture layouts were evaluated in Siemens NX. When the FWD GM Two-Mode transmission was paired with the four available donated engines, the 1.3L diesel engine was found to be the only engine that would fit within the available space. Based on the results from PSAT and GREET, viable vehicle architectures were assigned normalized scores for five vehicle parameters: performance (towing, acceleration, etc.), fuel economy, WTW greenhouse gasses, emissions and WTW petroleum energy usage. An aggregate of the five scores was used to rank the architectures and the top three shown in Table 2, were selected.

(See Table 2 after last section of paper)

The top architecture is a EREV20 vehicle with all-electric range of approximately 20 miles. It uses a 1.3L diesel engine, Two-Mode transmission, and Magna rear drive motor. This design was found to have the best overall performance across the five vehicle parameters. The second architecture is similar to the top choice but does not use the Magna rear drive motor. This design meets the competition VTS requirements and is mechanically simpler than the top choice but this design will increase the duty cycle of the two mode transmission, as well as failing to be classified as an EREV. To minimize the two-mode transmission temperature, a blended charge depleting strategy is required and dynamic performance will be conditionally limited. The third architecture uses the 2.4L Ecotec engine, BAS+ motor generator, Magna rear drive motor. The performance of this architecture was less competitive than the top two choices and it requires a more complex charging system with a controllable DC-DC to step up the output from the BAS+ voltage to the energy storage system voltage.

FUEL SELECTION AND WELL-TO-WHEEL INFLUENCE

The most viable fuel options for the ERAU team is a combination of electricity and either B20 or E85. GREET was used to estimate the properties for each fuel option shown in Table 3. Electricity has the lowest fuel cost per mile, B20 has lower greenhouse gas emissions than E85, while E85 has less petroleum energy than B20.

(See Table 3 after last section of paper)

The amount of electrical energy storage on the vehicle may influence the fuel selection. As shown in Figure 1, approximately 50% of daily travel distances are less than 28 miles. Assuming there is not an opportunity to recharge the vehicle during the day, a vehicle with a 28 mile charge depleting range would be used about 50% of the time.

(See Figure 1 after last section of paper)

For plug-in hybrid vehicles, a Utility Factor (UF) is used to measure the percentage of travel that uses electrical energy. The utility factor versus charge depleting range is shown in Figure 2. This curve was calculated using the 6th order polynomial shown in Equation 1, where RCD is the charge depleting range. This equation was provided by the

competition, as the SAE standard J1711 has not yet been finalized. This equation cannot be verified at this time. To analyze the influence of utility factor on vehicle performance, baseline PHEV models were created in PSAT.

(See Figure 2 after last section of paper)

$$UF = 1 - \exp\left(-\left[0.52P_{n} - 7.282P_{n}^{2} - 26.37P_{n}^{3} + 79.08P_{n}^{4} - 77.36P_{n}^{5} + 26.07P_{n}^{6}\right]\right)$$
$$P_{n} = R_{CD}/400$$

Equation 1: Utility Factor Calculation [ANL]

Since propelling a vehicle using electrical energy is more efficient Pump-to-Wheel (PTW) than using thermal engines, a larger utility factor will result in a higher combined fuel economy for most vehicles. As shown in Figure 3, increasing the charge depleting range will increase the combined fuel economy for the baseline architectures. These curves were created using Equation 2, where the charge depleting (CD) and charge sustaining (CS) fuel economies were determined using PSAT for the baseline designs. This equation also came from the competition organizers, ANL.

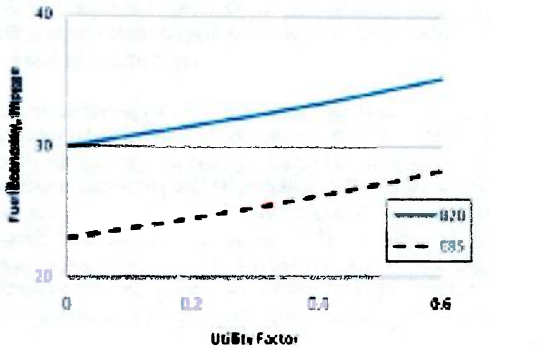

Figure 3. Influence of Utility Factor on Corrected Fuel Economy for EcoEagles Selected Architecture

$$mpgge\_PHEV = \frac{2}{\frac{(UF)}{mpgge_{CD}} + \frac{(2-UF)}{mpgge_{CS}}}$$

Equation 2: PHEV UF Weighted Fuel Efficiency [ANL]

Because of the high carbon dioxide emissions from producing electricity, the well-to-wheel greenhouse gas emissions are not improved as the utility factor increases when using the EcoCAR electricity mix, as shown in Figure 4. Increasing the utility factor had little effect on the production of greenhouse gasses under these assumptions.

The amount of greenhouse gasses produced per kilometer was calculated using Equation 3. The well-to-pump (WTP) values were provided by the EcoCAR organizers and were 699 g/kWhr for electricity production, 1.57 g/kWhr for E85 production and 1.99 g/kWhr for B20 production. The PTW values were found using GREET to be 162 g/kWhr for E85 and 170 g/kWhr for B20. The energy consumed in the charge depleting and charge sustaining modes was calculated using PSAT. While the GHG values per kWhr for E85 and B20 are similar, the E85 architecture consumes more energy per km than the B20 architecture. As a result, the B20 architecture has lower GHG emissions.

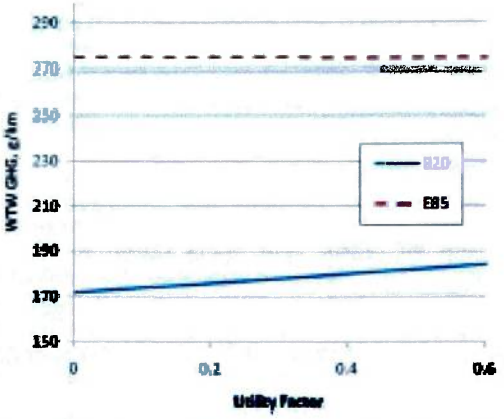

Figure 4. Influence of Utility Factor on Greenhouse Gas Production for EcoEagles Selected Architecture

$$GHG = (GHG_{CD,WTW} + GHG_{CD,PTW})(UF) + (GHG_{CS,WTW} + GHG_{CS,PTW})(1 - UF)$$
$$GHG_{CD,WTW} = (699)(Energy_{CD}) + (1.57)(Energy_{CD}) + (1.99)(Energy_{CD})$$
$$GHG_{CD,PTW} = (162)(Energy_{CD}) + (170)(Energy_{CD})$$

Equation 3: UF-Weighted WTW Greenhouse Gas Emissions

As shown in Figure 5, petroleum energy usage (PEU) can be substantially reduced by increasing the utility factor. The utility factor corrected PEU equation is effectively the same equation used for GHG emissions but with PEU coefficients. The WTP PEU coefficients were provided by the EcoCAR organizers. The WTP petroleum energy used to make: E85 is 0.0832kWhr/kWhr, B20 is 0.0642 kWhr/kWhr, and electricity is 0.0785 kWhr/kWhr. The petroleum energy in each fuel was determined from GREET to be: 0.263 kWhr/kWhr for E85, 0.812 kWhr/kWhr for B20, and 0 kWhr/kWhr for electricity.

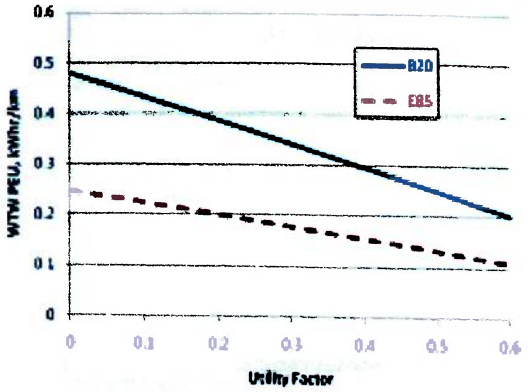

Figure 5. Influence of Utility Factor on Petroleum Consumption

A large utility factor is beneficial for each performance metric for the B20 architecture and generally beneficial for the E85 architecture. The size of the battery pack was limited by space, weight and manufacturer. The selected battery pack yields a utility factor of approximately 0.43 with the baseline E85 and B20 architectures.

Of the available liquid fuels, B20 is the top choice for ERAU. When compared to the E85 architecture with a utility factor of 0.43, the B20 architecture has better fuel economy, lower greenhouse gasses but higher petroleum energy use. Another factor in this selection is the list of supported engines, which included 1.3L diesel, 2.0L diesel, 1.6L gas and 1.8L gas engines. After review, it was determined that the 2.0L diesel engine and 1.6/1.8L gas engines do not fit in the Saturn Vue when combined with the two-mode transmission without significant chassis modifications.

VEHICLE POWERTRAIN MODELING, SIMULATION AND ANALYSIS

High-level calculations were done in order to develop some system boundaries, before modeling specific powertrain configurations. Using the road load equation, Table 4 below was developed with MATLAB, which shows the minimum peak power required at the wheel to meet either the required or desired acceleration times. The minimum peak wheel power required is 76.5 kW, while the minimum desired is 135 kW. This sets very early peak power requirements for the powertrain. A high-level analysis was also developed in order to calculate the maximum grade that the vehicle can climb. This determined that the minimum required power was only 30.6 kW. This also sets very early sustainable power requirements for the drivetrain.

(See Table 4 after last section of paper)

Many unique driveline configurations were considered and analyzed in PSAT with various modifications. The architectures could be grouped generally as: mild hybrid (BAS+), combined hybrid (two-mode), and a plug-in combined hybrid. The majority of the configurations were designed to make use of the available donated components. For these models, some modification was required to provided models and initialization files. These modifications included creating a new battery pack, creating a Magna eRDM motor model, and creating a charge depleting control strategy for the two-mode architecture through state-flow and developing custom drive cycles. The top three architectures were analyzed in more detail using the UDDS, HWFET, and US06 [8] drive cycles in charge depleting and charge sustaining modes.

A number of problems were encountered with the PSAT models as components were introduced into previously untested combinations. For example, the two-mode control system did not initially accept diesel engines but with assistance from ANL, these issues were overcome. Creating and modifying the control strategies presented the largest challenge. The control system for this analysis was a stock power-split controller found in PSAT; the models would have drastically different results with varied control systems, as they would affect power distribution, regenerative braking, and charge/discharge profiles. Charge depleting control strategies were created to model EREV performance but with few existing charge depleting control strategies to reference, the performance of these control strategies was unrefined. Development of a detailed charge depleting control system will be required to improve model accuracy, as well as final vehicle performance.

The fuel economies of the top three architectures were determined by analyzing the charge sustaining and charge depleting portions of the PSAT results, as opposed to the stated fuel economies from PSAT. This analysis was necessary because the fuel economy reported by PSAT does not take into the amount of electrical energy used. If a vehicle has a large battery and is analyzed over a short drive cycle, it would use little-to-no fuel, resulting in an infinite fuel economy. The electrical and fuel energy consumed during the test ranges were used to get the economy for the charge-depleting or charge-sustaining portions of the drive cycle. The data for the US06 was not included due to inconsistencies in the operation of the charge depleting control strategy for this drive cycle. The results for the top three architectures are shown in Table 5.

(See Table 5 after last section of paper)

As can be seen in Table 5, the team's first choice has the highest fuel economy for both city and highway. The added rear electric motor provides additional regenerative braking and torque smoothing, which increases the city fuel economy.

The second choice economies are almost as good, with identical MPGGE-CS and slightly lower MPGGE-CD values. The parallel configuration using the 2.4L E85 engine and BAS+ system has substantially lower results. The combination of the less efficient E85 engine and more complex control strategy required to blend the BAS+ motor with the Magna eRDM reduces the apparent efficiency of the 3rd choice architecture. Note that there is no charge-depleting control mode for the BAS+ system at highway speeds.

Using the charge-depleting ranges of the architectures determined using PSAT for the UDDS city cycles, the UF for each configuration was determined. The state of charge (SOC) of the top choice architecture for the UDDS, US06 and HWFET driving cycles is shown in Figure 6. The results from these PSAT simulations were used to determine the charge-depleting ranges.

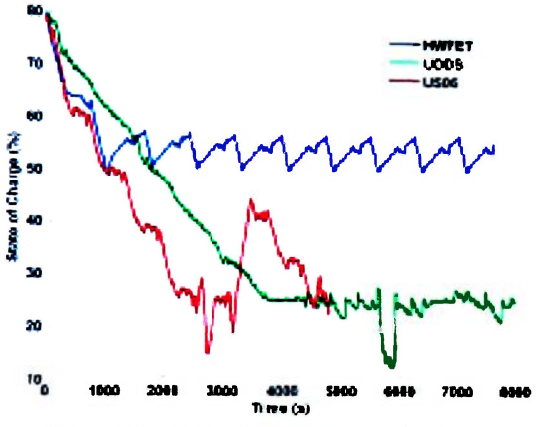

Figure 6. SOC for CD Control Strategy (1st Choice Architecture)

The UF was calculated using 6th order polynomial in Equation 1 and the charge-depleting range for each cycle. The charge-depleting and charge-sustaining energies and ranges, along with their corresponding UF(s) are presented below in Table 6.

(See Table 6 after last section of paper)

The acceleration, braking, and towing performance for each architecture was modeled, with the acceleration values coming from PSAT simulations. Simple math models were created to estimate the towing and braking performance. The acceleration, towing, and braking results are presented below in Table 7.

Table 7. Acceleration and Braking Summary

	1.3L B20 2-Mode eAWD	1.3L B20 2-Mode FWD	2.4L E85 BAS+ eAWD
Tow 0-45 mph	7.30 s	8.30 s	8.20 s
Brake 60-0 mph	41-46 m	41-46 m	41-46 m
Accel. 0-60 mph	8.70 s	9.60 s	9.10 s
Accel. 50-70 mph	5.30 s	5.60 s	5.20 s

The towing capacity of the three top architectures was determined using a combination of PSAT and a simple Matlab model. The results indicate that the top three architectures will meet the competition VTS requirements for towing (680 kg, up a 3.5% grade, for 20 continuous minutes), assuming the battery has 35% SOC or greater. The top architecture has the Magna eRDM motor available for assistance. The towing capacity results are presented below in Table 8.

(See Table 8 after last section of paper)

Upon review of the presented data, several conclusions have been drawn concerning component selection:

- A diesel (B20) engine is preferred over a gasoline (E85) engine, due to the efficiency gains
- A larger battery is preferred over a smaller one, due to the increase in the CD range and UF
- The 1.3L and two-mode with added electric RWD is preferred over the FWD-only 1.3L and two-mode design, due to an increase in power, efficiency and reduced two-mode motor duty cycle

Proposed Architectures

A performance-based decision matrix was devised in order to help determine the best-case driveline configuration. This method took into account the various performance and environmental impact scores of the competition. Data from GREET and PSAT was also taken into account. The values were ranked, showing the most advantageous drivelines. This matrix is presented below in Table 9, and it encompasses all vehicles that were investigated.

(See Table 9 after last section of paper)

Thus, the EcoEagles' chosen architecture was determined to include a 1.3 L GM diesel engine, using B20 fuel, connected to the FWD GM Two-Mode transmission, along with a RWD

provided by the 55 kW Magna motor. The Electrical Energy Storage System is composed of four 25S2P 32 5 V 12 8 kWh A123 Li-ion battery modules, connected in series. This gives an estimated all-electric range of 20-25 miles, and the resultant UF as presented here.

SUMMARY/CONCLUSIONS

The PSAT model results generally agree with the overall fuel economy and available GM component data, as were determined from initial software testing, but there were some differences. The model parameters are typically determined by curve fitting component data collected under specific operating conditions. The actual operating conditions of the vehicle (e.g. engine temperature or ambient temperature) may vary, resulting in shifts in the model parameters, which are not accounted for in the model. Modeling the amount of parameter shift and the dynamics of the shift would increase the accuracy of the model, at the cost of making the model more complex. Model accuracy may be improved by increasing the complexity of the component models and performing more detailed parameter fitting, at the cost of increasing the development time of the design. However, this investment is likely to be very valuable, as a benefit of developing an accurate model is the ease with which it can be manipulated to produce reliable results, unlike a physical component that cannot be changed.

The cost benefit of adapting to a virtual design philosophy is huge, as it allowed a team of student engineers to extensively modify an existing GM design that they were not previously familiar with, and determine performance characteristics of several different possible designs. All of this was done without any physical automotive hardware, and was performed in much less than a year. However, it is important that accurate models be used, which requires the expertise of numerous fields, along with heavy physical plant verification. This infrastructure will require investment, but it represents where the industry is moving.

REFERENCES

1. Gonder, J., Markel T., Simpson A., Thornton M. "Using GPS Travel Data to Assess the Real World Driving Energy Use of Plug-In Hybrid Electric Vehicles (PHEVs)" 2007, NREL Report Number NREL CP-540-40353

2. Adigrewitz, W., Ahmad, A., Semiburg, J. "Hardware In The Loop Simulator in UAV Rapid Development Life Cycle" 2007, ICIUS2007-A006

3. Jung, D., Tsiotras, P. "Modeling and Hardware-in-the-Loop Simulation for a Small Unmanned Aerial Vehicle" 2007, AIAA

4. Motorizer, J. (MS). "High-Level Modeling, Supervisory Control Strategy Development, and Validation for a Proposed Power-Split Hybrid-Electric Vehicle Design" 2005, Ohio State University

5. Medisetti, P. (MS) "Real Time Simulation and Hardware-In-Loop Testing of a Hybrid Electric Vehicle Control System" 2007, University of Akron.

6. ANL. PSAT 6.2. Computer Software. UChicago Argonne, LLC, Argonne, IL. 2008

7. ANL. GREET 1.7. Computer Software. UChicago Argonne, LLC, Argonne, IL. 2007

8. EPA. http://www.epa.gov/nvfel/methods/rsd4dd.htm

CONTACT INFORMATION

Vincent J. Sabatini
VJSabatini@gmail.com

ACKNOWLEDGMENTS

The authors would like to thank the EcoCAR organizers and the PSAT teams for their assistance in developing and debugging the PSAT models used in the analysis. They would also like to thank GM for providing

ABBREVIATIONS

AWD
All-Wheel Drive

BAS+
Belt Alternator Starter

B20
20% Biodiesel, 80% Standard Diesel

CD
Charge Depleting

CIDI
Compression Ignition Direct Injection (Diesel Vehicle)

CS
Charge Sustaining

E85
85% Ethanol, 15% Standard Gasoline

eRDM
Electronic Rear Drive Module

EREV
Extended Range Electric Vehicle

FWD
Front Wheel Drive

GHG
Green House Gases

GREET
Greenhouse Gases, Regulated Emissions, and Energy Use in Transportation

HEV
Hybrid Electric Vehicle

HWFET
Highway Fuel Economy Test

MPGGE
Miles per Gallon, Gasoline Equivalent

PEU
Petroleum Energy Usage

PHEV(XX)
Plug-in Hybrid Electric Vehicle (Charge Depleting Range in miles)

PSAT
Powertrain Systems Analysis Toolkit

PTW
Pump-to-Wheel

RWD
Rear Wheel Drive

SI
Spark Ignition (Gasoline Vehicle)

SOC
State of Charge (Battery Percentage)

UDDS
Urban Dynamometer Driving Schedule

UF
Utility Factor

US06
Supplemental FTP Driving Schedule (Aggressive)

WTP
Well-to-Pump

WTW
Well-to-Wheel

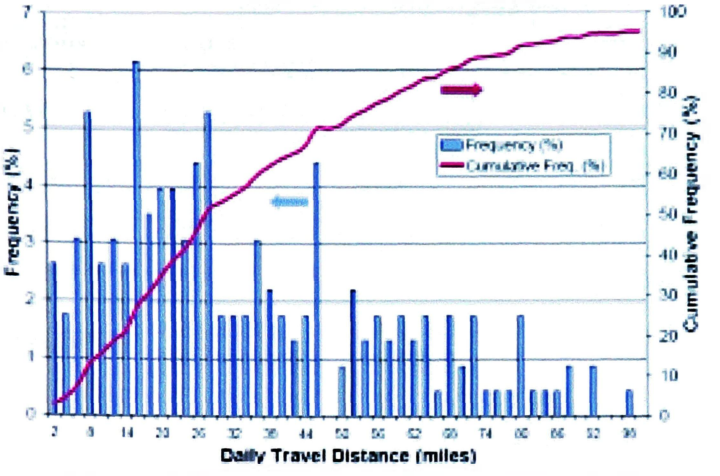

Figure 1. Daily Driving Distance Distribution (St. Louis) [1]

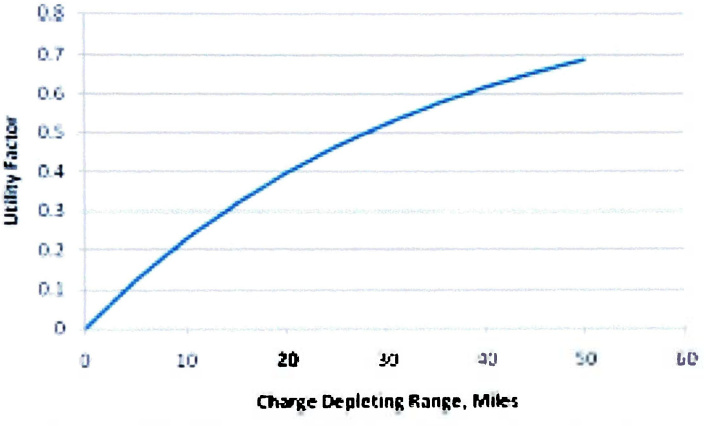

Figure 2. Utility Factor as a Function of Charge Depleting Range

Table 1. Vehicle Technical Specifications

Specification	Competition		EcoEagles
EcoCAR	Production Vue	Competition Requirement	Projected
Accel 0-60	10.6 s	≤14 s	8.7
Accel 50-70	5.7 s	< 10 s	5.3
UF Weighted FE	8.3 L/100km (28.3 mpgge)	7.4 L/100km (32 mpgge)	6.25 L/100km 10.43 UF) (37.7 mpgge)
Towing Capacity	680 kg (1500 lb)	≥680 kg @ 3.5%, 20 min @ 72 kph (45 mph)	680 kg
Cargo Capacity	.83 m3	Height: 457mm (18") Depth: 686mm (27") Width: 762mm (30")	Height: 457mm (18") Depth: 686mm (27") Width: 762mm (30")
Passenger Capacity	5	≥4	4
Braking 60 - 0	38 m - 43 m (123 - 140 ft)	< 51.8 m (170 ft)	41m - 46m
Mass	1758 kg (3875 lb)	< 2268 kg (5000 lb)	1974 kg
Starting Time	≤ 2 s	≤ 15 s	10s
Ground Clearance	198 mm (7.8 in)	>178 mm (7 in)	180 mm
Range	> 580 km (360 mi)	> 320 km (200 mi)	500 km

Table 2. Top Three Architecture Choices

Ranking	Engine	Fuel	Drive	Generator	Energy Storage	Rear Drive
Top Choice	1.3L Diesel	B20	AWD	Two-mode	320V - 10.7 kWhr Li-Ion	Magna eRDM
2nd Choice	1.3L Diesel	B20	FWD	Two-mode	320V - 10.7 kWhr Li-Ion	none
3rd Choice	2.4L Ecotec	E85	AWD	BAS+	320V - 10.7 kWhr Li-Ion	Magna eRDM

Table 3. Fuel Comparison Matrix (GREET)

	Grid-Independent SI HEV: E85	Grid-Connected SI HEV: E85	Grid-Independent CIDI HEV: BD20	Grid-Connected CIDI HEV: BD20	Grid-Independent Fuel Cell G.H2	Electric Vehicle
Total Energy (kW-hr)	2.31	1.98	2.09	1.84	1.07	1.07
Petroleum Energy (kW-hr)	0.36	0.26	0.77	0.54	0.01	0.05
GHGs (g/kW-hr)	274	315	227	278	251	314
Energy Used per mile (kW-hr/mi)	0.96	0.36	0.89	0.35	0.63	0.41
Fuel Energy (kW-hr)	0.96	0.24	0.89	0.23	0.63	0.00
Elec. Energy (kW-hr)	0.00	0.12	0.00	0.12	0.00	0.41
Avg Cost per mile	$0.12	$0.09	$0.09	$0.07	$0.21	$0.05

Table 4. High Level Acceleration Power Requirements

Time (s)	Desired or Required?	Speeds (mph)	Power (W)
10	Desired	0-60	97500
14	Required	0-60	71250
20	Desired	0-90	12250
5	Desired	50-70	13500
10	Required	50-70	76500

Table 5. CS&CD Fuel Economies (MPGGE)

	UDDS	HWFET
1.3L B20 2-Mode eAWD - Charge Depleting	59	53
1.3L B20 2-Mode eAWD - Charge Sustaining	30	38
1.3L B20 2-Mode FWD - Charge Depleting	50	49
1.3L B20 2-Mode FWD - Charge Sustaining	30	38
2.4L E85 BAS+ eAWD - Charge Depleting	35	N/A
2.4L E85 BAS+ eAWD - Charge Sustaining	23	36

Table 6. Utility Factor Summary

	1.3L B20 2-Mode eAWD			1.3L B20 2-Mode FWD			2.4L E85 BAS+ eAWD		
	UDDS	US06	HWFET	UDDS	US06	HWFET	UDDS	US06	HWFET
CD ES Energy (Wh)	5896	5896	3216	1608	1608	2680	3430	3216	0
CD Fuel Energy (Wh)	5942	45435	5966	2896	17898	7392	8482	69541	0
CD Total Energy (Wh)	11838	51331	9182	4504	19506	10072	11912	72757	0
CD Distance (mi)	20	32	14	6	13	14	12	50	0
CS ES Energy (Wh)	0	0	536	0	0	0	0	0	860
CS Fuel Energy (Wh)	97266	52322	84114	9864	3985	83908	139405	83759	100306
CS Total Energy (Wh)	97266	52322	84650	9864	3985	83908	139405	83759	101166
CS Distance (mi)	81	32	89	8	3	89	91	53	103
Utility Factor	0.416			0.464			0.421		

Table 8. Towing Capacity Summary

	Velocity (m/s)	Cont. Power (W)	Grade (degrees)	Grade (%)	Energy (MJ)	Notes:
1.3 L + Two-mode + Magna	20.12	77300	6.25	10.95	10.25	1st Choice
1.3 L + Two-mode	20.12	56050	4.31	7.54	10.25	2nd Choice
2.4 Eco +Magna	20.12	70594	5.64	9.87	10.25	3rd Choice

NOTE: 2.4 L Eco has 123 kW Peak Power, 1.3 L Diesel has 68.3 kW Peak Power

Table 9. Architecture Decision Matrix

Option	Perform.	Fuel Economy	WTW GHG	Tailpipe Emissions	WTW PEU	Norm. Score	Rank
2.4L Production Vue	3.7	2.0	2.0	2.0	2.0	0.0	
1.3L B20 2-mode AWD HEV	2.0	2.0	5.8	9.2	2.0	3.5	
1.3L B20 2-mode AWD PHEV10	2.0	6.3	8.2	9.7	2.5	6.4	
1.3L B20 2-mode AWD PHEV20	3.0	10.0	10.0	10.0	5.2	10.0	1
1.3L B20 2-mode FWD HEV	2.0	2.0	5.6	9.2	2.0	3.4	
1.3L B20 2-mode FWD PHEV10	2.0	6.2	8.0	9.7	2.4	6.3	
1.3L B20 2-mode FWD PHEV20	3.0	10.0	9.9	10.0	5.2	9.9	2
2.4L E85 BAS+ AWD HEV	5.6	2.0	2.0	2.0	6.6	2.5	
2.4L E85 BAS+ AWD PHEV10	7.5	4.8	2.0	2.2	8.6	5.0	
2.4L E85 BAS+ AWD PHEV20	10.0	8.8	2.0	4.2	10.0	9.3	3

NOTE: Tailpipe emissions refer to only the PTW emissions of the vehicle, which are scored separately.